MASTERARBEIT | MASTER'S THESIS

Titel | Title

Polyphosphazene Copolymers for Biomedical Applications

verfasst von | submitted by

Juliane Rumpelsberger BSc

angestrebter akademischer Grad | in partial fulfilment of the requirements for the degree of

Master of Science (MSc)

Wien | Vienna, 2024

Studienkennzahl lt. Studienblatt | Degree programme code as it appears on the student record sheet:	UA 066 862
Studienrichtung lt. Studienblatt | Degree programme as it appears on the student record sheet:	Masterstudium Chemie
Betreut von | Supervisor:	Assoz. Prof. Mag. Dr. Christian Kowol

ZUSAMMENFASSUNG

In den letzten Jahren wurde viel Forschung im Bereich der Polymere betrieben, welche für biomedizinische Applikationen verwendet werden. Polymere haben sich hinsichtlich ihrer Verwendung weiterentwickelt, beginnend von der Anwendung in Maschinen, in der Automobilindustrie, für Bauanwendungen, Verpackung, in der Elektronikindustrie, und vielen mehr, wurden Polymere auch schnell im medizinischen Bereich für die Massenproduktion von Kanülen, Einwegspritzen, Handschuhen, sterilisierbaren Verpackungen und Operationsequipment für die Medizintechnik verwendet.
Neue Polymere wurden entwickelt, die speziellen Anforderungen gerecht werden mussten, damit sie innerhalb des menschlichen Körpers Verwendung finden konnten. Diese Polymere wurden nicht nur als Prothesen und Implantate verwendet, sondern sogar für spezialisierte, biomedizinische Anwendungen, wie der Verwendung als Wirkstoffträgerpolymere, genützt.

Solche Wirkstoffträgerpolymere müssen definierten Anforderungen entsprechen. Sie müssen Abbaubarkeit unter physiologischen Bedingungen aufweisen und dabei nur nicht-toxische Abbauprodukte hinterlassen, weiters müssen Löslichkeit unter physiologischen Konditionen, sowie hinreichende Stabilität gegeben sein. Das Ziel dieser Arbeit war es, polyphosphazen-basierte Copolymere zu synthetisieren, welche man für derartige biomedizinische Anwendungen verwenden kann. Polyphosphazene wurden synthetisiert, welche mit verschiedenen Linkern reagiert wurden, um durch nachfolgende Copolymerisationen ‚Bottlebrush' Polymere zu erhalten. Einerseits wurden über den sogenannten ‚grafting from' Ansatz mit Polyglutaminsäure polymerisiert. Weiters wurden Polyphosphazen poly-N-(2-hydroxypropyl)methacrylamid Bottlebrush-Copolymere über den "grafting to" Ansatz synthetisiert, wobei Click-Chemie genützt wurde. Das wurde durchgeführt, um verschiedene polyphosphazen-basierte Copolymere herzustellen, welche über vorteilhafte Eigenschaften verfügen, wie verschiedene Stabilitäten in wässrigen Systemen und verschiedene Bindungsstellen oder funktionelle Endgruppen. Diese Copolymere waren geplant für die kontrollierte Wirkstoffgabe und deshalb wurde auch versucht, einen Peptidwirkstoff auf diese Copolymere anzubringen, sowie eine weitere Hydrazin-Funktionalität, welche zum Anbringen verschiedenster Wirkstoffe genützt werden kann.

ABSTRACT

In recent years, extensive research has been conducted in the field of polymers for biomedical applications. Polymers have evolved in their use, starting from applications in machinery, the automotive industry, construction, packaging, and the electronics industry, to being rapidly adopted in the medical field for the mass production of cannulas, disposable syringes, gloves, sterilizable packaging, and surgical equipment for medical technology. Furthermore, new polymers have been developed to meet specific requirements for their use within the human body. These polymers are not only employed as prostheses and implants, but even for specialized biomedical applications such as drug carrier polymers.

The essential requirements for such drug carrier polymers are clearly defined, being degradable under physiological conditions, leaving only non-toxic degradation products, and exhibiting solubility and sufficient stability under physiological conditions. The aim of this work was to synthesize polyphosphazene-based copolymers for such biomedical applications. Polyphosphazenes were synthesized, reacted with various linkers, and further copolymerized to obtain bottlebrush polymers. On the one hand, a “grafting-from” approach with polyglutamic acid was followed. On the other hand, a polyphosphazene- poly-*N*-(2-hydroxypropyl)methacrylamide copolymer was prepared by the “grafting-to” approach, utilizing click chemistry. This was done to produce various polyphosphazene-based copolymers with advantageous properties, such as different stabilities in aqueous systems and various binding sites or functional end groups. These copolymers were intended for controlled drug delivery, and further investigated regarding conjugation with a peptide drug, as well as an additional hydrazide functionality for direct conjugation with carbonyl functionalized drugs.

Acknowledgements

First, I would like to thank Prof. Christian Kowol for supervising my thesis. Although the practical work was not conducted in Vienna, you always had an open ear for my questions and concerns during the thesis. I am beyond grateful for the support.

Secondly, I would like to thank Assoz. Univ.-Prof. Dr. Ian Teasdale and Dr. Paul Strasser for their support throughout my thesis and the opportunity to work on this fascinating project at the ICP in Linz.

I would also like to thank Nico Vennemann, Michael Kneidinger, Hannes Mitter, Sonja Brandner, Martina Huber, Peter Prka, Christina Walliser and Verena Schinegger. You made the time I spent at the ICP unforgettable. I could not have wished for better colleges. Thank you for the fun time in between and after work.

Lastly, I want to thank my family for the huge emotional support and reassurance they provided me. Thank you, Mama and Papa, Leni, Hansi, Oma, and thank you Erik! Without all of you, I would not have been able to complete my thesis. You were there for me when I was struggling, but you were also there to celebrate every single cornerstone leading to the finalization of the thesis.
I could go on and on about all the things I have to thank my family and friends for, but I will come to an end here! Even if I did not mention all of you by name: Thank you!

TABLE OF CONTENTS

1. Introduction

1.1. Polymers for biomedical applications as drug carriers

In the field of drug delivery, certain obstacles hinder promising small molecular drugs from exploiting their full potential. In multiple cases, the drugs are not able to reach the targeted site of action in required concentrations due to early clearance from the blood stream. This affects effectiveness of the drug, necessitating higher concentrations of the drug to be administered, often leading to increased numbers of unwanted, negative side effects. Furthermore, solubility of rather hydrophobic drugs is limiting applications. To overcome these limitations, polymeric materials were investigated as drug carrier systems. These polymers for biomedical applications must share certain, unarguable characteristics to help improve pharmacokinetics.

For polymeric drug carriers, water solubility is vital [1]. Insufficient solubility can lead to aggregation, followed by an immune response and clearance from the human body [2; 3]. As many drugs on the market exhibit poor aqueous solubility, polymer-drug conjugates can resolve the issue. Some polymers offer superior hydrophilicity due to their structure. The polymers discussed in the subsequent subchapters, poly-*N*-(2-hydroxypropyl)methacrylamide (pHPMA) and poly-α-L-glutamic acid (PGA) are readily water soluble. Naturally, hydrophobic polymeric structures would need to be altered by applying hydrophilic coatings or formation of micellar structures [4]. However, besides solubility, stability under physiologic conditions is crucial as well. Conjugation of protein drugs onto polymers can prevent the drug from premature degradation by proteolytic enzymes, enhancing stability. Furthermore, stability is improved by the high molecular weight introduced by polymeric carriers. Generally, higher molecular weight results in a longer plasma half-life for intravenously administered water soluble polymer-drug conjugates, since the higher molecular weight and increased hydrodynamic radius prevents the drugs from early elimination by renal clearance [5; 6]. Enhanced stability further leads to prolonged plasma circulation. The drug can therefore reach the site of action in higher concentrations, particularly when further modifications allow for targeted release of the drug [7]. Finally, geometry is another key factor for the conjugates' stability. Renal clearance can be overcome by more rigid polymers with increased number of chain ends; such polymers are hindered in passing the pores in kidneys and thus being removed by renal clearance [5].

Although, stability and prolonged circulation is therefore clearly necessary to ensure the administration of the drug to the targeted site, after the drug is released, degradability of the polymeric carrier is highly wanted. Ideally, polymers for biomedical applications are degradable inside the human body after a set time frame. Most current biomedical polymers, such as PEG

and pHPMA, are based on a carbon backbone and hence not degradable [8]. Copolymerization to block– or bottlebrush structures can help overcome the issue of insufficient degradability [5]. Enhanced degradability can ensure that the polymers can be cleaved into excretable byproducts, minimizing long-term accumulation in the body. Therefore, the development of degradable copolymers is essential for the safe and effective use of polymers in biomedical applications. A promising candidate is the class of polyphosphazenes (PPz), which allows a variety of co-polymers to be synthesized, as well as a tuned degradation for specified applications [9].

Lastly, polymers in drug delivery systems must be non-toxic and non-immunogenic. pHPMA and PGA are inherently non-toxic and non-immunogenic, as shown by various studies [10; 11]. For PPz, the toxicity and immunogenicity are depending on the substituents introduced onto the polymers' backbone [12]. Therefore, careful selection and modification of these substituents are crucial to ensure biocompatibility. Extensive *in vivo* and *in vitro* studies are necessary to evaluate the safety profile of these modified polymers [13]. As becomes apparent from the discussed topics above, potential candidates for polymers for biomedical applications as drug carriers have to fulfil a catalogue of desired characteristics to be taken into consideration.

1.2. Polyphosphazenes

Polyphosphazenes, short PPz, are polymers consisting of a backbone of covalently linked alternating phosphorous and nitrogen atoms. The dπ - pπ bonds are not interacting with each other, resulting in stability on the one hand, and high flexibility of the P-N bonds on the other hand. This allows almost free rotation of the P-N bond, which facilitates substitution on the d orbitals of the P atom [14]. The general structure is shown in Figure 1, with the rest group - R commonly being of organic nature [15].

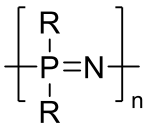

Figure 1: General structure of polyphosphazenes.

When carrying such organic rest groups, polyphosphazenes are referred to as poly(organo)phosphazenes. Due to the ability of adding different moieties onto the phosphorus atom by so-called macromolecular substitution reactions, the properties of polyphosphazenes are manifold. One can tune the solubility, the behaviour under physiological conditions, the overall structure of the macromolecule, and the degradation rate [16]. This allows a broad band of applications, also in the field of biomedicine.

1.2.1. Synthesis of polyphosphazenes

The first reported preparation of a polyphosphazene polymer, more precisely a poly(dichloro)phosphazene, was conducted by Stokes in 1897. The reaction, starting from hexachlorotriphosphazene, yielded an insoluble, crosslinked polymer [17]. In 1965, Allock and Kugel published a synthesis method resulting in a linear (un-crosslinked), soluble, fully substituted, high molecular weight poly(organo)phosphazene [18]. They were polymerizing hexachlorotriphosphazene and subsequently substituted the chlorine atoms on the resulting polydichlorophosphazene $(NPCl_2)_n$ with either sodium alkoxide or phenoxide. Thereby preventing crosslinking and yielding a soluble poly(organo)phosphazenes $[NP(OR)_2]_n$. The number of repeating units of these polymers were reportedly ranging from 3 up to 15000.

From this starting point, different synthesis methods for polyphosphazenes were explored. Nowadays, two different methods for the synthesis of the linear precursor

poly(dichloro)phosphazene have been broadly established, namely the ring-opening polymerization or the cationic living polymerization.

The ring-opening polymerization is the traditionally used method, using hexachlorocyclotriphosphazene as starting material. The method allows for simple upscaling and high molecular weight polymers, however the control over the polymerization is low and typically higher dispersities are obtained. In general, the monomer is heated up to 250°C to initiate the reaction, illustrated in Figure 2, although temperatures of 300°C or higher have to be prevented to avoid crosslinking and formation of rubber-like polyphosphazenes [19; 15]. Furthermore, the ring-opening reaction is sensitive to moisture and air, necessitating dry solvents or a reaction *in vacuo* and the starting material hexachlorocyclotriphosphazene needs to be as pure as possible, requiring recrystallization or sublimation prior to the reaction. To improve the control over, as well as the yield of the reaction, catalysts like $AlCl_3$ or BCl_3 have been introduced.

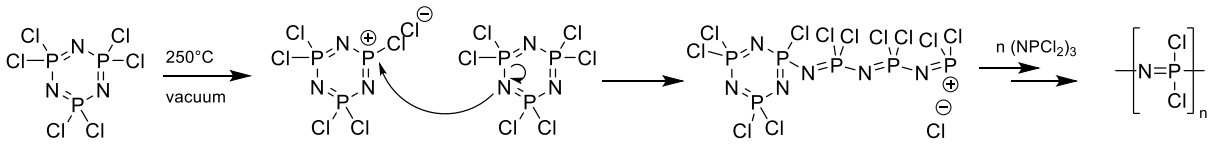

Figure 2: Ring opening polymerization of hexachlorocyclotriphosphazene to obtain the precursor molecule poly(dichloro)phosphazenes.

The second well established method is the living cationic polymerization. It allows for increased control over the reaction and targeted molecular weight of the resulting poly(dichloro)phosphazenes, however, the required synthesis of the monomer trichlorophosphoranimine ($Cl_3PNSiMe_3$) complicates the approach [15]. The reaction can either be initiated with PCl_5 [20] or a tertiary phosphine (R_3PCl_2), whereby the latter ensures monodirectional growth *via* the blocked chain end and enables the functionalization of the end-group. The reaction mechanisms are shown schematically in Figure 3 [15].

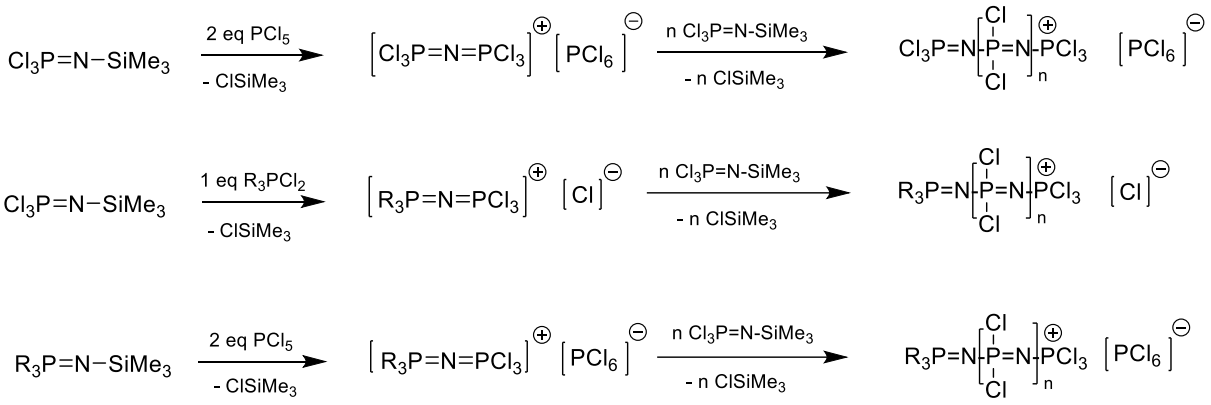

Figure 3: Synthesis pathways of poly(dichloro)phosphazenes via the living cationic polymerization.

Since poly(dichloro)phosphazene is highly reactive and labile towards hydrolysis and subsequent main-chain degradation, as described in Chapter 1.2.2., the Cl moieties are substituted during a so-called macromolecular substitution reaction to prevent premature degradation [21; 22]. Various substituents, namely alcohols and amines, can be introduced onto the PPz backbone, governing the bulk properties of the final polymer such as solubility, potential degradability, reactivity as well as macromolecular architecture. The general procedure of the macromolecular substitution is illustrated *via* an exemplary amine in Figure 4.

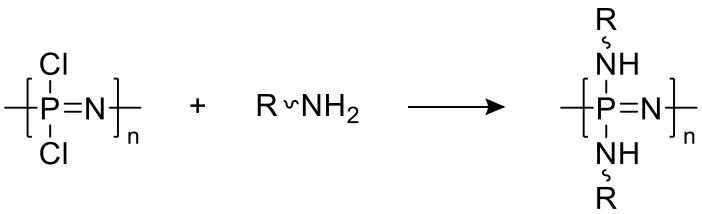

Figure 4: Schematic representation of the macromolecular substitution reaction of poly(dichloro)phosphazene with an organic amine species, yielding a poly(organo)phosphazene.

Overall, polyphosphazenes provide a promising synthetic platform for the preparation of (co-)polymers for biomedical application, offering a broad spectrum of properties and structural possibilities.

1.2.2. Degradation of polyphosphazenes

As already described above, polyphosphazenes enable a broad array of properties, including potential degradability with a tuneable degradation rate. The degradation proceeds *via* a hydrolytic cleavage of the backbone and is mainly governed by the hydrophilicity of the polymer and the accessibility for water to attack at the phosphorous centre. Furthermore, the degradation rate is increased at a lower pH [23]. In detail, a substituent is first cleaved forming hydroxyphosphazene which is subsequently further degraded, finally resulting in phosphates and ammonium salts [23]. The general mechanism of degradation, again with an exemplary poly(amino)phosphazene, is depicted in Figure 5.

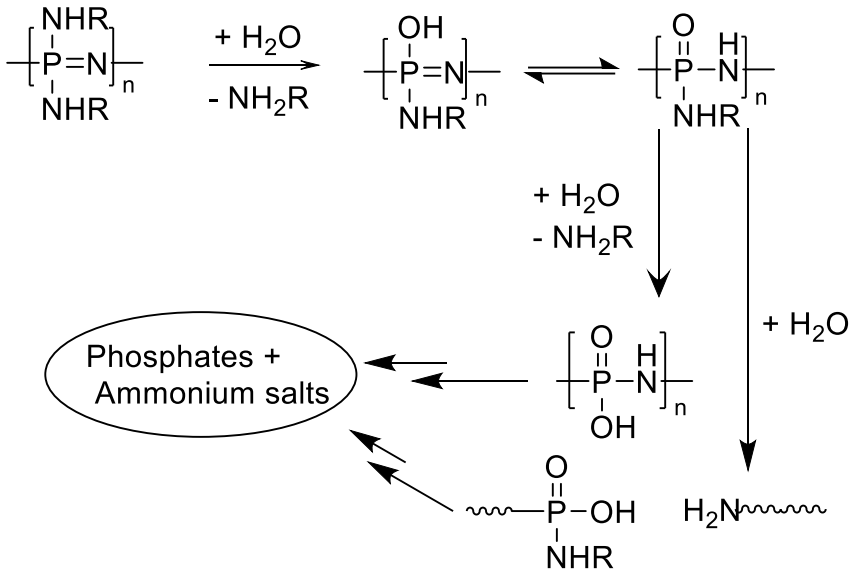

Figure 5: Degradation mechanism of poly(organo)phosphazenes.

Regarding the degradation products, the polymer completely degrades into phosphates and ammonium salts along with the cleaved side groups, enabling a completely biocompatible system by carefully selecting appropriate macrosubstituents [24; 22].

1.2.3. Architectural design of Polyphosphazenes

The broad variety of polyphosphazenes was already highlighted above, rooted in the vast library of possible macrosubstituents. This unique feature of the macromolecular substitution reaction can further be used for architectural design of polyphosphazene polymers and co-polymers. Copolymerization with other polymers, either *via* 'grafting to' or 'grafting from' approaches, results in branched polymers, such as comb-like or bottlebrush polymers [25; 26]. Structures with a lower grafting density are referred to as comb-like polymers instead of bottlebrush polymers [27]. Additionally, star-like or dendritic architectures are feasible as well [28; 26; 29; 30].

In this work, the focus was laid on synthesizing bottlebrush polymers consisting of a backbone and densely grafted side chains, resulting in high molecular weight 'bottlebrush' structures (Figure 6) [31].

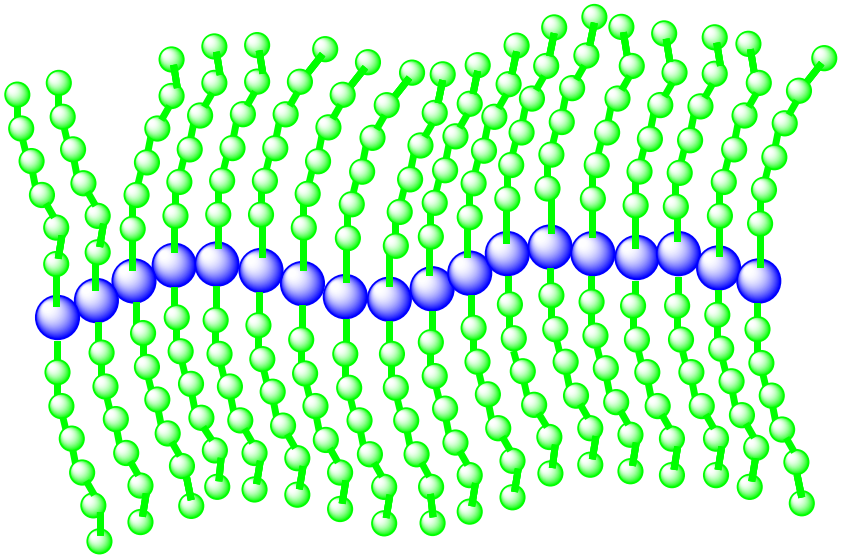

Figure 6: Schematic visualisation of a bottlebrush copolymer.

Bottlebrush polymers can be characterized by their chemical composition as well as three main structural parameters, namely the length of the backbone, the length of the sidechains, and the grafting density [32]. Each parameter is tuneable independently, influencing the properties of the final material. In comparison to their linear analogues, bottlebrush polymers provide several advantages including higher feasible molecular weights, often improved solubility and multifunctionality, positioning them as promising candidates for polymer therapeutics [33]. Furthermore, bottlebrush polymers can self-assemble to structures up to the

nano meter area. This is allowing for applications in the fields of stimuli responsive coatings, photonics, and drug delivery [33].

1.2.4. Polyphosphazenes in biomedicine

Based on the broad spectrum of properties, the potential and tuneable degradation and biocompatibility of polyphosphazenes as well as possible architectural design, this class of materials finds manifold application in the field of biomedicine. Polyphosphazenes can for example be used as scaffold for tissue engineering [21]. Providing structural support for bones to grow back in the right structure and direction whilst healing. Grafting fluorophores onto the polymers' backbone allows monitoring by fluorescence imaging and application in the field of bioimaging. This can be employed, for example, to investigate the pharmacodynamics and pharmacokinetics of the macromolecule and conjugated drugs in *vivo* [21]. In the field of cancer research, bioimaging can be used to follow the pathway of metabolites related to tumor tissue [34]. Another significant area where polyphosphazenes show great potential is drug delivery. The tuneable side chain functionality of polyphosphazenes also allows for the introduction of various functional groups, which can be used for polymer-drug conjugates and even enable stimuli-responsive drug release [12; 35].

1.3. Poly-*N*-(2-hydroxypropyl)methacrylamide

Poly-*N*-(2-hydroxypropyl)methacryamides (pHPMA), depicted in Figure 7, are hydrophilic, water-soluble polymers that have been extensively studied in the last years [8]. They are non-toxic, non-immunogenic and biocompatible, making them a viable candidate for applications in the field of biomedical polymers, like usage as drug carrier *via* polymer-drug conjugates [36]. Nevertheless, their non-degradability inside *in vivo* and thereby limited clearance from the body *via* renal clearance, restricts applications for pHPMA.

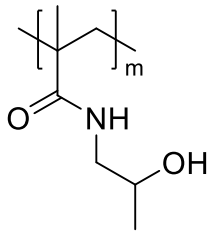

Figure 7: General structure of poly-N-(2-hydroxypropyl)methacrylamide.

1.3.1. Synthesis of poly-*N*-(2-hydroxypropyl)methacrylamide

A commonly used way of synthesizing pHPMA is *via* the monomer N-(2-hydroxypropyl)methacrylamide. The double bond on the methacrylamide is exploited for radical polymerizations of pHPMA [10]. As free radical polymerizations result in broad molecular weight distributions, controlled ways were investigated. Matyjaszewki *et al.* first found a way to control the radical polymerization by employing the atom transfer radical polymerization ATRP. The polymers still had rather broad dispersities, as well as low conversions, so further research was done. McCormick *et al.* then synthesized the first pHPMA in 2005 with well-defined molecular weight distributions. The group used the method of reversible addition fragmentation chain transfer RAFT. However, the reaction conditions, as well as the transfer agents, needed to be selected carefully for this method [37; 10]. The respective reaction conditions can vary for the polymerization, having different reagents and conditions, as reported in literature [38–40]. The general reaction for the polymerization of HPMA *via* RAFT polymerization in aqueous media is shown in Figure 8 [10].

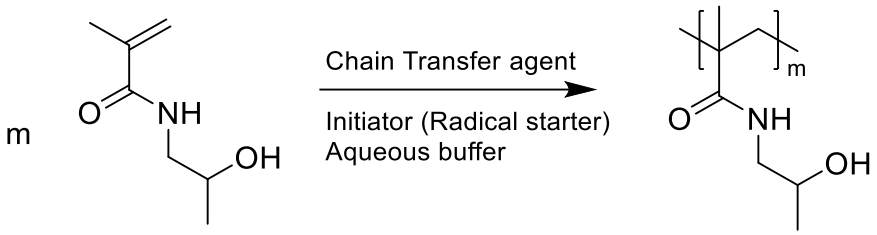

Figure 8: Synthesis of pHPMA via RAFT polymerization in aqueous media.

1.3.2. Degradation of poly-*N*-(2-hydroxypropyl)methacrylamide

As already mentioned in the previous subchapter, pHPMA is hardly degradable, like most C-based polymers, and cannot be hydrolytically cleaved inside the human body. pHPMA can solely be excreted *via* glomerular filtration in the kidneys. However, this is only possible up to a certain molecular weight, which amounts about 50000 $g.mol^{-1}$ [41; 42]. The exact values depend on the architecture of the respective polymer (i.e. star-shaped or linear) and the type of polymer [42]. Therefore, when targeting biomedical applications *in vivo*, the macromolecular weight of pHPMA needs to be controlled. This enables glomerular filtration and hence excretion of the macromolecule from the body.

1.3.3. Applications for poly-*N*-(2-hydroxypropyl)methacrylamides

pHPMA has been extensively studied for usage as a drug carrier [42–45]. Its hydrophilicity facilitates its use within the human body, alongside its non-immunogenic character in contrast to the well-researched PEG [46]. Moreover, it is possible to reach sufficiently high molecular weights of pHPMA, ensuring extended lifetime in the blood stream and hence higher concentrations of the polymer drug conjugate can reach the tumor site [46].

pHPMA as drug carrier for anti-cancer drugs has first reached clinical trials in the 1990s [41]. Namely, it was a conjugate of polyHPMA with doxorubicin, named PK1. The studies were terminated due to minimal to no response from patients with different types of cancer. Other clinical studies with polymer-drug conjugates like paclitaxel, camptothecin, or platinated followed over the years. However, none of these conjugates made it further than phase II [41]. The major drawback of these conjugates were the insufficient molecular weight, and associated problems with accumulation in tumor tissue. In response, research was conducted to increase the molecular weight, bringing out diblock- and multiblock copolymers, either *via*

direct copolymerization or click-chemistry. The poly(organo)phosphazene-co-poly(*N*-2-(hydroxypropyl)methacrylamide bottlebrush copolymers synthesized in the framework of this thesis were intended to fulfil the mentioned requirements of overall high molecular weight, whilst containing pHPMA chains below the renal clearance limit.

1.4. Poly-α-L-glutamic acid

Poly-α-L-glutamic acid, PGA, is a polymer that consists of repeating units of the non-essential amino acid glutamic acid or glutamate. Its general structure is depicted in Figure 9 [47].

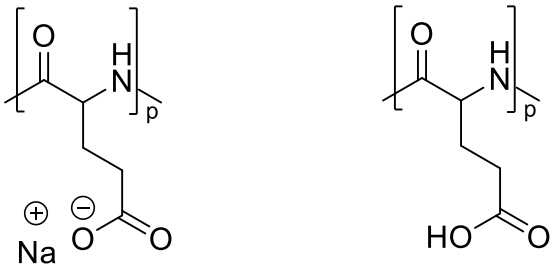

Figure 9: Poly-α-L-glutamate (left) and poly-α-L-glutamic acid (right).

PGA offers very advantageous characteristics for biomedical applications. PGA is biocompatible, non-toxic, as well as edible and its salt form is highly water soluble [48]. Additionally, PGA is readily degradable inside the human body. In presence of proteinases, polypeptides degrade into their respective α-amino acids, which are further metabolizable inside the human body [49].

The functional group of the carboxylic acid further enables simple conjugation with various other functional groups, giving access to a broad spectrum of structural possibilities. The sum of these properties makes PGA a promising candidate for multiple applications, including the biomedical field. For example, hydrogels made of poly-α-L-glutamic acid were used for tissue regeneration [50]. Furthermore, applications of poly-α-L-glutamic acid used as carrier molecule were reported [51; 52; 11].

1.4.1. Synthesis of poly-α-L-glutamic acid

Poly-α-L-glutamic acid is typically synthesized *via* ring opening polymerization of γ-benzyl-L-glutamate N-carboxyanhydride, yielding controlled molecular. The resulting intermediate poly(γ-benzyl-L-glutamate) (PBLG) subsequently needs to be deprotected. The polymerization and subsequent deprotection are schematically illustrated in Figure 10, under the conditions employed in this work.

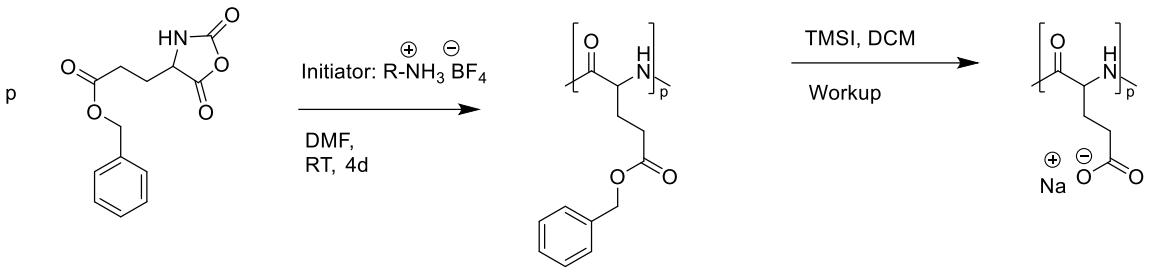

Figure 10: Ring opening polymerization of N-carboxyanhydride and subsequent deprotection of PBLG, giving poly-α L-glutamate.

Although various reagents and reaction conditions can be utilized for the ring opening polymerization and subsequent deprotection of PGA [53; 54], the detailed conditions within this thesis were selected on adapted and optimized literature procedure. Primary amine tetrafluoroborate salts, for example, allow for a better control over the dispersity, as well as the molecular weight. Furthermore, this specific initiator combination enables a scale up to multigram level, thus replacing used hydrochloride salt initiators [47]. Deprotection with TMSI provides soft reaction conditions, ensuring the retention of the α-L-configuration of the polymer. In contrast, simple hydrolysis using NaOH can potentially lead to racemization. In addition, acidic hydrolysis at lower pH values could accelerate unwanted and premature hydrolysis of the PPz backbone [53].

1.5. Click Chemistry: Copper catalysed Azide-Alkyne-Cycloaddition

The copper catalysed Azide-Alkyne-Cycloaddition, briefly CuAAC, is a powerful tool in the field of so called 'Click chemistry'. Click chemistry refers to chemical reactions, which are per definition simple to conduct, thus offering high yields, granting stereospecificy, allowing facile purification and leaving few to no byproducts [55; 56]. The concept of the copper catalysed azide-alkyne-cycloaddition under the reaction parameters used in this work was first published by Meldal *et al.* in 2001. Starting from the dipolar 1,3 Huisgen cycloaddition,1,4- and 1,5-disubstituted triazoles were obtained [57]. Meldal *et al.* managed to exclusively obtain the 1,4-disubstituted 1,2,3-triazole product, assuring a regiospecific product, without leaving by-products like 1,5-disubstituted triazoles [56]. The mechanism of the cycloaddition is depicted in Figure 11 [58].

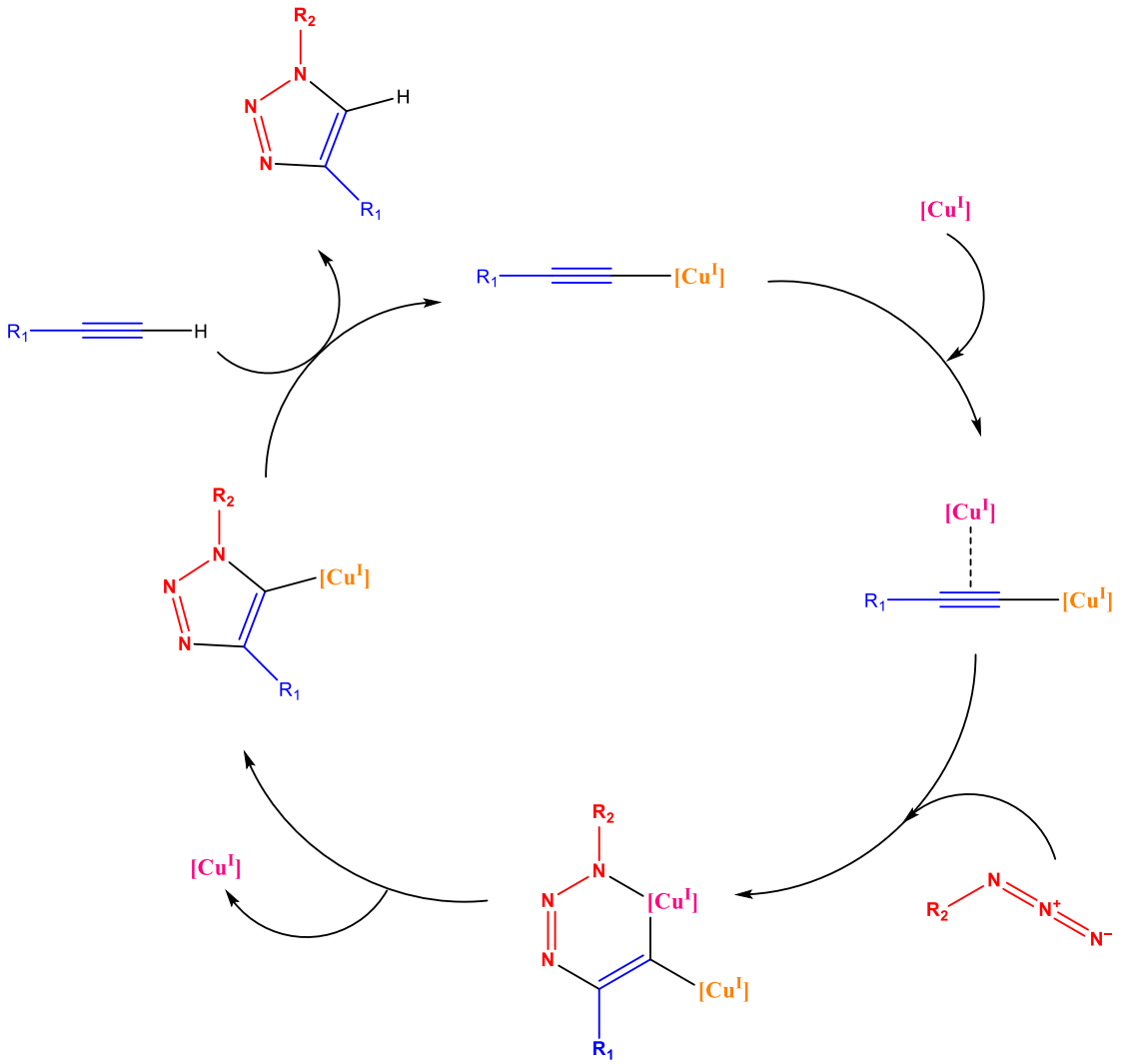

Figure 11: General reaction mechanism of a copper catalysed azide-alkyne-cycloaddition.

In general, the CuAAC is not sensitive to reaction conditions and reagents. For example, a broad spectrum of solvents is accessible. The CuAAC can be conducted either in aqueous or protic media, aprotic media, as well as under inert conditions. Moreover, the reactivity, yet high selectivity of organic azides in reactions are exploited. Thus, CuAAC offers a high tolerance for different functional groups on the rest groups -R that remain unaffected during CuAAC [55].

2. Aim of the thesis

The objective of this thesis was to utilize poly(organo)phosphazenes for the synthesis of various copolymers intended for application as polymer therapeutics

The first part involved the synthesis of novel polyphosphazene-poly-*N*-(2-hydroxypropyl)methacrylamide (pHPMA) graft copolymers (PPz-g-pHPMA) *via* CuAAC click chemistry reactions. pHPMA are highly promising biomedical polymers, however, hampered by their non-degradable character in vivo and hence restricted molecular weight. To overcome these restrictions, a PPz-g-pHPMA bottlebrush polymer was designed, combining a degradable PPz backbone with excretable pHPMA side chains and overall achieving higher molecular weights while retaining the bulk character of pHPMA. To this end, polyphosphazenes with different linkers bearing alkyne functionalities were synthesized. The PPz backbones were further reacted with pHPMA side chains *via* CuAAC and characterized regarding the conversion of the reaction and achievable molecular weight.

In the second part of the thesis, the synthesis of poly(organo)phosphazene–poly-α-L-glutamic acid graft copolymers (PPz-g-PGA) and their use as macromolecular carriers for a peptide cancer drug will be described. The conjugation reactions were conducted *via* peptide coupling reactions, resulting in a novel polymer-peptide drug conjugate, and characterized regarding the achieved loading.

The third and final part involved the continuing development of the PPz-g-PGA carrier system by incorporation of a hydrazide linker onto the PGA side groups to provide accessible attachment sites for carbonyl groups. Additional conjugation sites and conjugation chemistry should broaden the applicability of the developed carrier system for different therapeutics and simplify the coupling procedures.

3. Experimental

Nuclear magnetic resonance (NMR) spectra were measured on a *Bruker® Avance 300* spectrometer (300,01 MHz).

The GPC measurements in organic medium were conducted on a *Viscothek GPC$_{max}$®* at 60°C with DMF containing 10 mM LiBr as eluent and a flow rate of 0.75 ml.min^{-1}. Prior to injection, the samples were filtered through a 0.2 µm PTFE syringe filter. The samples were detected with a light scattering (LS) and refractive index (RI) detector. The molecular weights were calculated based on a conventional calibration of the RI detector with linear polystyrene standards from PSS (*Polymer Standard Service GmbH*).

The aqueous GPC measurements were conducted on an *Agilent Technologies 1260 Infinity II* device, with Milli-Q-water with 0.1 M $NaNO_3$ and 0.0251%w/w NaN_3 as eluent. The flow rate was 0.5 ml.min^{-1}. Prior to injection, samples were filtered through a 0.2 µm nylon syringe filter. Detection was conducted with an UV-vis detector from *Agilent*, a refractive index detector RI-501 from *Shodex* and a *TREOS II* light scattering detector from *Wyatt technology*.

Water was removed by freeze drying on an *Alpha 1-2 LDplus* freeze drying system *Christ*. Ultrafiltration was performed with *Vivaspin 20* tubes (3 kDa molecular weight cut-off) from *GE Heathcare*. Dialysis was conducted with regenerated cellulose dialysis tubes from *Spectrum Laboratories, Inc.*, with different molecular weight cut-offs (MWCO) of 1 kDa, 3.5 kDa and 6-8 kDa.

The pHPMA was provided by Dr. Juraj Kronek from the Slovak academy of science.

The peptide drug used for the synthesis of the polymer – drug conjugate was provided by Dr.^{in} Cornelia Roschger from the MED Campus of the Johannes Kepler University. For patent reasons, no structure or detailed analytical data can be shown.

3.1. Polyphosphazene Synthesis

The syntheses of the poly(dichloro)phosphazenes were performed according to Strasser *et al.* [23]. All reactions were performed in the glove box under argon atmosphere to prevent degradation of the labile poly(dichloro)phosphazenes.

3.1.1. Synthesis of Poly(dichloro)phosphazenes with a triphenylphosphine end group

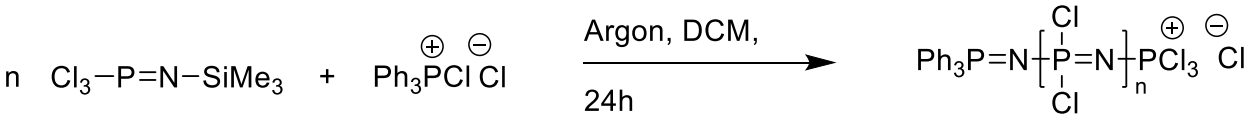

Figure 12: Synthesis of the poly(dichloro)phosphazene with triphenylphosphine end group

Targeting a poly(dichloro)phosphazene with 50 repeating units, 30 mg (98 %; 1 eq; 0,090 mmol) of the initiator dichlorotriphenyl-λ^5-phosphane was dissolved in around 2 ml of dry DCM. 990 mg (50 eq; 4,42 mmol) of the monomer Cl_3-P=N-$SiMe_3$ was dissolved in around 3 ml of DCM as well and added dropwise to the initiator while stirring. The reaction mixture was stirred for 24 h at room temperature and subsequently reacted with one of the prepared linkers *in situ* during the macromolecular substitution reaction.

3.1.2. Synthesis of Poly(dichloro)phosphazenes with a diphenylstyrenphosphine end group

An end-group functionalized poly(dichloro)phosphazene was prepared according to the procedure from Strasser *et al.* [53].

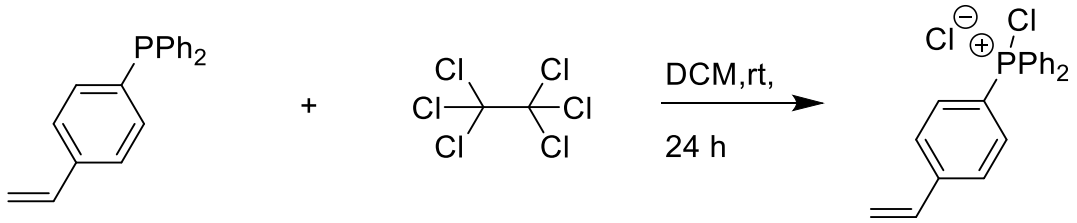

Figure 13: Schematic synthesis of the functional initiator dichlorodiphenyl(4-styrene)phosphane.

First, 4-(diphenylphosphino)styrene was chlorinated by dissolving 10 mg (1 eq; 34,68 mmol) in ~2 millilitres of dry DCM. 9.069 mg (1,1 eq; 38,15 mmol) of hexachloroethane was dissolved in ~1 ml dry DCM as well, added to the solution and stirred for 24 h at room temperature in the glove box.

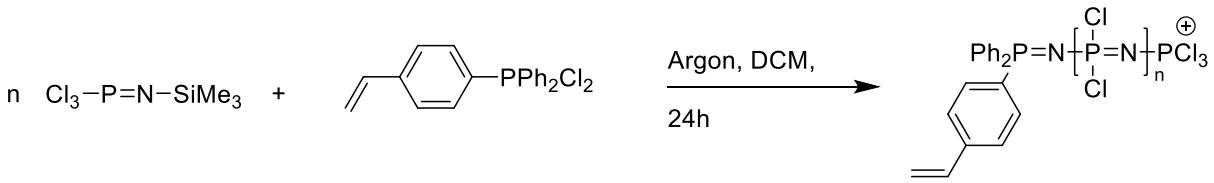

Figure 14: Synthesis of poly(dichloro)phosphazene with a diphenylstyrenephosphin end group.

For a poly(dichloro)phosphazene with 75 repeating units, 584 mg (75 eq; 2,601 mmol) of the monomer Cl_3-P=N-$SiMe_3$ were then dissolved in ~3 millilitres of DCM and added dropwise under stirring directly to the initiator solution. The polymerization reaction was continued for 24 h at room temperature and subsequently used for the macromolecular substitution reaction as described above.

3.2. Linker Synthesis

The NMR spectra for all the linkers with the respective repetitions can be found in the appendix.

3.2.1. Synthesis of L-Propargylglycine amide linker

The propargylglycine amide was prepared according to Madhu *et al.* [59].

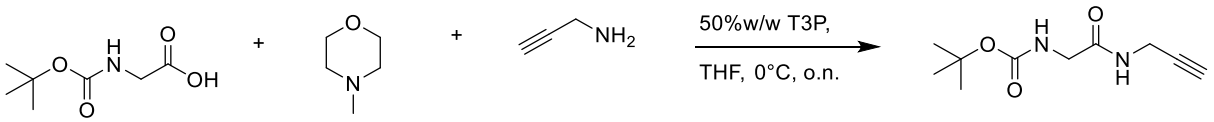

Figure 15. Synthesis of Boc protected propargylglycine.

2,5 g (1 eq, 14,27 mmol) of Boc-glycine-OH were dissolved in 40 ml of THF and cooled to 0 °C in an ice bath. 21,79 g 50% w/w T3P (2,4 eq; 34,25 mmol) in THF and 1,88 ml of 4-methylmorpholin (1,2 eq; 1,73 g, 17,12 mmol) were added, and the reaction was stirred for

10 minutes at 0 °C. Afterwards, the ice bath was removed, 1,09 ml of propargylamine (1 eq; 0,79 g; 14,27 mmol) were added slowly and the reaction was stirred overnight.
Subsequently, the solvent was evaporated and the product was purified by taking it up in 200 ml of EtOAc and washing it with 200 ml of a 10% w/w HCl solution, 200 ml of a 10% w/w solution of Na_2CO_3 and finally with 200 ml of Brine. The organic phase was collected, the solvent was evaporated under *vacuo*, and the product was further dried in the oven at 60°C.

Next, the Boc protection group was removed. To this end, 5 ml (4,5 eq; 65 mmol) TFA were added to the Boc-propargylglycine in 20 ml DCM. The reaction was stirred for 2 h at room temperature and the solvent was subsequently evaporated on the rotavapor. The product was purified by alternatingly solving in toluene and MeOH and evaporating the solvent in-between on the rotary evaporator completely to carry out residual TFA. After a white solid was obtained after evaporation, the product was dried under vacuum and further dried in the drying oven at 65°C overnight.
The reaction yielded 1,62 g (7,47 mmol, 52%) of a yellowish-brownish white solid.

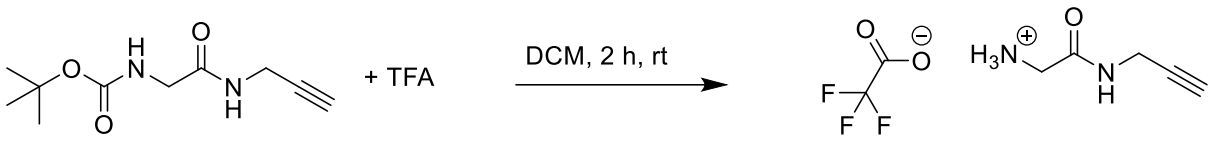

Figure 16: Deprotection of Boc-propargylamine with TFA.

Boc-propargylglycine amide:
^{1}H, 300 MHz, $CDCl_3$: δ= 4.07 (d, J= 5.4, 2.6 Hz, 2H), 3.82 (d, J=5.8 Hz, 2H), 2.23 (t, J=2.6 Hz, 1H), 1.44 (s, 9H) ppm.

Propargylglycine amide:
^{1}H, 300 MHz, DMSO-d6: δ= 3.95 (dd, J=5.5 Hz, 2.5 Hz, 2H), 3.56 (s, 2H), 3.19 (t, J=2.5 Hz, 1H) ppm.

3.2.2. Synthesis of L-Propargylglycine ester linker

The propargylglycine ester was prepared according to Rothemund *et al.* [60].

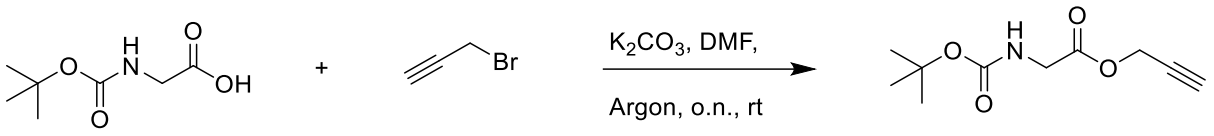

Figure 17: Synthesis of Boc protected propargylglycine ester.

First, 3 g of Boc-Glycine (1 eq; 17,25 mmol) and 2,89 g K_2CO_3 (1,14 eq, 19,67 mmol) were dissolved in 10 mass equivalents of DMF (60 ml). The mixture was put under argon, cooled in an ice bath, and 1,74 ml (1,14 eq; 2,32 g; 19,53 mmol) propargyl bromide were added slowly with a syringe under stirring. After the addition was completed, the ice bath was removed and the reaction was stirred over night at room temperature. For purification, the solid was filtered off and the filtrate was dried under vacuum. The intermediate was taken up in 50 ml of EtOAc, and washed 3 times with 50 ml brine each. The organic phase was then dried with $MgSO_4$, filtered, and dried on the rotary evaporator.

In the next step, deprotection was conducted directly. 3 g of Boc-propargylglycine ester (17,13 mmol; 1 eq) was dissolved in 5 ml of dioxane, put under argon atmosphere, and 10,7 ml (2,5 eq; 42,8 mmol) of 4 M HCl in dioxane was added. The reaction was stirred overnight. For purification, the solvent was evaporated and the solid residue was washed two times with 40 ml cold Et_2O and once with 300 ml of cold Et_2O and dried in the vacuum drying chamber.

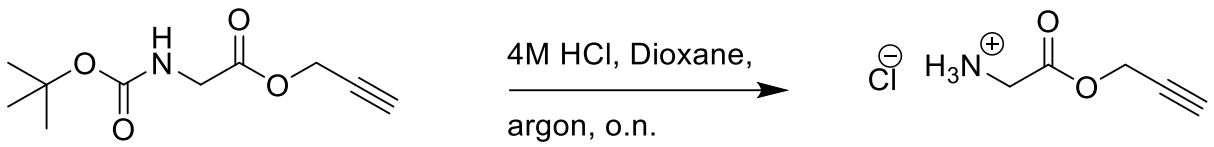

Figure 18: Deprotection of Boc-Propargylglycine ester with HCl.

The reaction yielded 1,3513 g (9 mmol; 52%) of a white to light brown solid.

Boc-propargylglycine ester:

^{1}H, 300 MHz, DMSO-d6: δ= 4.72 (d, J=2.4 Hz, 2H), 3.71 (d, J=6.1 Hz, 2H), 3.56 (t, J=2.4 Hz, 1H), 1.38 (s, 9H) ppm.

Propargylglycine ester:

^{1}H, 300 MHz, DMSO-d6: δ= 4.84 (d, J=2.5 Hz, 2H), 3.83 (s, 2H), 3.69 (t, J=2.4 Hz, 1H) ppm.

The Boc-propargylglycine ester was also deprotected with TFA according to 3.2.1., yielding 2,05 g (9,07 mmol; 53%) of a white to light brown solid.

Propargylglycine ester:
^{1}H, 300 MHz, DMSO-d6: δ= 4.73 (d, J=2.5 Hz, 2H), 3.72 (d, J=6.1 Hz, 2H), 3.56 (t, J=2.5 Hz, 1H), 1.39 (s, 9H) ppm.

^{1}H, 300 MHz, DMSO-d6: δ= 8.47 (s, 3H, -NH_3^+), 4.84 (d, J= 2.5 Hz, 2H), 3.88 (s, 2H), 3.66 (t, J= 2.4 Hz, 1H) ppm.

3.2.3. Synthesis ^{t}butyl(2-(2-(2-aminoethoxy)ethoxy)ethyl)carbamate linker

The synthesis was conducted according to Strasser *et al.* [53].

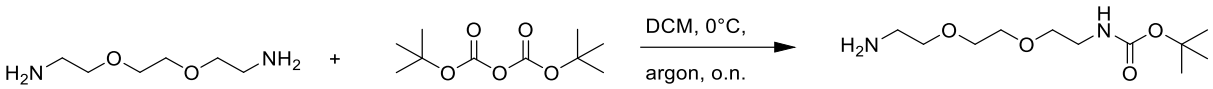

Figure 19: Synthesis of tbutyl(2-(2-(2-aminoethoxy)ethoxy)ethyl)carbamate.

First, 27 ml (1 eq; 27,41 g; 185 mmol) of 2,2'-(ethylendioxy)-bisethylamine were added into a 500 ml 3 neck round bottom flask. 200 ml of DCM were added under stirring, the mixture was put under argon and cooled with an ice bath. 4,01 g (0,1 eq; 18,37 mmol) of di-tertbutyl-dicarbonate was weighed in, dissolved in 200 ml DCM, put under Ar and added dropwise to the bisethylamine solution over the course of 5 hours. After complete addition, the ice bath was removed, and the reaction mixture was stirred overnight under argon.

For purification, the solution was transferred into a 1 neck round bottom flask, and DCM was removed under reduced pressure. The raw product was taken up in 150 ml of DCM and 150 ml dH_2O, and transferred into a separation funnel. The organic phase was then washed subsequently with 2x 100 ml dH_2O. The aqueous phases were combined, and extracted with 1x 150 ml DCM. Then, the organic phases were combined, and washed with 1x 100 ml Brine. The organic product phase was then dried with $MgSO_4$, filtered, and the solvent was evaporated on the rotary evaporator. For additional drying, the product was stored in the vacuum drying chamber at 60°C for one night, before storage under inert conditions in the glove box.

The reaction yielded 3,78 g (15,2 mmol; 83% yield) of a viscous, colourless liquid.

^{1}H, 300 MHz, $CDCl_3$: δ= 3.55 (s, 4H), 3.46 (m, 4H), 3.25 (q, J= 5.3 Hz, 2H), 2.82 (t, J=5.2 Hz, 2H), 1.48 (s, 2H), 1.37 (s, 9H) ppm.

3.2.4. Synthesis of β-Alanyl-Boc-hydrazide linker

The synthesis of β-alanyl-Boc-hydrazide was conducted according to Teasdale *et al.* [35].

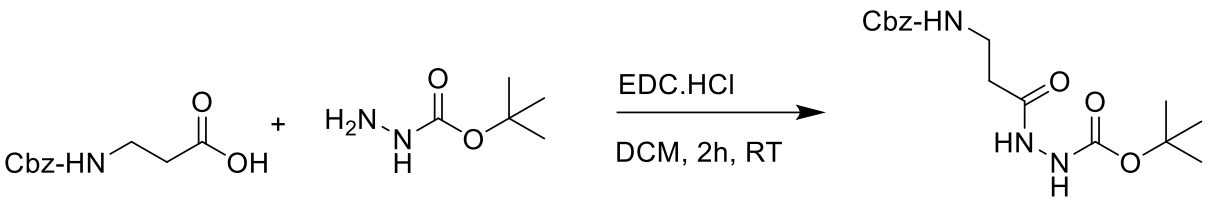

Figure 20: Synthesis of Z-β-alanyl-Boc-hydrazide.

First, Z- β-alanyl-Boc-hydrazide was synthesized. Thereto, 2,50 g (1 eq; 11,2 mmol) of Z-β-alanine-OH was weighed in a round bottom flask. 1,48 g (1 eq; 11,2 mmol) tert-butylcarbazate (Boc-hydrazide) was added, as well as 2,255 g (1,05 eq; 11,755 mmol) of *N*-(3-dimethylaminoprpyle)-N'-ethylcarbodiimide.HCl (EDC.HCl). The mixture was dissolved in 100 ml DCM, and stirred for 2 hours at room temperature.

For purification, the reaction mixture was washed with 100 ml of 0,1 M acetic acid, and the aqueous phase was extracted three times with 25 ml DCM each. The organic phases were combined, and washed with 2x 100 ml 0,1 M acetic acid, subsequently with 2x 100 ml saturated $NaHCO_3$ solution, and lastly with 100 ml dH_2O. The organic phase was dried with $MgSO_4$, filtered and the solvent was removed under reduced pressure.

The reaction yielded 3,39 g (10,05 mmol; 89%) of a white solid.

In the next step, the benzyl-carbonyl (Cbz) protection group had to be removed.

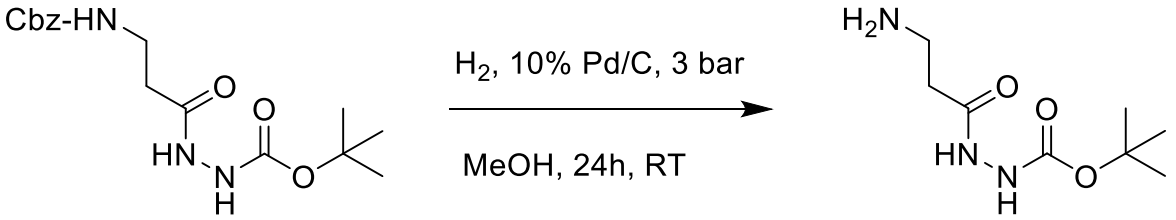

Figure 21: Deprotection of Z- β-alanyl-Boc-hydrazide.

For the deprotection, 3,39 g (10.05 mmol) of the Z- β-alanyl-Boc-hydrazide were weighed in and dissolved in 102 ml of MeOH. 203 mg of Pd/C were dissolved in roughly 2 millilitres of MeOH, and added carefully to the Z- β-alanyl-Boc-hydrazide. Subsequently, a hydrogenation reaction was conducted, at 3 bar pressure H_2 for 24 hours.
For purification, the mixture was then filtered through Celite, and the solvent was evaporated under *vacuo*.
The reaction yielded 1,6773 g (8,25 mmol; 82%) of a viscous, colourless liquid.

Z-β--alanyl-Boc hydrazide:
^{1}H, 300 MHz, DMSO-d6: δ= 7.33 (m, 5H), 5.00 (s, 2H), 3.20 (q, J=6.8 Hz , 2H), 2.27 (t, J=7.4 Hz, 2H), 1.38 (s, 9H) ppm.

β -alanyl-Boc hydrazide:
^{1}H, 300 MHz, $CDCl_3$: δ= 3.07 (t, J= 5.7 Hz, 2H), 2.43 (t, J=5.7 Hz, 2H), 1.45 (s, 9H) ppm.

3.3. Macromolecular Substitution

The macromolecular substitution reaction, also called macrosubstitution, was conducted using the poly(dichloro)phosphazene synthesized above and attaching one of the previously synthesized linkers. The macrosubstitution reactions always took place in the glove box under argon atmosphere, due to the lability of the poly(dichloro)phosphazene starting material when getting in contact with water. The procedure was adapted from Henke *et al.* [61]. The general reaction mechanism is shown in Figure 22.

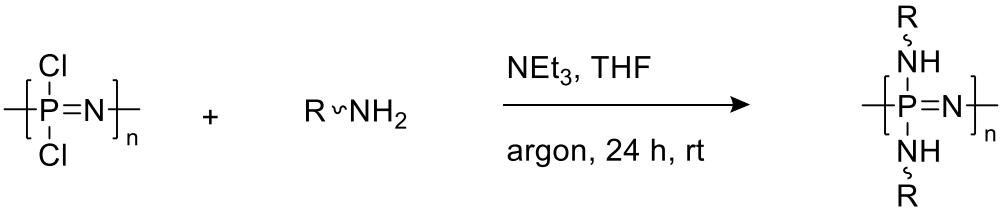

Figure 22: Macromolecular substitution reaction, exemplary shown for any linker R-NH_2.

The procedure described in the following, is the macrosubstitution of the ^{t}butyl(2-(2-(2-aminoethoxy)ethoxy)ethyl)carbamate linker onto the poly(dichloro)phosphazene [62]. The procedure was performed for each linker analogously.

The poly(dichloro)phosphazene solution in DCM, prepared according to Chapter 3.1, was directly reacted further in the glove box. 1,615 g (2,5 eq, 6,5025 mmol) of the ^{t}butyl(2-(2-(2-aminoethoxy)ethoxy)ethyl)carbamate linker were dissolved in ~30 millilitres of THF and 0,9026 ml of NEt_3 (2,5 eq; 0,658 g; 6,5025mmol) was solved in ~5 millilitres of THF as well and transferred to the linker. The synthesized poly(dichloro)phosphazene (2,601 mmol, 1 eq; 308 mg, n=75) was then added dropwise under stirring to the mixture, and the reaction was left in the glove box at room temperature, under stirring, for 24 hours. Afterwards, the mixture was taken out of the glove box, filtered through a paper filter and the solvent was evaporated. For purification, the product was dialysed against and EtOH with a molecular weight cut-off of 1 kDa for 24h. MilliQ® water was used as the medium for 1 hour, changing the medium every 15 minutes. Afterwards the medium was changed to EtOH, with regular changes of the medium. The reaction yielded 1,2835 g (2.36 mmol of repeating units; 91% yield) of a clear, slightly yellowish, soft solid.

The macrosubstitution reactions yielded different products, depending on the respective linker attached. NMR spectra for all of them, with repetitions conducted, can be found in the appendix.

PPz with propargylglycine amide linker:

The product was dialysed with a MWCO of 1 kDa and the reaction yielded 337 mg (0,98 mmol of repeating units, 22% yield) of an orange-brownish, medium soft solid.

^{1}H, 300 MHz, MeOD: δ= 4.06 (m, 2H), 3.69 (m, 2H), 2.64 (m, 1H) ppm.
^{31}P, 121.49 MHz, MeOD: δ= 3.00 ppm.

PPz with propargylglycine ester linker:

The product was dialysed with a MWCO of 1 kDa and the reaction yielded 295 mg (0,85 mmol of repeating units, 19% yield) of a waxy, yellowish-whiteish-brownish solid.

^{1}H, 300 MHz, DMSO-d6: δ= 4.69 (m, 2H), 3.69 (m, 2H), 3.44 (m, 1H) ppm.
^{31}P, 121.49 MHz, DMSO-d6: δ= 0.55 ppm.

PPz with ^{t}butyl(2-(2-(2-aminoethoxy)ethoxy)ethyl)carbamate linker:

The reaction yielded 1,2835 g (2.36 mmol per repeating unit; 91% yield) of a see-through, slightly yellowish, soft solid.

^{1}H, 300 MHz, $CDCl_3$: δ= 3.59 (m, 8H), 3.29 (m, 2H), 3.08 (m, 2H), 1.44 (s, 9H) ppm.
^{31}P, 121.49 MHz, $CDCl_3$: δ= 4.23 ppm.

3.4. Synthesis of PPz-g-pHPMA

For the synthesis of the novel PPz-co-pHPMA, different general procedures of a copper catalysed azide-alkyne-cycloaddition were used according to adapted literature [63–66]. The different procedures carried out can be found in the following. The different approaches are discussed in the chapter 'Results and Discussion'.

Procedure 1:

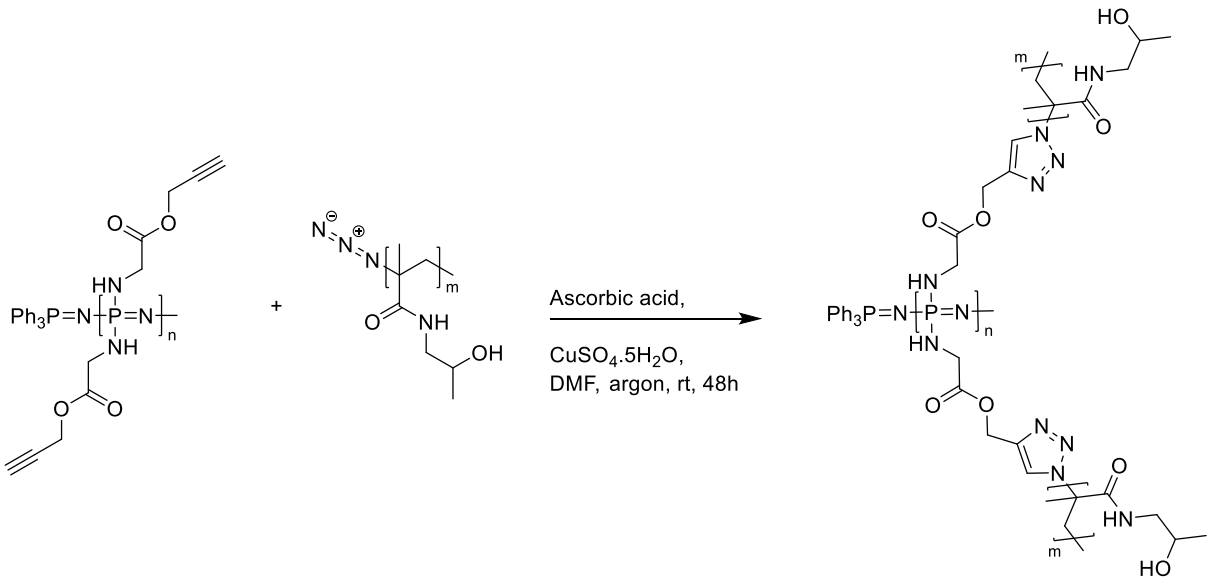

Figure 23: Synthesis of PPz-co-pHPMA via grafting to approach following Procedure 1 (via copper catalysed azide-alkyne cycloaddition).

The first approach was conducted following an adapted procedure of Fokin and Sharpless *et al.* [63].

The reaction was conducted by weighing in 1 eq of the PPz bearing the propargylglycine ester linker (0,83 g; 2,78 mmol), and 20 mg of pHPMA (ICP-IT-4; 0,2 eq; 0,56mmol). Then, 1 ml of a sodium-L-ascorbate solution (c= 1,66 mg.ml^{-1}; 0,003 eq; 0,0084 mmol) and 1 ml of a $CuSO_4.5H_2O$ solution (c= 1,04 mg.ml^{-1}; 0,0015 eq; 0,00417mmol) were added. The solvent for all stock solutions was a 50:50% v/v mixture of H_2O and EtOH. The reaction was then stirred for two days at room temperature. For purification, dialysis was conducted for 24 hours in EtOH using a 3.5 kDa MWCO. The solvent was subsequently evaporated and the product was stored under argon.

Procedure 2:

The second approach was conducted according to adapted literature [67].
First, 20,7 mg of a PPz with a propargylglycine ester linker was weighed in (1 eq; 0,0769 mmol). 1,44 mg $CuSO_4.5H_2O$ in dry DMF was added *via* adding 1 ml of a 10x stock solution (c=1,44 $mg.ml^{-1}$) to the PPz (0,075 eq; 5,77 µmol). 3,38 mg of anhydrous ascorbic acid in dry DMF was also added *via* a stock solution (c= 3,38 $mg.ml^{-1}$) to the PPz (0,29 eq; 22,03 µmol). The solution was stirred at room temperature, and put under an inert argon atmosphere. 30,7 mg of the pHPMA were weighed in (ICP-IT-4; 0,05 eq; 0,003845 mmol), dissolved in 1ml of dry DMF, and added to the PPz mixture.
The solution was stirred for 2 days under inert conditions at room temperature.
For purification, the raw product was dialysed with a MWCO of 3.5 kDa for 1,5 hours against MilliQ water, and further 23 hours against EtOH, with regular changes of the medium. The solvent was subsequently evaporated and the product was stored under argon.

Procedure 3:

For the third approach, the synthesis was conducted according to **Procedure 2**. Only the pHPMA was changed, from ICP-IT-4 to ICP-IT-6, changing the molecular weight of around 35900 $g.mol^{-1}$ to around 8000 $g.mol^{-1}$.

Procedure 4:

For the fourth approach, the synthesis was conducted according to **Procedure 3**. Only the reaction temperature was changed from room temperature to 5°C.

Procedure 5:

This approach number 5 investigated the influence of the Cu-species on the conversion, directly employing $Cu^{(I)}$ to see if problems with the reduction of the $Cu^{(II)}$ species might lead to a decrease in conversion. **Procedure 5** was adapted from Androvič et *al.* [64].
20,7 mg PPz with propargylglycine ester (1 eq; 0,0769 mmol) were weighed in and dissolved in 207 µl DMAc. 61,5mg pHPMA (ICP-IT-6; 0,1 eq; 0,00769mmol) were weighed in as well, dissolved in 605 µl DMAc, and added to the PPz solution. The mixture was degassed with argon, and left under an argon atmosphere. A catalytic amount of $Cu^{(I)}Br$ (2,7 mg) was added, and the reaction was stirred for 24 hours at room temperature under argon. For purification,

the mixture was then precipitated in 150 ml of cold Et_2O, and centrifugated for 10 minutes at 4000 rpm. After drying, the product was stored under argon.

Procedure 6:

Procedure 6 was conducted analogously to **Procedure 2**, changing the PPz bearing propargyl glycine ester to a PPz bearing a propargyl valine ester. Briefly, 20,7 mg of a PPz with a propargylvaline ester linker was weighed in (1 eq; 0,0769 mmol). 1,44 mg $CuSO_4.5H_2O$ in dry DMF was added *via* a stock solution to the PPz (0,075 eq; 5,77 µmol). 3.38 mg of anhydrous ascorbic acid in dry DMF was also added *via* a stock solution to the PPz (0,29 eq; 22,03 µmol). The solution was stirred at room temperature, and put under an inert argon atmosphere. 30,7 mg of the pHPMA were weighed in (ICP-IT-6; 0,05 eq; 0,003845 mmol), dissolved in 1ml of dry DMF, and added to the PPz mixture.
The solution was stirred for 2 days under inert conditions at room temperature.
For purification, the raw product was dialysed with a MWCO of 3.5 kDa for 1,5 hours against MilliQ water, and further 23 hours against EtOH, with regular changes of the medium. The solvent was subsequently evaporated and the product was stored under argon.

Procedure 7:

Procedure 7 was conducted analogously to **Procedure 5**, changing the PPz bearing propargyl glycine ester to a PPz bearing a propargyl valine ester and including TBTA as additional catalyst, to improve conversion of the CuAAC, as suggested in literature [65]. 20,7 mg PPz with propargylvaline ester (1 eq; 0,0769 mmol) were weighed in and dissolved in 207 µl DMAc. 61,5mg pHPMA (ICP-IT-6; 0,1 eq; 0,00769mmol) were weighed in as well, dissolved in 605 µl DMAc, and added to the PPz solution. The mixture was degassed with argon, and left under an argon atmosphere. Finally, catalytic amounts of $Cu^{(I)}Br$ (2,7 mg) and TBTA (4,1 mg) were added, and the reaction was stirred for 24 hours at room temperature under argon. For purification, the mixture was then precipitated in 150 ml of cold Et_2O, and centrifugated for 10 minutes at 4000 rpm. After drying, the product was stored under argon.

3.5. Synthesis of PPz-co-PGA

The synthesis of the copolymer of polyorganophosphazene with poly-α-L-glutamic acid was conducted according to Strasser *et al.* [53] and Baumgartner *et al.* [54]. Here, the polyorganophosphazene with the attached ^{t}butyl(2-(2-(2-aminoethoxy)ethoxy)ethyl)carbamate linker was used. In the first step, the Boc-protected linker on the PPz had to be deprotected, forming the macroinitiator.

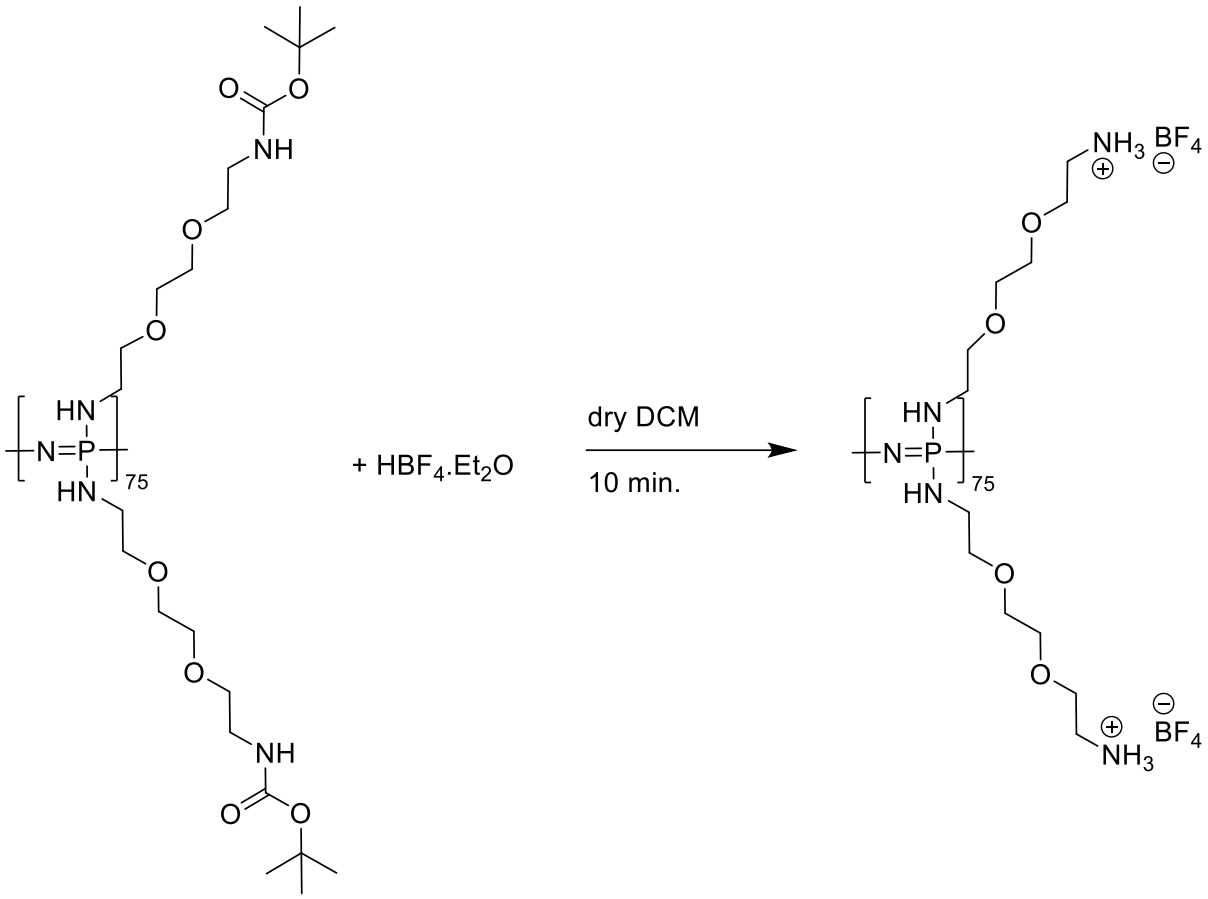

Figure 24: Deprotection of PPz with carbamate linker.

Thereto, 304 mg of the polymer (1 eq; 0,564mmol) was weighed in, dissolved in 50 ml anhydrous DCM, and 460 µl (6 eq; 3,3847 mmol) of $HBF_4.Et_2O$ was added under vigorous stirring, very slowly. After the addition was completed, the mixture was stirred further for 10 minutes, and the precipitate was filtered with a paper filter. It was washed 5x with 50 ml cold Et_2O each, and subsequently resolved with MeOH. The MeOH was evaporated on a rotary evaporator, and the product was further dried in the vacuum drying oven.
The reaction yielded 207,1 mg (0,40 mmol; 70%) of a white, lightly brownish, sticky solid.

In the next step, the poly-benzyl-L-glutamic acid was grafted from the linker, using the $-NH_3^+$ / BF_4^- salt group as macroinitiator.

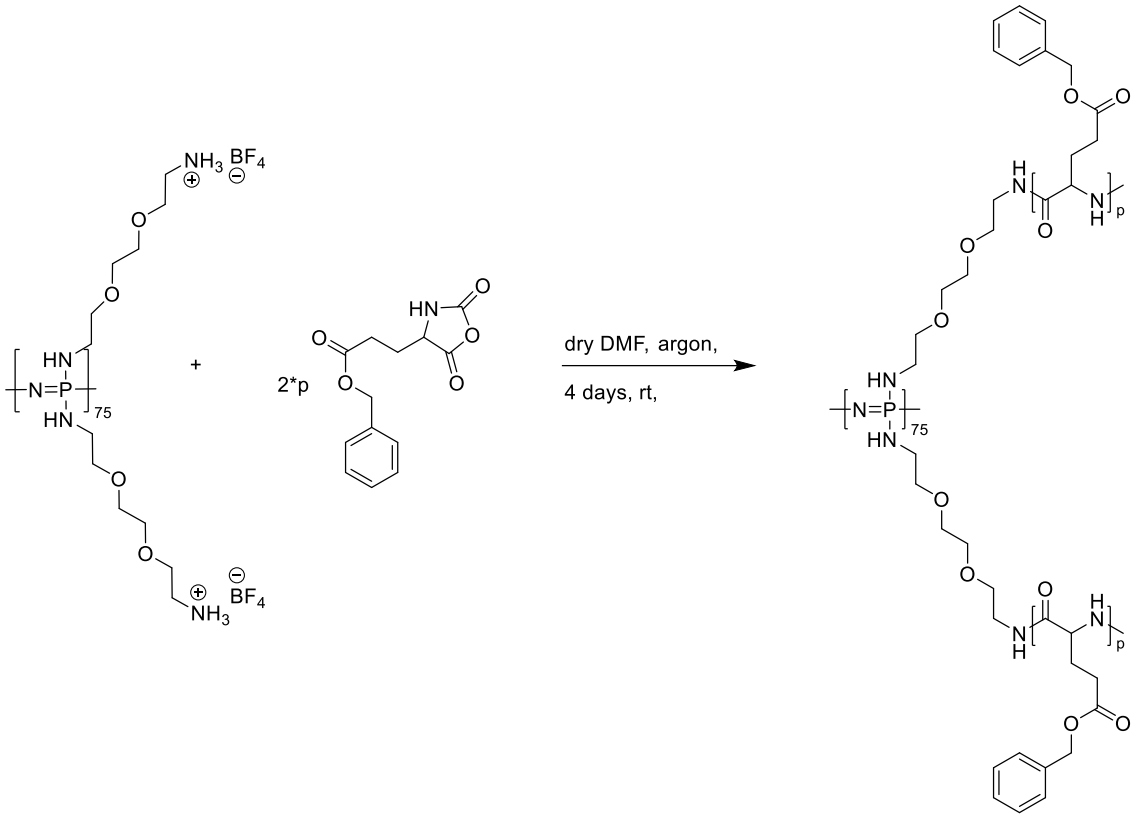

Figure 25: Synthesis of benzyl-protected PPz-Co-PGA, via a 'grafting from' approach.

First, 30.5 mg (1 eq; 0,0592 mmol) of the deprotected PPz were weighed in and transferred into the glove box. 1,64 g of 5-Benzyl-L-glutamate-*N*-carboxyanhydride (NCA) (100 eq; 5,92mmol, p=50 per chain) were weighed in a vial, dissolved in 15,5 ml dry DMF (0,38 mol.l^{-1} NCA solution), and subsequently added to the PPz. The mixture was vortexed, and then stirred for 4 days in the glove box under argon. The copolymer was then precipitated in Et_2O, ten times the volume of DMF used (155 ml Et_2O), and centrifuged at 4000 rpm for 10 minutes and the solvent was decanted off.
Drying at room temperature in the fume hood yielded 644 mg (0,0288 mmol; 48%) of a clear, soft solid.

Finally, the PPz-Co-PGA had to be deprotected.

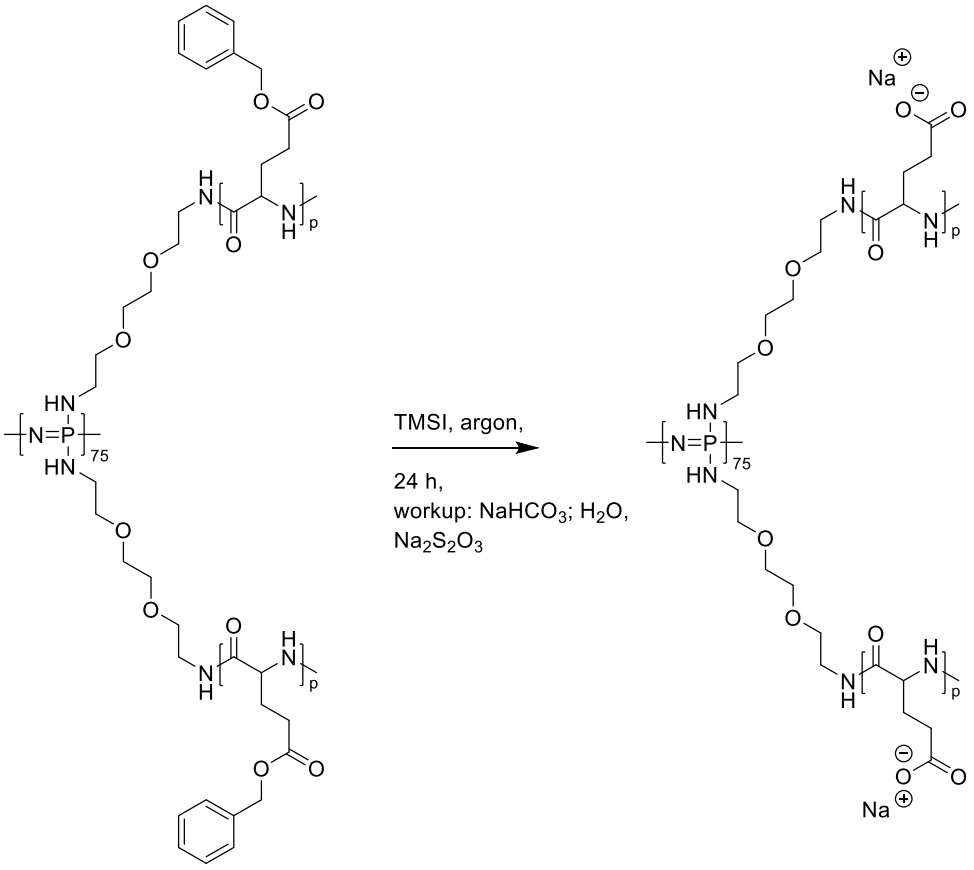

Figure 26: Deprotection of the benzyl-protected PPz-co-PGA.

Thereto, 300 mg of the benzyl-protected PPz-Co-PGA (1 eq; 1,379 mmol of repeating units) was weighed in, transferred into the glove box and dissolved in 5 ml of anhydrous DCM. Per equivalent of PGA repeating unit 6 equivalents of TMSI (1,18 ml; 8,279 mmol) were added dropwise. The reaction was stirred for 24 hours at room temperature in the glove box. Then, the mixture was transferred out of the glove box and the solvent was evaporated. The residue was taken up in 5 ml of saturated $NaHCO_3$, and 5 ml of MilliQ water. Minimal amounts of $Na_2S_2O_3$ were added until the solution turned from brownish to white and the reaction was stirred for 24 hours at room temperature.

For purification, the product was washed with 3x 5 ml cold Et_2O. Then, the product was dialyzed for 48 hours against MilliQ water with a MWCO of 3.5 kDa. The product was freeze dried, yielding 161 mg (0,01043 mmol; 80% yield) of a white, cloudy, fluffy PPz-co-PGA.

Benzyl-protected PPz-co-PGA:

^{1}H, 300 MHz, DMSO-d6: δ= 7.26 (m, 5H), 5.08 (m, 2H), 2.84 (m, 1H), 2.49 (m, 4H) ppm.

^{31}P, 121.49 MHz, DMSO-d6: δ= n.a.

PPz-co-PGA:
^{1}H, 300 MHz, D_2O: δ= 4.29 (s, 1H), 2.24 (d, J=7.4 Hz, 2H), 1.95 (m, 2H) ppm.
^{31}P, 121.49 MHz, D_2O: δ= n.a.

3.6. Loading of peptide drug onto PPz-co-PGA

The loading of the novel peptide drug was conducted based on the general procedure described by Baumgartner *et al.* and slightly adapted [54].

Procedure 1:

First, 40 mg (1 eq; 0,264 mmol of repeating units) of the PPz-co-PGA was weighed in and dissolved in 4 ml of MilliQ water (c=10 mg.ml^{-1}). Next, 10,4 mg of EDC.HCl (0,2 eq; 0,053 mmol) was dissolved in 104 µl of MilliQ water (c= 100 mg.ml^{-1}), as well as 6,2 mg of N-Hydroxysuccinimide (NHS) in 62 µl of MilliQ water (0,2 eq; 0,053 mmol, c= 100 mg.ml^{-1}), and both solutions were added to the copolymer. 417 µl of MES buffer (1M, 10x) was added, and the reaction was incubated under stirring for 15 minutes at room temperature. Meanwhile, 1,6 mg of DMAP (0,05 eq; 0,013 mmol) was dissolved in 33 µl of DMF (c= 50 mg.ml^{-1}), and 20 mg of the peptide drug (0,05 eq; 0,013 mmol) was dissolved in 2 ml of DMF (c= 10 mg.ml^{-1}). The DMF solutions were added to the reaction solution, followed by 620 µl of a 10x PBS buffer. The reaction was stirred for 2 days at room temperature.
For purification, the product was dialysed against MilliQ for 1 hour, followed by EtOH for 24 hours with a MWCO of 3.5 kDa. Afterwards, the product was further purified by ultrafiltration with a molecular weight cut off of 6-8 kDa.

Procedure 2:

Procedure 2 was conducted analogously to **Procedure 1**, except solving the peptide drug in MilliQ water instead of DMF. Furthermore, the order of addition was altered, adding the 10x PBS buffer ahead of the peptide solution.

Procedure 3:

First, 200 mg of the benzyl-protected PPz-co-PGA were weighed in (1 eq; 0,00894 mmol). The polymer was then transferred into the glove box and dissolved in 0.2 ml of dry DMF. 1 mg of Cy5 was weighed in (0,17 eq., 0,0015 mmol, 5 wt% loading) and added to the polymer solution

with 2 times 0.5 ml dry DMF each. The mixture was stirred for 24 hours in the glove box at room temperature, in the dark. Afterwards, the solution was precipitated in 50 ml cold Et_2O, and centrifuged for 10minutes at 4000 rpm. The precipitate was dried in the dark, and the benzyl-deprotection was conducted according to Chapter 3.5. Finally, the peptide drug was conjugated onto the Cy5-labelled PPz-co-PGA carrier. To this end, 40 mg (1 eq; 0,264 mmol of repeating units) of the PPz-co-PGA was weighed in and dissolved in 4 ml of MilliQ water (c=10 $mg.ml^{-1}$). Next, 10,4 mg of EDC.HCl (0,2 eq; 0,053 mmol) was dissolved in 104 µl of MilliQ water (c= 100 $mg.ml^{-1}$), as well as 6,2 mg of N-hydroxysuccinimide (NHS) in 62 µl of MilliQ water (0,2 eq; 0,053 mmol, c= 100 $mg.ml^{-1}$), and both solutions were added to the copolymer. 417 µl of MES buffer (1M, 10x) was added, and the reaction was incubated under stirring for 15 minutes at room temperature. 20 mg of the peptide drug (0,05 eq; 0,013 mmol) was dissolved in 2 ml of MilliQ water (c= 10 $mg.ml^{-1}$) and added to the reaction solution. The reaction was then stirred for 2 days at room temperature.

For purification, the product was dialysed against MilliQ for 1 hour, followed by EtOH for 24 hours with a MWCO of 3.5 kDa. Afterwards, the product was further purified by ultrafiltration with a molecular weight cut off of 6-8 kDa.

3.7. PPz-co-PGA with hydrazide linker

The functionalization of the PPz-co-PGA with the prepared hydrazide linker was conducted according to Baumgartner *et al.* [54].

Procedure 1:

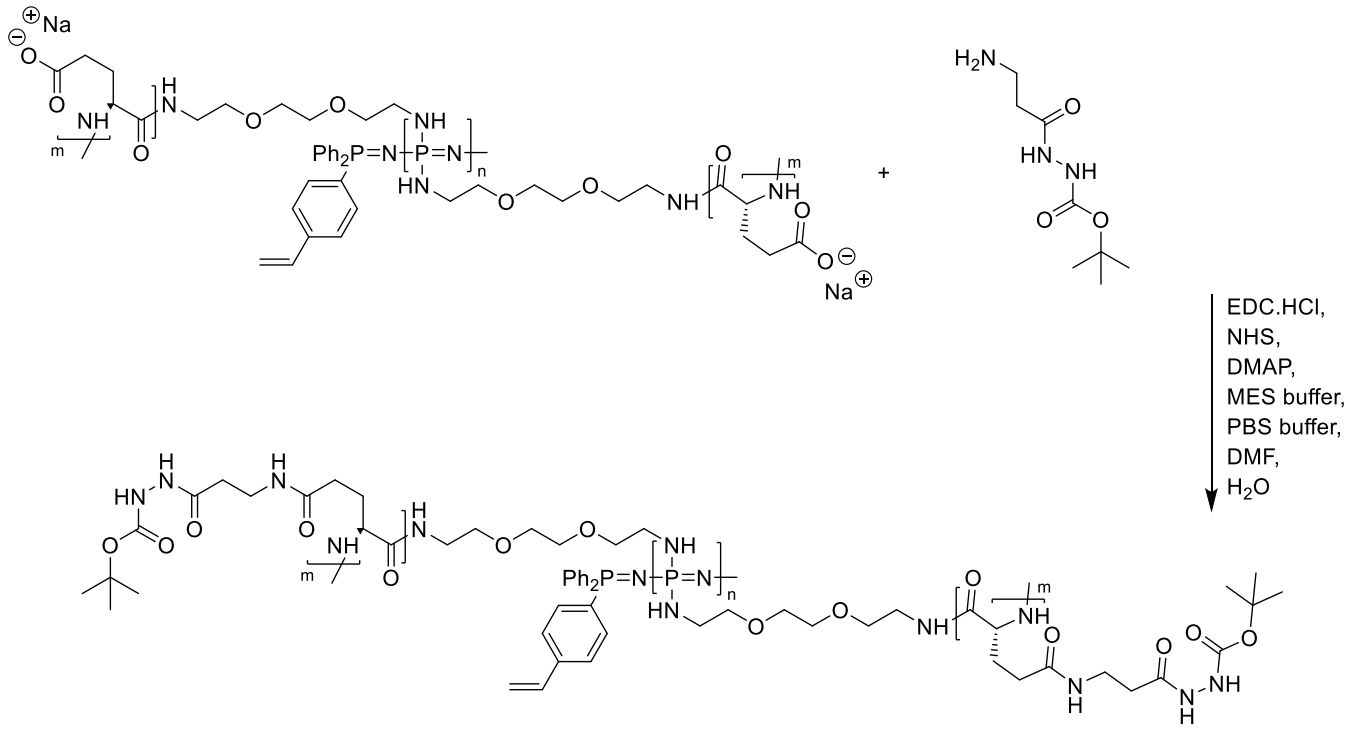

Figure 27: Synthesis of a PPz-co-PGA bearing a hydrazide linker according to Procedure 1.

50 mg of the PPz-co-PGA (1 eq; 0,33 mmol of repeating units) was dissolved in 5 ml MilliQ water. 12,9 mg EDC.HCl (0,2 eq; 0,066 mmol) was dissolved in 129 µl MilliQ water and 7,8 mg NHS in 78 µl MilliQ, and each was added to the polymer solution. 520 µl 1M MES buffer (10x) was subsequently added and the solution was incubated for 15 minutes at room temperature while stirred. Then, 2 mg of DMAP (0,05 eq; 0,017 mmol) in 40 µl DMF, and 33,6 mg of the hydrazide linker (0,5 eq for 50% loading; 0,165 mmol) were added, as well as 775 µl of a 10x PBS buffer. The reaction was stirred for 48 hours at room temperature.

For purification, dialysis was performed for 24 hours against EtOH with 6-8 kDa MWCO. Additionally, ultrafiltration was performed, with a MWCO of 30 kDa. The polymer was subsequently freeze dried and stored under argon.

Procedure 2:

Procedure 2 was conducted analogously to **Procedure 1**, except a Cy5-labelled PPz-co-PGA. was used as described in Chapter 3.6.

4. Results and discussion

4.1. Results for PPz-co-pHPMA

CuAAC reactions were investigated for the preparation of bottlebrush copolymers based on a PPz backbone and pHPMA side chains. To this end, different reaction conditions were screened and evaluated based on gel permeation chromatography and nuclear magnetic resonance spectroscopy. In detail, the reaction conversion was estimated based on GPC measurements and the area under the curve of the respective polymer signals in the RI detector trace, correlating to their concentration.

Procedure 1:

The first procedure was conducted according to Fokin et al. [55], with a 50% v/v mixture of EtOH and MilliQ water as solvent, $CuSO_4$ as catalytic species and sodium ascorbate as reducing agent. This commonly used procedure appears to support the copper acetylides in the reactive state in aqueous solutions [55]. For the in situ reduction of Cu(I) to Cu(II), sodium ascorbate was used due to a preferable reducing power compared to ascorbic acid [66]. The success of the cycloaddition was confirmed by GPC measurements (Figure 28), in which the formation of PPz-co- pHPMA polymer can be seen in peak ‘A’, clearly distinct from the signals of the pure PPz and pHPMA constituents. Nevertheless, a second peak ‘B’ indicates the presence of unreacted pHPMA in the mixture, overlapping with the signal of pure pHPMA.

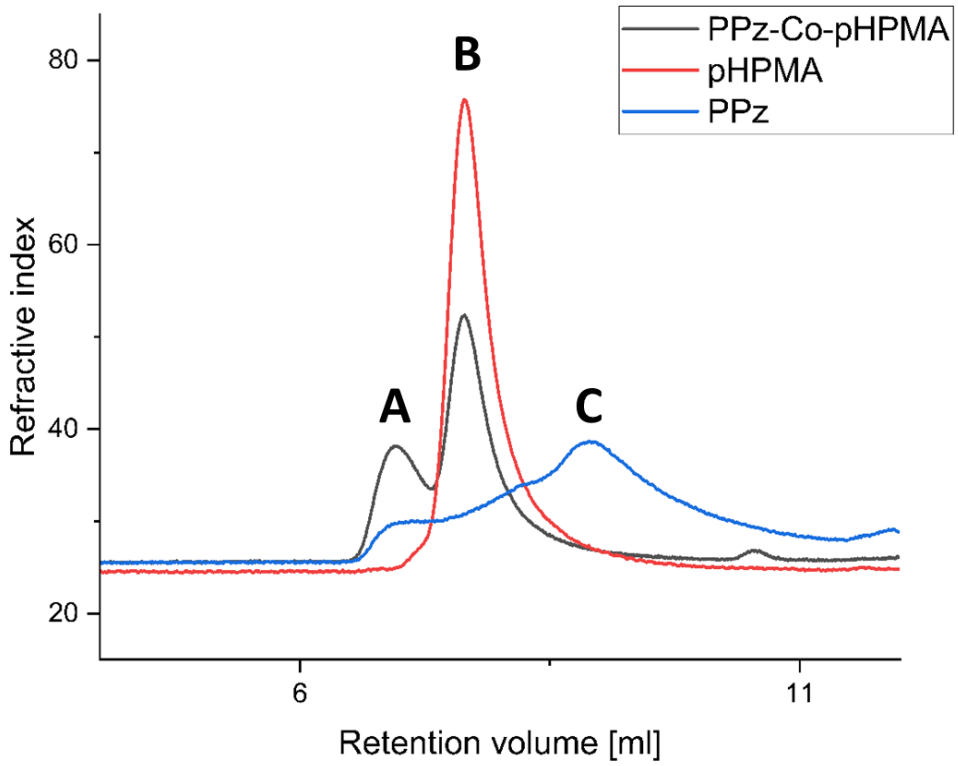

Figure 28: GPC measurement in DMF of PPz-Co-pHPMA, reacted in EtOH/H2O at rt for 2 days, using sodium ascorbate and $CuSO_4.5H_2O$ (Procedure 1).

Based on the areas under the curve for the two signals, a conversion of 30% could be calculated for **Procedure 1**, Table 1. Although a successful bottlebrush formation was achieved with **Procedure 1**, the low conversion warranted further screening of the reaction conditions to increase the conversion and avert complicated purification of the product mixture.

Table 1: GPC data for the CuAAc in EtOH / H_2O at room temperature (Procedure 1)

Peak	Đ	M_w [Da]	RI (Area)
A	1.48	208 517	6.55
B	1.09	28 993	15.53
A+B	2.39	83 728	22.22

Procedure 2:

In the second approach, the solvent was changed to DMF and the reducing agent to ascorbic acid, Figure 29 Again, a clear formation of the bottlebrush co-polymer could be seen based on the GPC measurements, Figure 29. A shift to a lower retention volume and hence higher molecular weight compared to pure pHPMA is apparent, and an increase in the reaction conversion can be already estimated.

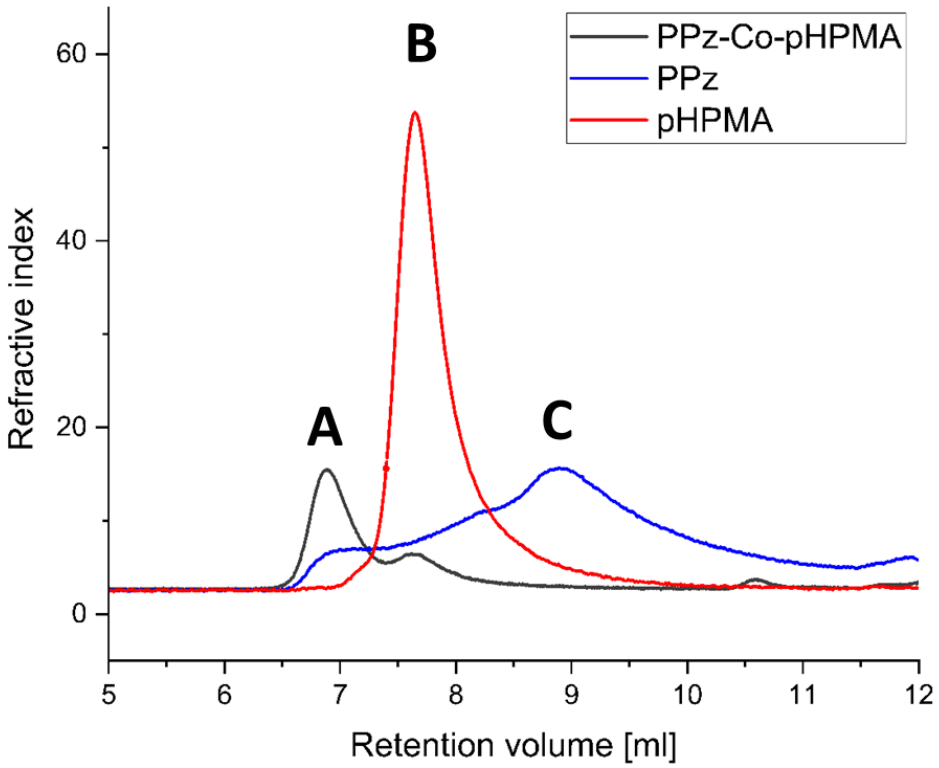

Figure 29: GPC measurement in DMF of PPz-Co-pHPMA, reacted in DMF at rt under argon for 2 days, using ascorbic acid and $CuSO_4.5H_2O$.

Detailed analysis of the areas under the curve of peaks A and B, the formed PPz-co-pHPMA and unreacted pHPMA, respectively, shows a conversion of about 81%, Table 2. Providing an increase by a factor greater than 2 compared to **Procedure 1**. The dispersity of the copolymer equals the dispersity of the first approach (1.48).

Table 2: GPC data for the CuAAc of PPz and pHPMA according to Procedure 2.

Peak	Đ	M_w [Da]	RI (Area)
A	1.48	215169	6.05
B	1.04	38569	1.56
A+B	2.02	187545	7.44

Since the pHPMA batch used employed rather high molecular weights (around 36000 $g.mol^{-1}$) an influence of the molecular weight of the side chains could not be excluded. Therefore, the reaction was repeated with a pHPMA of lower molecular weight (ICP-IT-6, $M_n \approx 8000$ $g.mol^{-1}$). The procedure followed **Procedure 3,** described in the experimental chapter (3.4).

Procedure 3:

The results for **Procedure 3**, employing a pHPMA of decreased molecular weight, can be found in Figure 30. The rise of peak ‘A’ in the chromatogram indicates the formation of the triazole coupled PPz-g-pHPMA. Nevertheless, a clear peak for unreacted pHPMA, peak ‘B’ can be seen as well.

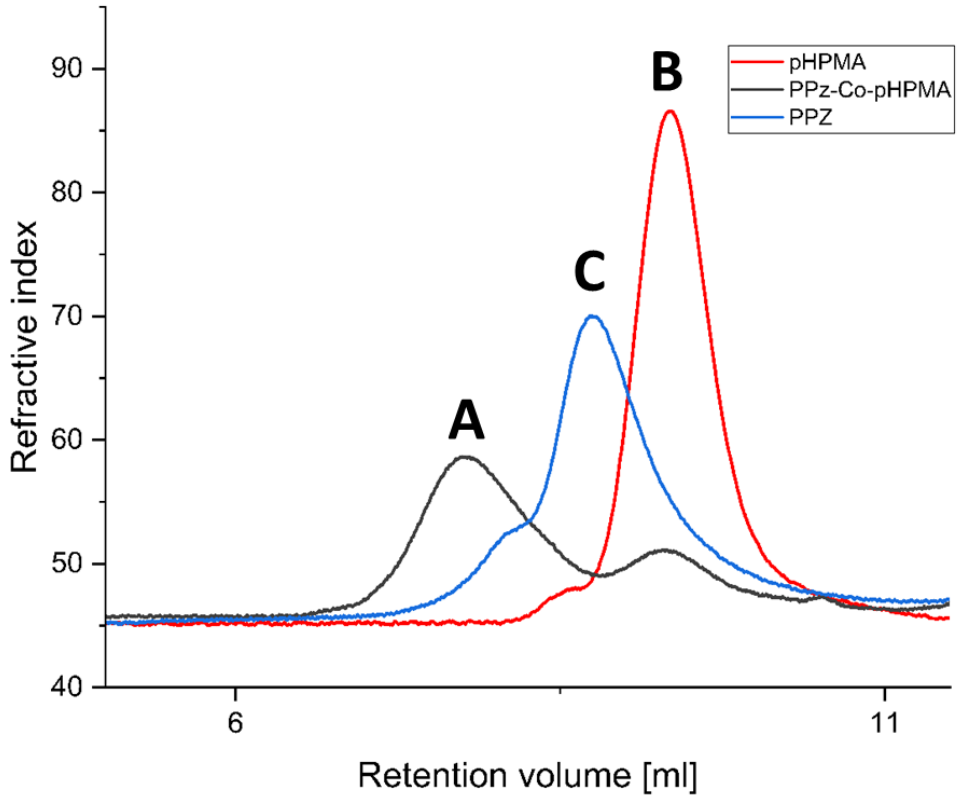

Figure 30: GPC measurement in DMF of PPz-Co-pHPMA, reacted in DMF at rt under argon for 2 days, using ascorbic acid and $CuSO_4.5H_2O$

The GPC data of **Procedure 3** is summarized in Table 3. A conversion of 75% was calculated from the peak area ratios of the product PPz-g-pHPMA and the unreacted pHPMA. The dispersity of the conjugated PPz-co-pHPMA is consistent with the dispersities for both previous approaches with Đ = 1.48.

Table 3: GPC data for the CuAAc in DMF at room temperature (Procedure 3)

Peak	Đ	M_w [Da]	RI (Area)
A	1.48	128.926	14.26
B	1.49	15.518	4.63
A+B	3.34	111.488	19.50

The NMR spectra of the polymer prepared by **Procedure 3** can be found in Figure 31 and Figure 32. Although it was not possible to determine the reaction conversion based on the NMR data, the signals could be correctly assigned to the expected structure with the

predominant pHPMA signals, exhibiting the expected ratio of 1:2:2:6. Due to the lower concentration of the PPz backbone in the copolymer, no signals could be clearly assigned in the ^{1}H NMR spectrum. Nevertheless the presence of PPz was confirmed by the ^{31}P NMR spectrum *via* the presence of the characteristic backbone signals of polyphosphazenes at around 1 ppm [68].

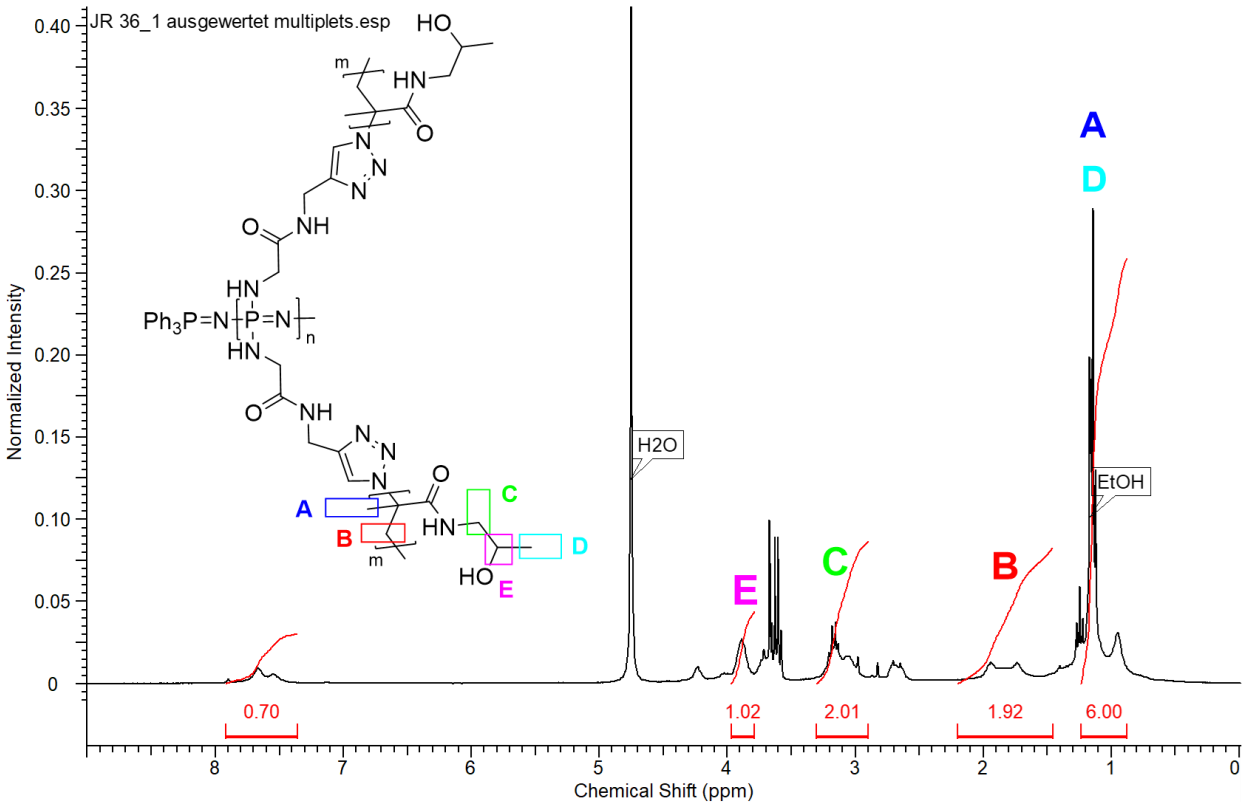

Figure 31: ^{1}H NMR of PPz-Co-pHPMA in D_2O, reacted in DMF at rt under argon for 2 days, using ascorbic acid and $CuSO_4.5H_2O$ (Procedure 3).

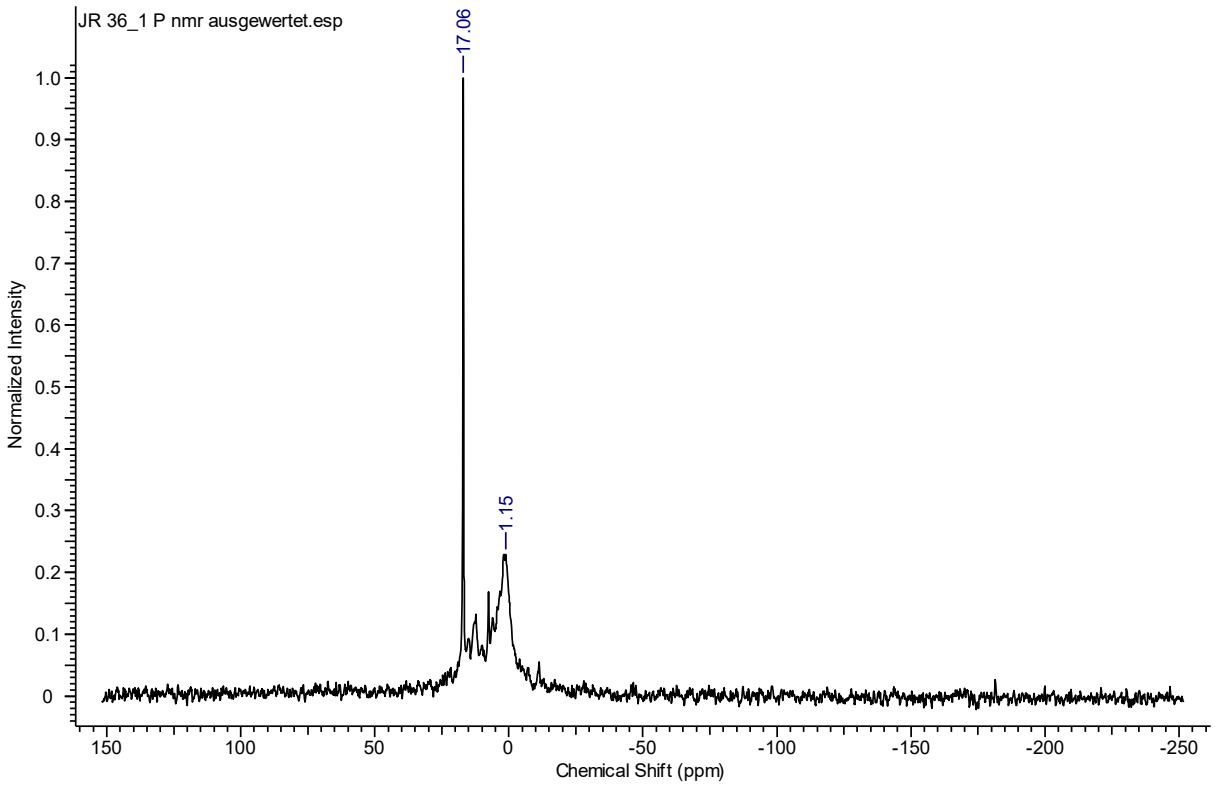

Figure 32: ^{31}P NMR spectrum of PPz-co-pHPMA, reacted in D_2O at rt under argon for 2 days, using ascorbic acid and $CuSO_4.5H_2O$ (Procedure 3).

^{1}H, 300 MHz, D_2O: δ= 7.63 (m, 1H, -OH), 3.89 (s, 1H, -CH), 3.16 (m, 2H, side chain -CH_2), 1.85 (m, 2H, main chain -CH_2), 1.10 (m, 6H, main + side chain -CH_3) ppm.
^{31}P, 121.49 MHz, D_2O: δ= 17.06, 1.15 ppm.

The peaks for the pHPMA are clearly detected, as mentioned above, and assigned to the structure. The ^{31}P NMR additionally confirms that the phosphorus from the backbone is detected and PPz is not degraded, as the shift is showing the characteristic peak of glycine substituted PPz at around 1 ppm [68].
For comparison, the GPC measurements of the PPz-g-pHPMA bottlebrush polymers bearing sidechain pHPMA of higher and lower molecular weight are shown in Figure 33.

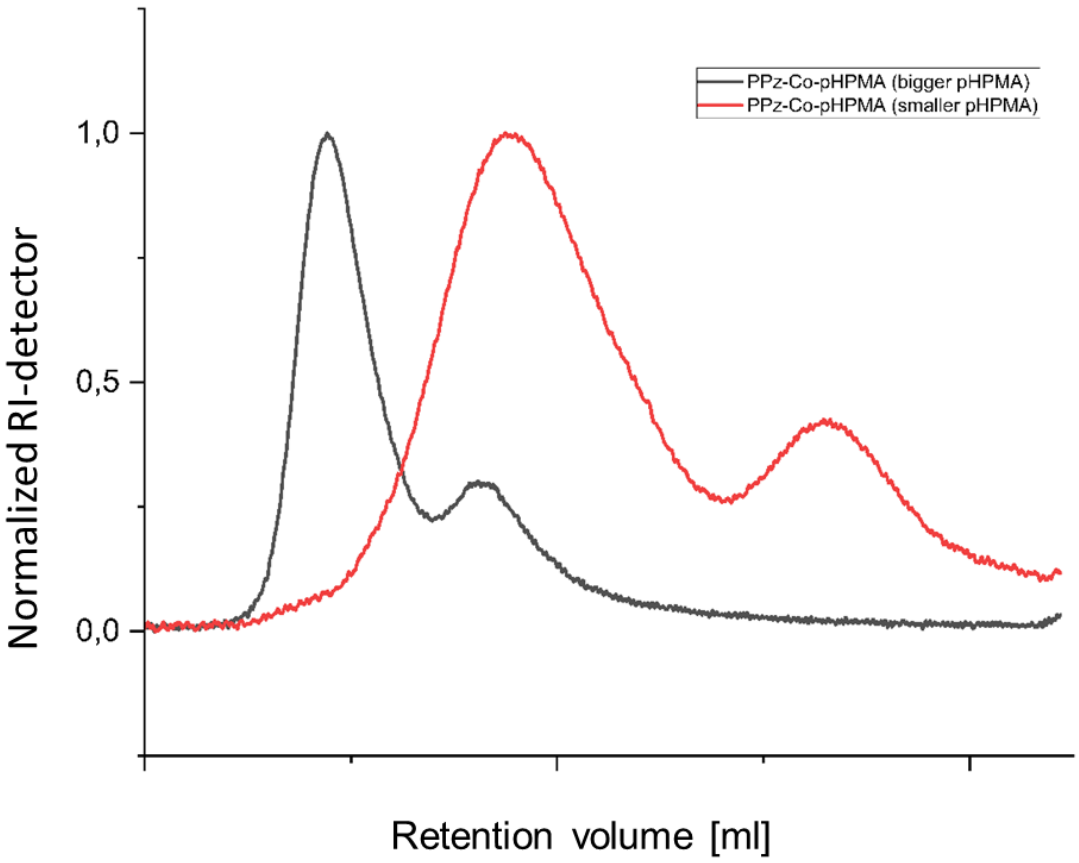

Figure 33: Comparison of the GPC measurements in DMF of PPz-co-pHPMA with pHPMA of Mn = 39000 Da (grey) and of Mn = 8000 Da (red).

As expected, a shift in the x-direction can be observed, based on the different M_w of the pHPMA side chains. The content of unreacted pHPMA is slightly lower for the copolymer bearing the pHPMA with an M_n = 39000 Da. When comparing directly the conversions of **Procedure 2** and **Procedure 3**, a marginally higher conversions of 80% compared to 75% could be calculated for the larger pHPMA, confirming the suitability of the approach for pHPMA of a broad range of different M_n.

Procedure 4:

To investigate the influence of the reaction temperature on the reaction conversion and possibly the dispersity, the reaction temperature was reduced to 5°C according to **Procedure 4**. The results are depicted in Figure 34, alongside the results from the most successful procedure, **Procedure 2,** as reference.

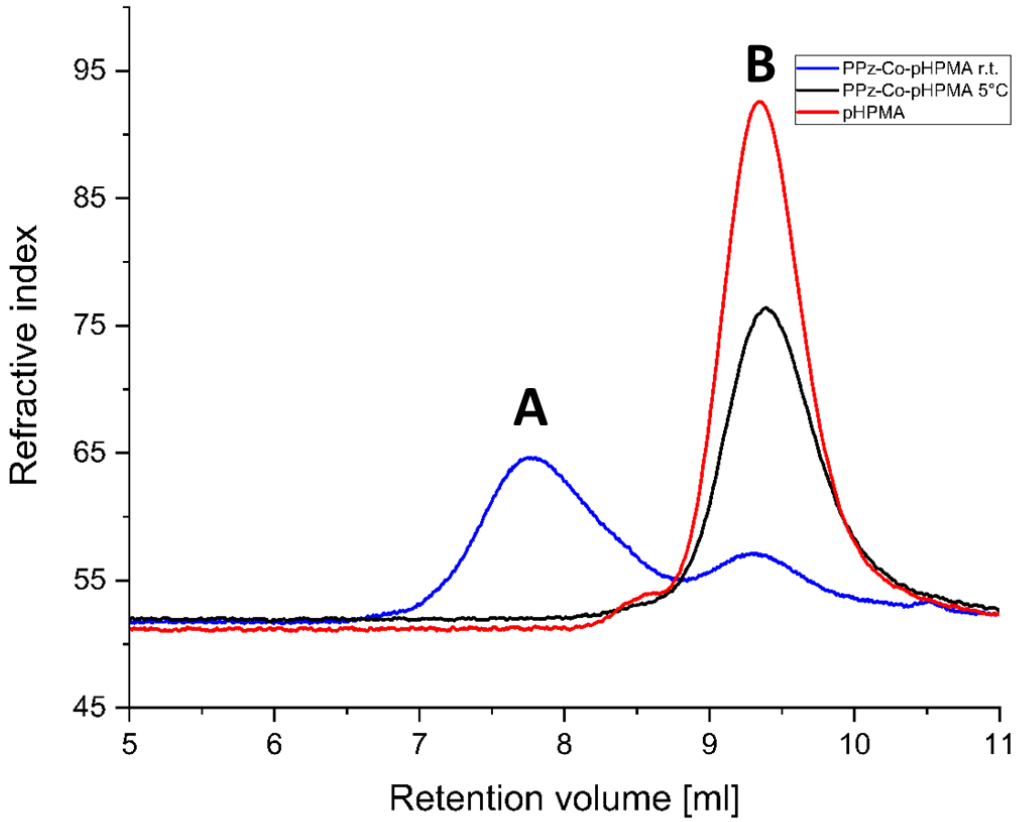

Figure 34: GPC measurement in DMF of PPz-co-pHPMA, reacted in DMF, using $CuSO_4.5H_2O$ and ascorbic acid, for 2 days under argon and 5°C (Procedure 4).

As can be clearly seen, the reaction at lower temperatures did not bring any improvement on the reaction conversion. On the contrary, no formation of the product could be observed according to the GPC chromatogram, Figure 34 and Table 4.

Table 4: GPC data for the CuAAc in DMF at 5°C (Procedure 4)

Peak	**Đ**	**M_w [Da]**	**RI (Area)**
A	-	-	-
B	1.032	10.886	20.87

Since no positive influence of the reduced reaction temperature on the reaction could be seen, the influence of the copper species on the click reaction was investigated as well.

Procedure 5:

Following **Procedure 5**, the copper species was changed from $Cu^{(II)}SO_4$ to $Cu^{(I)}Br$. Since the active species in the CuAAC is $Cu^{(I)}$, no reduction of $Cu^{(II)}$ to $Cu^{(I)}$ is thereby necessary and the catalytic species can be used directly.
The corresponding GPC chromatogram of the approach is depicted in the Figure 35.

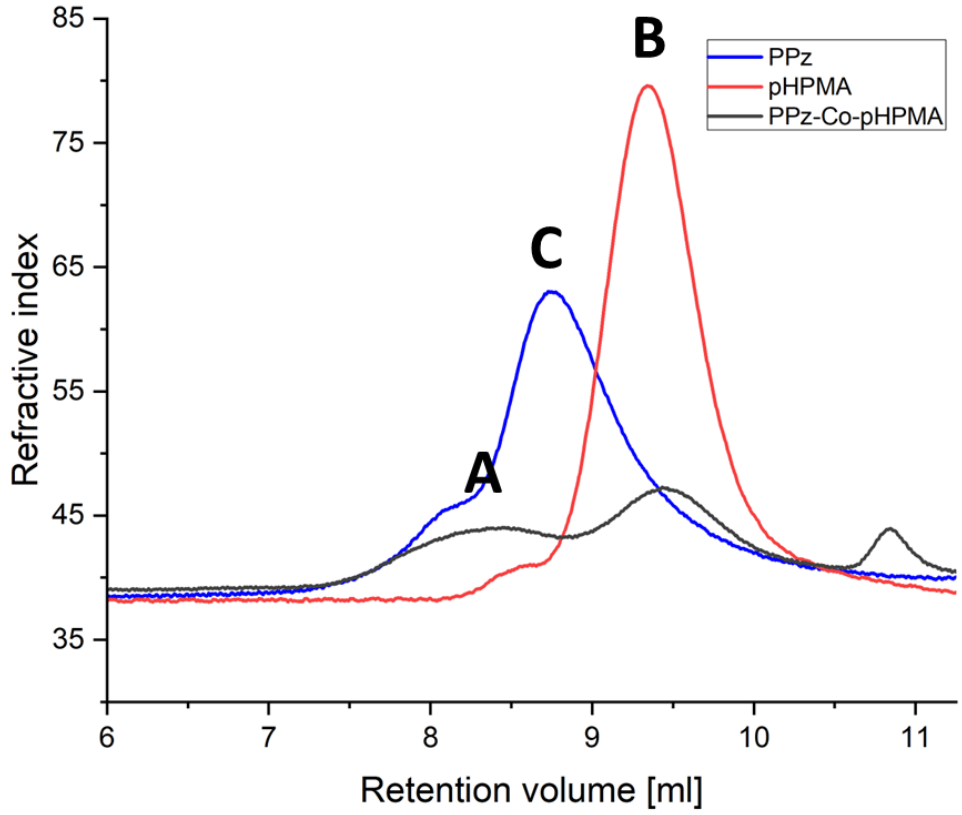

Figure 35: GPC measurement in DMF of PPz-Co-pHPMA, reacted in DMAc, with CuBr and TBTA at rt under argon for 1 day (Procedure 5).

A slight shift towards a higher molecular weight, peak A, can be observed. Nevertheless, a clear peak corresponding to residual, free pHPMA can be clearly seen as well, peak B.
The GPC data can be found in Table 5. Although the dispersity could be slightly improved down to Đ = 1.20, only a conversion of 37% could be achieved, significantly below the results of **Procedure 2** and **Procedure 3** with 81% and 75%, respectively**.**

Table 5: GPC data for the CuAAc with Cu(I)Br in DMAC (Procedure 5)

Peak	Đ	M_w [Da]	RI (Area)
A	1.20	43.774	7.14
B	1.02	17.915	12.02

Procedure 6 & Procedure 7:

In the final approach, the influence of the linker species on the PPz backbone was investigated. To this end, the glycine linker was substituted for a valine species, increasing the steric bulk on the amino acid side group, and influencing the expected degradation rate of the PPz-backbone.

The success of the reactions was again controlled by GPC measurements and the chromatograms are shown in Figure 36.

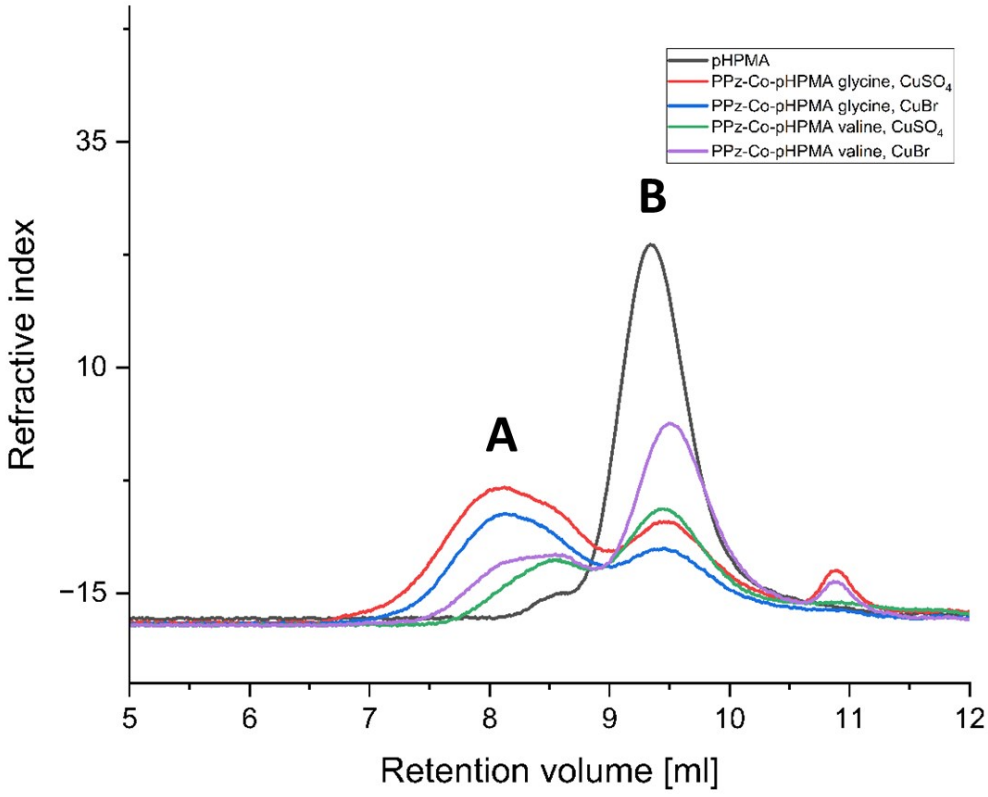

Figure 36: GPC measurement in DMF of PPz-Co-pHPMA, comparing different linker species (glycine versus valine) and reaction conditions (Procedure 6 and Procedure 7).

Overall, the reaction with the valine substituted PPz did not lead to increased product formation compared to the glycine linker, compare Table 6. Neither for **Procedure 6** nor for **Procedure 7**, with drops in conversion down to 38 and 33%, respectively. Interestingly, addition of TBTA did allow for an increased conversion of 65% when using $Cu^{(I)}Br$ and glycine substituted PPz compared to **Procedure 5**.

Table 6: GPC data for the CuAAc with valine substituted PPz instead of glycine substituted PPz (Procedure 6 and Procedure 7)

Peak	Đ	M_w [Da]	RI (Area)	Calculated conversion
A PPz-Glycine, $CuSO_4$	1.11	79.790	22.88	**66%**
B PPz -Glycine $CuSO_4$	4.00	13.958	10.83	
A PPz-Glycine, CuBr	1.58	74.438	15.25	**65%**
B PPz -Glycine CuBr	1.08	14.370	7.90	
A PPz-Valine, $CuSO_4$	1.39	53.705	6.98	**38%**
B PPz -Valine $CuSO_4$	1.02	13.186	11.61	
A PPz-Valine, CuBr	1.14	55.152	9.01	**33%**
B PPz -Valine CuBr	1.07	9.638	18.89	

In summary, the formation of a PPz-pHPMA bottlebrush polymer could be observed according to GPC measurements, with a maximum conversion of 81% according to **Procedure 2**. Additional optimizations are undoubtedly feasible to further increase the conversion given the "click character" of the CuAAC. At present, purification *via* ultrafiltration or dialysis can effectively eliminate the unreacted pHPMA, resulting in the isolation of the PPz-g-pHPMA conjugate. Overall, a novel PPz-co-pHPMA could be synthesized, confirmed by GPC measurements.

4.2. Results for PPz-co-PGA with peptide therapeutic

The PPz-co-PGA, which was synthesized according to literature procedures as described in chapter 3.5., was further used to attach a novel peptide therapeutic onto it. The methodology employed a widely utilized peptide coupling protocol, leveraging the amino terminus of the peptide therapeutic and the carboxyl groups of the PGA side chains to form a peptide bond. The results of the different procedures employed are detailed below.

Procedure 1:

The first attempt to couple the peptide drug onto the PPz-co-PGA *via* a peptide coupling reaction did not yield a successful reaction. The peptide drug exhibited insufficient solubility in DMF, possibly due to a majority of hydrophobic groups compared to hydrophilic ones and a resulting disadvantageous peptide folding. Hence, solubility tests were conducted. The results are detailed in Table 7.

Table 7: Solubility of the used peptide drug.

Peptide Solubility	DMF	MilliQ	MES	0.1 M HCl	0.1 M NaOH	EtOH	PBS
Good (colourless solution)		x	x			x	
Medium (opaque solution)	x			x			x
Bad (undissolved residues)					x		

Despite good solubility in water, the DMF content in the reaction solution of **Procedure 1** appeared to be too high to allow for a solubilization of the peptide drug.

Procedure 2:

Based on the results of the solubility tests the procedure was adapted, solving the peptide drug in MilliQ water instead of DMF and reducing the overall DMF content in the reaction solution. Additionally, the 10x PBS buffer was added to the mixture prior to the peptide solution to achieve a nearly neutral pH value in contrast to the slightly acidic pH of the MES-buffered reaction. This should improve the peptide solubility, since the drug's solubility was superior in neutral MilliQ water compared to acidic or basic solutions. The results of this approach are presented in Figure 37.

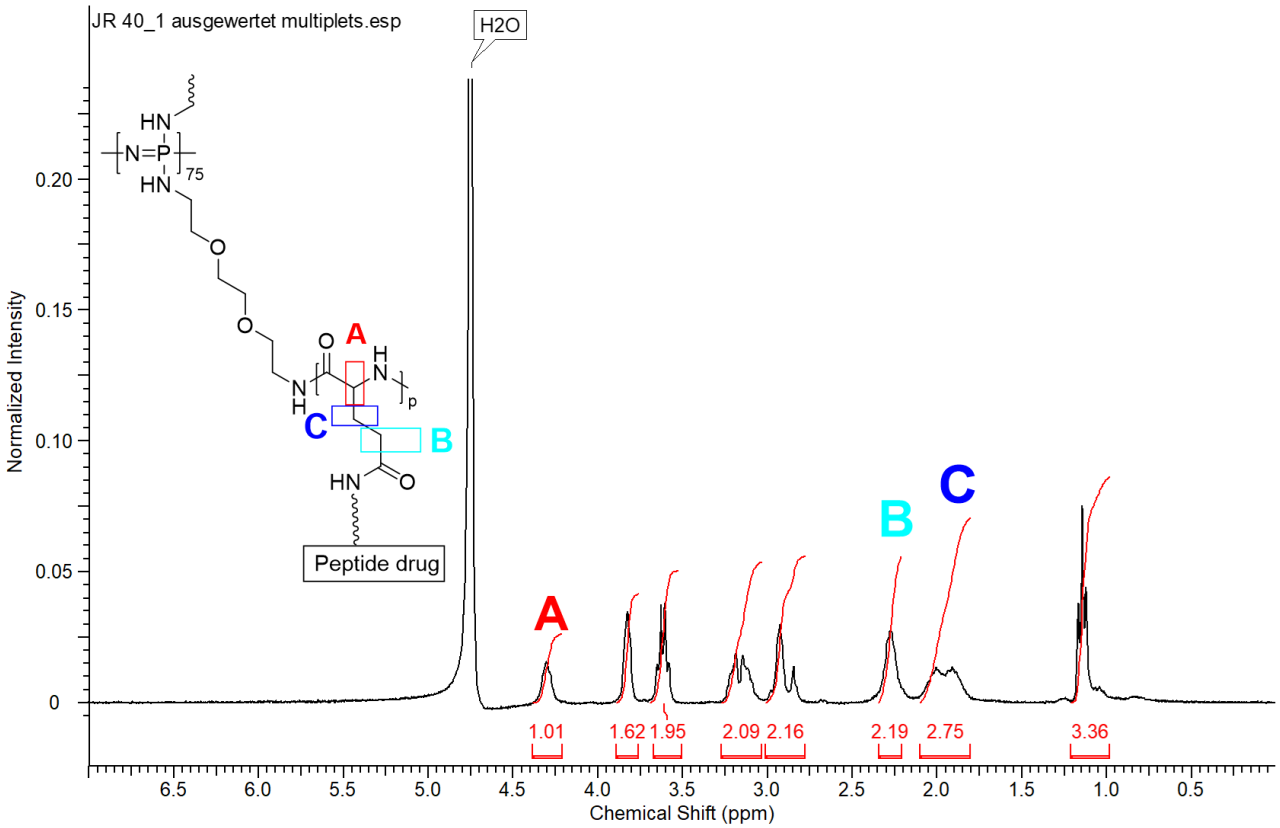

Figure 37: ^{1}H NMR spectrum in D_2O of PPz-co-PGA with peptide therapeutic, following Procedure 2.

^{1}H, 300 MHz, D_2O: δ= 3.95 (m, 1.5H), 3.85 (m, 0.5H), 3.83 (m, 1.5 H), 3.62 (d, J=7 Hz, 2H), 3.15 (m, 2H), 1.14 (t, J=7 Hz, 3H); 4.31 (m, 1H, PGA), 2.27 (m, 2H, PGA), 1.95 (m, 2H, PGA) ppm.

From the ^{1}H-NMR spectrum most of the characteristic peaks of the peptide therapeutic can be assigned for the PPz-co-PGA peptide conjugate. Nevertheless, quantification of the attempted loading indicated a loading above the targeted degree of 5 mol%, hinting on unidentified impurities overlapping with the assignable peaks of the peptide drug.

Nevertheless, the material was tested *in vitro* as a proof-of-principle for the evaluation of the PPz-co-PGA as a nanocarrier for the peptide therapeutic. For the study, A549 cells were used. A549 cells are obtained from a human epithelial cell line, more exact from basal cell carcinoma tissue. This cell line is a commonly used model cell line for alveolar type II epithelial cells (ATII) in research and testing for different respiratory diseases [69; 70].

The cells were incubated with increasing concentrations of the polymer-peptide conjugate. Consequently, the cytotoxicity of the conjugate was assessed. The results of the studies are summarized in Tables 8 and Table 9.

Table 8: Cell cytotoxicity test on A549 cells, determining cell viability after incubation with increasing concentrations of PPz-co-PGA with peptide drug for 24 hours.

A549	24h									
	0	**0.5mg/ml**	**250µg/ml**	**125µg/ml**	**62.5µg/ml**	**31.25µg/ml**	**15.63µg/ml**	**7.8µg/ml**	**3.9µg/ml**	**Brush alone 0.5mg/ml**
	100	62,38	60,95	72,05	77,05	74,31	90,82	99,11	100,76	86,50
	100	54,79	55,05	61,85	69,15	78,84	83,73	87,84	98,94	78,97
	100	54,05	60,90	68,08	76,27	93,36	90,23	86,84	101,73	77,78
median	**100**	**54,79**	**60,90**	**68,08**	**76,27**	**78,84**	**90,23**	**87,84**	**100,76**	**78,97**

Table 9: Cell cytotoxicity test on A549 cells, determining cell viability after incubation with increasing concentrations of PPz-co-PGA with peptide drug for 72 hours

A549	72 h									
	0	**0.5mg/ml**	**250µg/ml**	**125µg/ml**	**62.5µg/ml**	**31.25µg/ml**	**15.63µg/ml**	**7.8µg/ml**	**3.9µg/ml**	**Brush alone 0.5mg/ml**
	100	44,06	64,54	70,67	82,70	76,66	85,32	85,45	91,70	83,70
	100	44,92	56,42	63,44	65,16	75,71	83,19	86,22	86,93	78,75
	100	35,95	53,95	68,10	71,21	83,12	90,46	91,53	86,23	91,55
median	**100**	**44,06**	**56,42**	**68,10**	**71,21**	**76,66**	**85,32**	**86,22**	**86,93**	**83,70**

The cells treated with the PPz-Co-PGA peptide drug conjugated showed significantly higher mortality compared to untreated cells, with a survivability around 55% after 24h and 45% after 72h for a concentration of 0.5mg/ml of the polymer-drug conjugate. Interestingly, the bottlebrush polymer alone also exhibited cytotoxicity, albeit only at the highest concentration of 0.5mg/ml and to a low effect with a cell survivability around 80%. Comparing cell survivability after 24 hours to after 72 hours, a clear beneficial effect of prolonged incubation time could be seen. Probably due continuous cleavage of the peptide drug from the copolymer carrier over time, increasing the amount of drug reaching the cells. Overall, a clear cytotoxic effect of the polymer-drug conjugate could be observed after 24h and 72h when compared to the pure bottlebrush copolymer, Figure 38, serving as a proof-of-concept of the suitability of the developed carrier system.

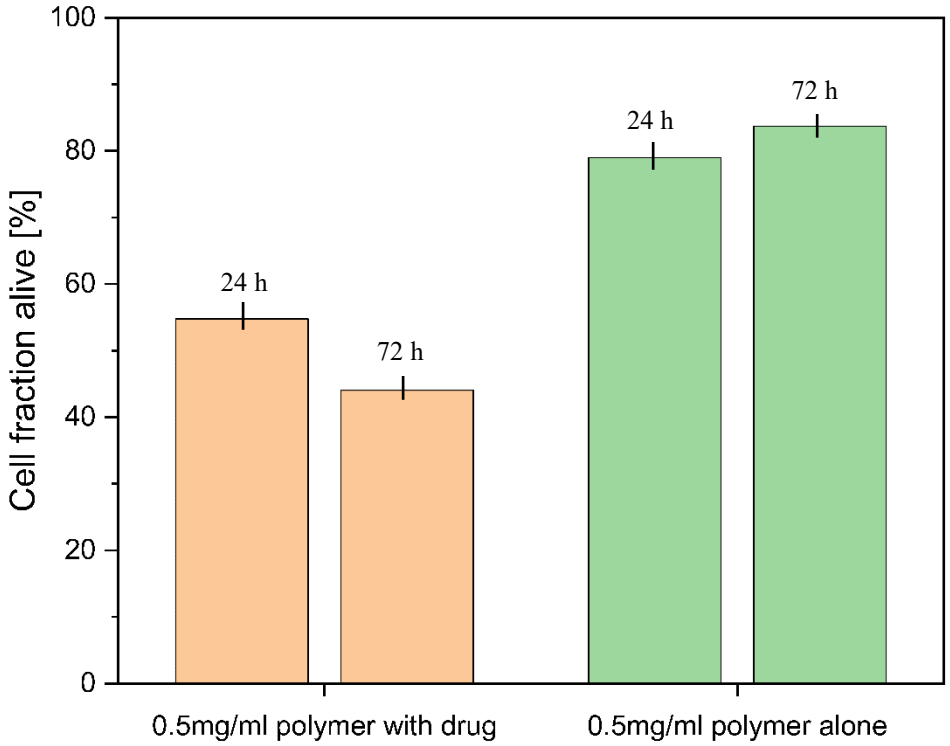

Figure 38: Cytotoxicity study on A549 cells, determining cell viability after incubation with 0.5mg/ml of PPz-co-PGA with peptide drug for 24h and 72h compared to cells treated with polymer solution alone.

Procedure 3:

In the next step, a PPz-co-PGA bottlebrush polymer labelled with a fluorophore was used to gather more information regarding the cell uptake and distribution of the polymer-drug conjugate. The labelling of the PPz-co-PGA was conducted according to the protocol of Strasser *et al*. [53], and the conjugation was subsequently performed as outlined in Chapter 3.6. addition of the PBS buffer was omitted due to an optimal pH range for the peptide coupling within the pH range of the utilized MES buffer. Furthermore, DMAP was excluded avoid any organic solvent during the reaction.

Based on a GPC measurement in aqueous media, Figure 39, a slight increase in M_w of the polymer-drug conjugate compared to the PPz-co-PGA bottlebrush polymer can be seen. Although only small, the molecular weight of the peptide therapeutic is low in comparison to the molecular weight of the PPz-co-PGA and only a loading of 5mol% was targeted.

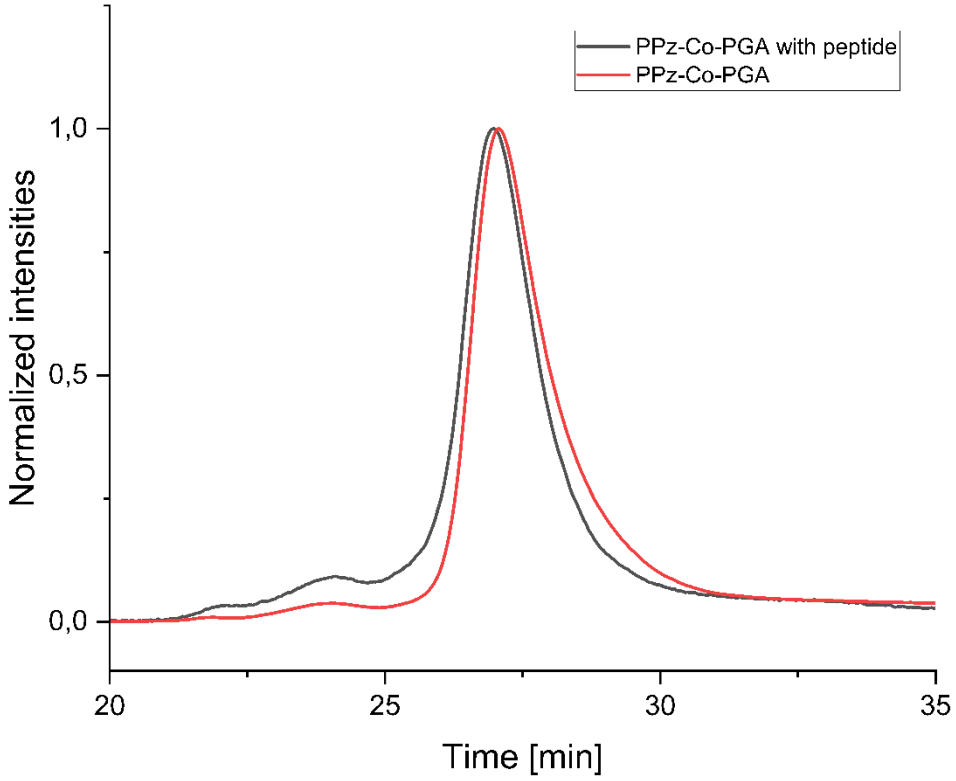

Figure 39: GPC measurement in aqueous medium of PPz-co-PGA with peptide therapeutic compared to PPz-co- PGA; both PGA species were labelled with Cy5.

In the ^{1}H-NMR spectrum, Figure 40, characteristic peaks of the peptide therapeutic can be identified. For quantification, the signal corresponding to the methylene residues of 3 leucine residues on the peptide were selected. Comparing the intensities of the glutamic acid moieties of the PGA side chains with the peptide peak (2:0.21) a loading of 2.5 mol% could be calculated, below the targeted 5 mol%. In comparison to **Procedure 2** a decreased loading efficient could be determined. Nevertheless, as mentioned above, an overestimated loading was determined for **Procedure 2**, most probably due to unidentifiably impurities.

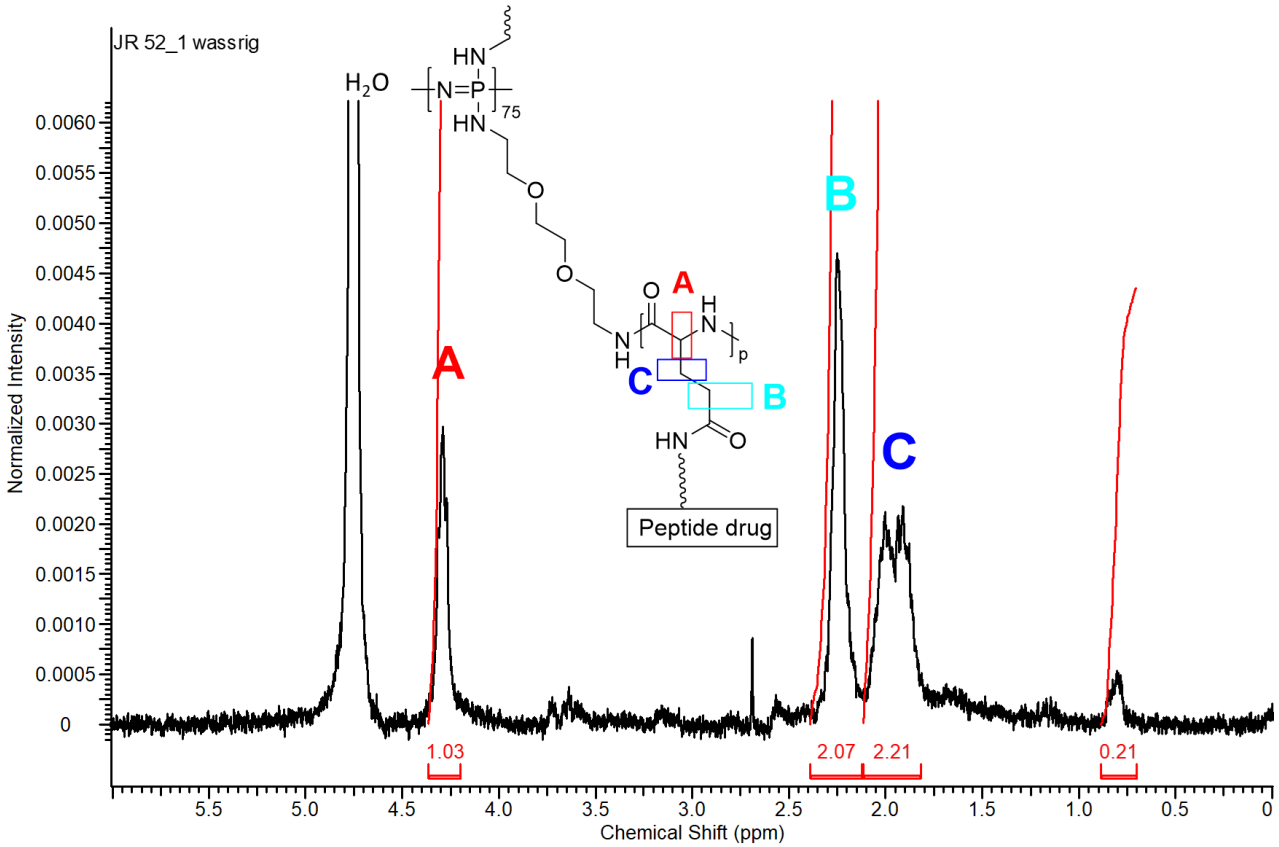

Figure 40: ^{1}H NMR spectrum in D_2O of PPz-co-PGA with peptide therapeutic; labelled with Cy5.

^{1}H, 300 MHz, D_2O: δ= 4.29 (m, 1H, PGA), 2.24 (m, 2H, PGA), 1.95 (m, 2H, PGA), 0.81 (m, 0.21H) ppm.

Overall, based on the presented data and the proof-of-concept of the cytotoxic effect of the polymer-drug conjugate, a successful preparation of a novel drug carrier based on a PPz-co-PGA bottlebrush and bearing a potent peptide drug was achieved.

4.3. Results for PPz-Co-PGA with hydrazide linker

In the final chapter, a hydrazide linker was coupled onto the PPz-co-PGA bottlebrush copolymer. The aim of coupling the hydrazide linker onto the PPz-co-PGA was to introduce a hydrazide functionality, enabling a simple and straight forward coupling of drugs. For example, reactions with ketone functionalities would result in formation of hydrazones [71]. Such hydrazone bonds can be used for targeted, stimuli responsive drug delivery, due to their pH responsive nature [72]. Etrych *et al.* have shown pHPMA doxorubicin conjugates sensitive to pH changes [73]. Lu et al. have shown similar results for pH responsive pullulan doxorubicin conjugates [74]. The reactions were conducted according to a standard peptide coupling protocol and further optimized.

Procedure 1:

The first approach followed standard peptide coupling protocols, employing the commonly used coupling reagents EDC.HCl and NHS. As can be seen in the ^{1}H-NMR spectrum, Figure 41, the signals of the coupled hydrazide linker can be clearly assigned. Signal F, corresponding to the Boc-protection groups, serves an integral of around 3.6, slightly below the expected 4.5 for a loading if 50%. Interestingly, signals D and E, corresponding to the methylene residues in the β-alanine moiety, showed increased integrals of around 2. This might be explained by overlapping signals with the PGA backbone, as well as unidentified impurities.

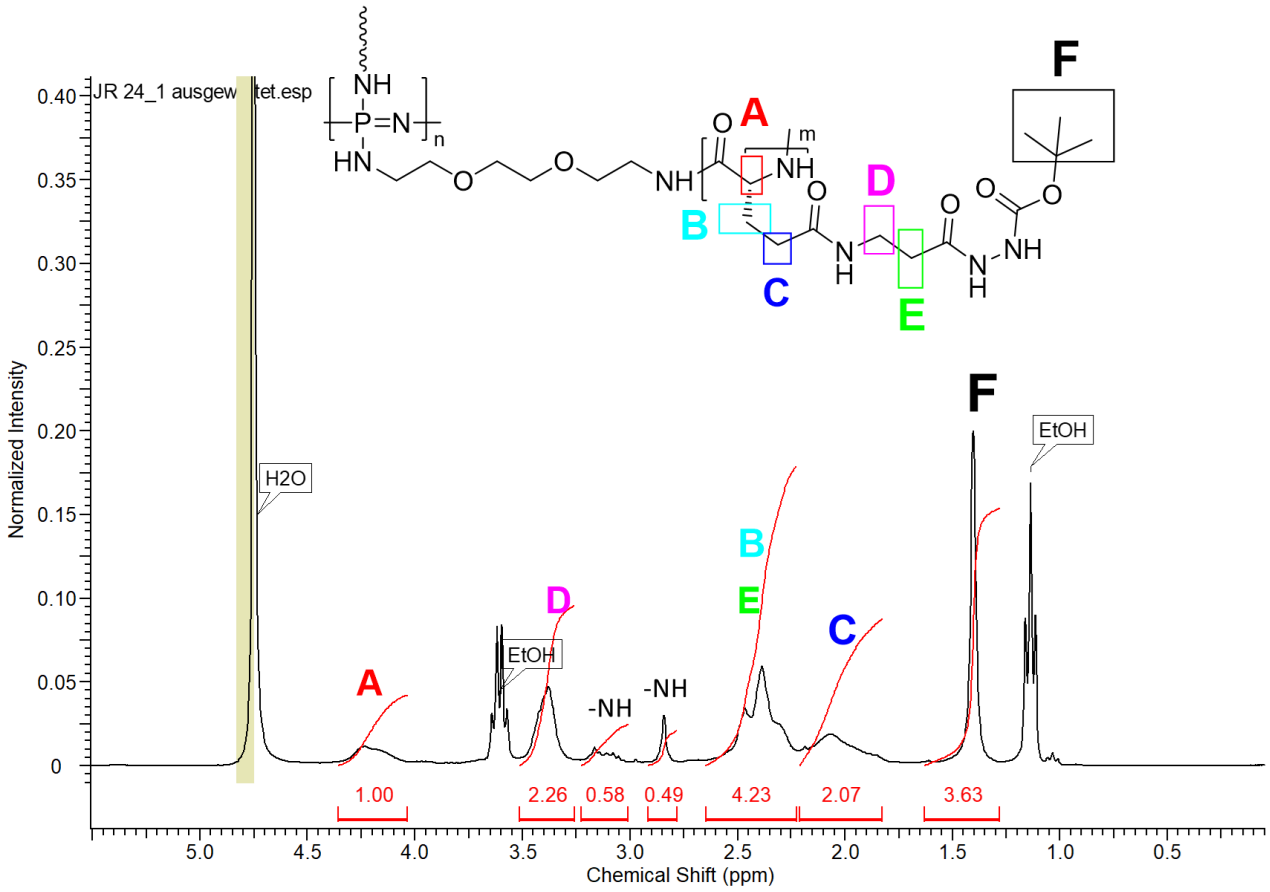

Figure 41: ^{1}H NMR spectrum in D_2O of β-alanyl-Boc hydrazide linker on PPz-co-PGA, targeting 0.5 eq per PGA repeating unit.

^{1}H, 300 MHz, D_2O: δ= 4.22 (m, 1H, PGA), 2.43 (m, 4H, PGA + Linker), 2.07 (m, 2H, PGA), 3.38 (m, 2H), 3.12 (m, 0.5H), 2.84 (m, 0.5H), 1.40 (br.s, 4H) ppm.
^{31}P, 121.49 MHz, D_2O: δ= n.a.

The observed intensities are as expected; all peaks corresponding to the attached hydrazide moiety could be assigned accurately and the intensities were consistent with the expected structure. The Boc peaks' intensity of the hydrazide linker at 1.40 ppm is about 4, slightly below the expected 4.5 for the targeted = 0.5 eq. coupling. The signal at 3.38 ppm corresponding to the -CH_2 group of the hydrazide linker exhibited an increased integral of 2.28 in contrast to the expected intensity of 1, which can be explained by overlapping impurities.
The phosphorous NMR could not be measured, as the intensity of the signal was too low due to low abundance of the phosphorous in the macromolecule.

Procedure 2:

To evaluate the success of **Procedure 2**, ^{1}H NMR measurements were conducted. The spectrum is presented in Figure 42, with the respective peaks of the hydrazide functionality and the PGA side chains assigned.

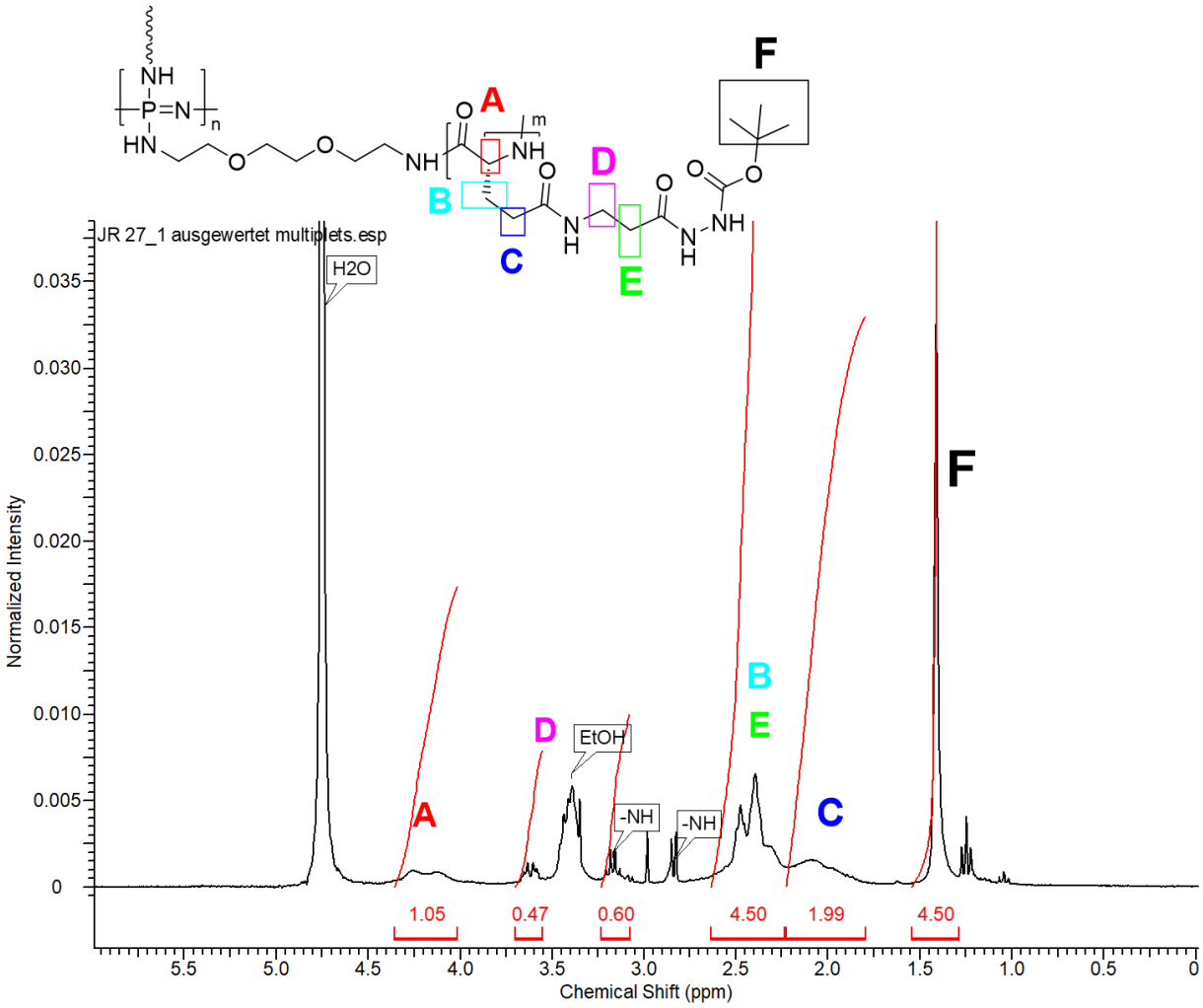

Figure 42: ^{1}H NMR in D_2O of β-alanyl-Boc hydrazide linker on PPz-co-PGA; 0.5 eq per repeating unit (Procedure 2).

^{1}H, 300 MHz, D_2O: δ= 4.18 (m, 1H, PGA), 2.38 (m, 4H, PGA + Linker), 2.00 (m, 2H, PGA), 7.90 (m, 0.04H), 3.62 (m, 0.5H), 3.16 (m, 0.75H), 1.41 (br. s, 4.5H) ppm.
^{31}P, 121.49 MHz, D_2O: δ= n.a.

Both the peaks of the PPz-co-PGA and from the hydrazide linker are present once again. The signal intensity for the -Boc group at 1.41 ppm exhibits the expected value of 4.47, suggesting that the reaction has proceeded to a certain extend. Nevertheless, some signal intensities deviate from the expected value. The peak at 3.62 ppm from a -CH_2 group of the hydrazide

linker should show an intensity of 1 for a loading of 0.5 eq per repeating unit PGA, however only 0.47 was observed. Also, the peak at 2.38 ppm should exhibit an intensity of 3 instead of 4, consisting of one proton for 0.5 eq of the -CH_2 peak of the hydrazide linker and 2 protons for the PGA.

Procedure 3:

The next attempt was performed using a PPz-co-PGA labelled with Cy5. This attempt adhered to **Procedure 3** as outlined in the experimental section.

Again, the ^{1}H-NMR spectrum, presented in Figure 43, confirms a successful reaction. The signal of the -Boc group of the hydrazide linker can be observed at 1.41 ppm, exhibiting the expected intensity of 4.60 for a loading of 50mol%. Nevertheless, as for **Procedure 1**, the signal D and E do not conform with the expected intensities.

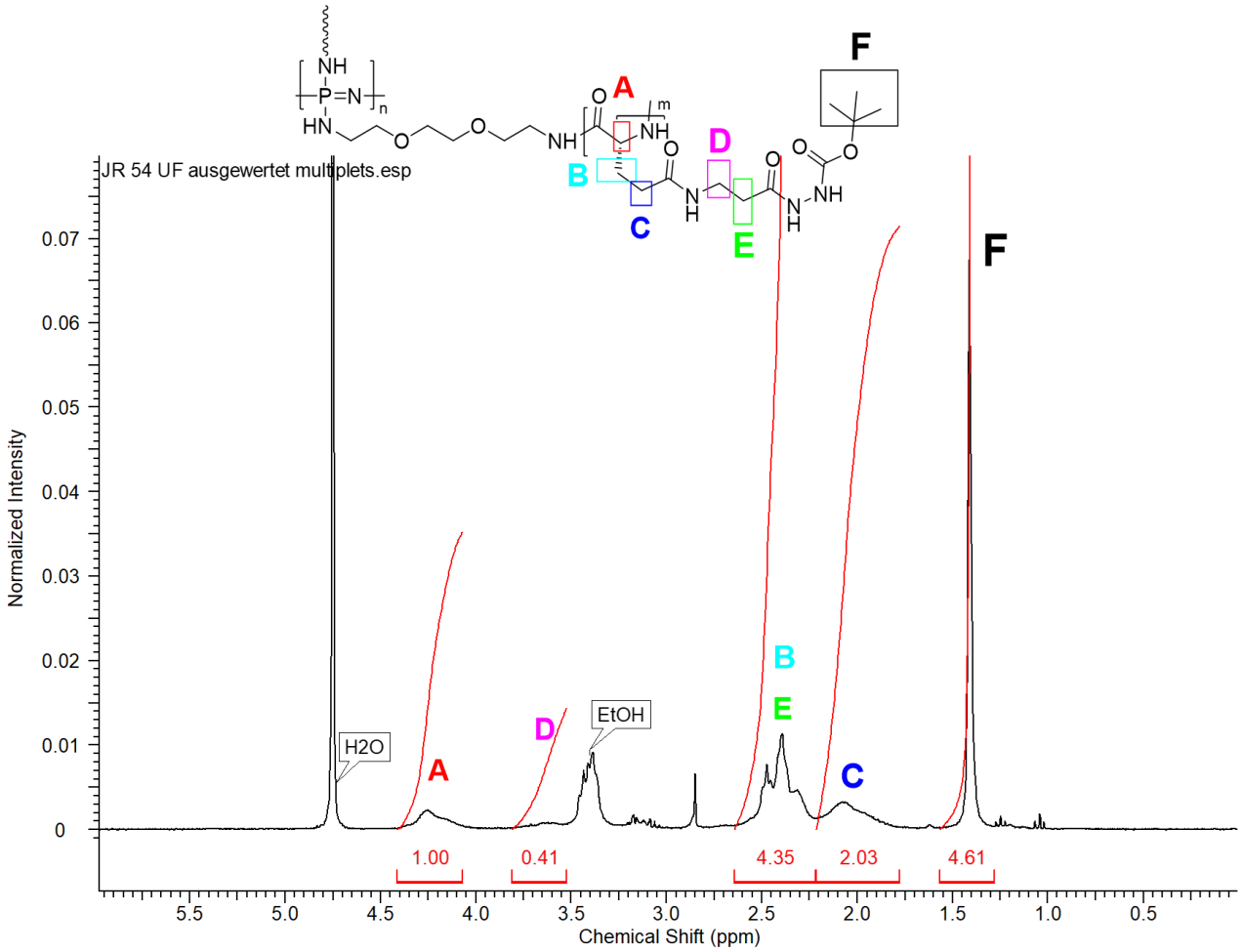

Figure 43. ^{1}H-NMR spectrum in D_2O from the PPz-co-PGA with the hydrazide linker (Procedure 3).

In addition to the NMR analysis, GPC measurements were performed to confirm the reaction by the expected increase in molecular weight, Figure 44 and Figure 45. The peak for the copolymer with the linker is shifted to higher molecular weights, compared to the PPz-co-PGA without hydrazide linker. However, a significant broadening of the peak can be observed, possibly originating from column interactions due to the increased hydrophobic character of the polymer. The shoulder at a retention time of about 21 minutes corresponds to a measurement artefact, due to reaching the end of the column separation. Overall, the higher molecular weight of the PPz-co-PGA with the hydrazide linker indicates, that the hydrazide linker did react onto the copolymer, as no reagents were present, which could have reacted onto the polymer and thus increase the M_w.

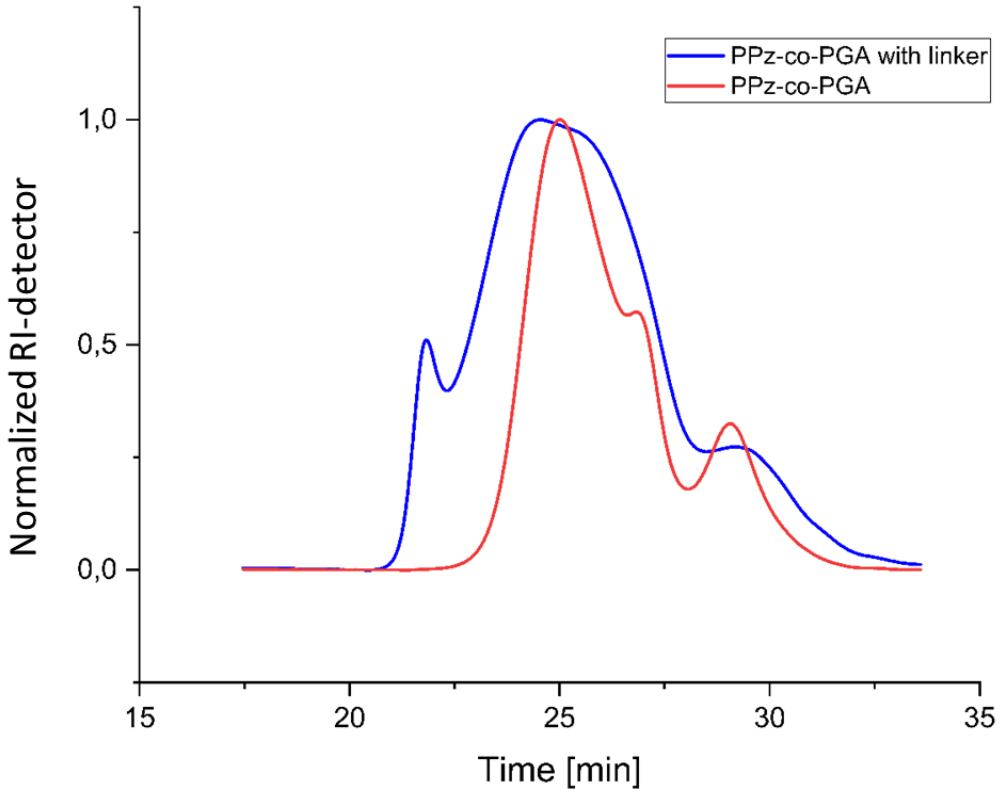

Figure 44: GPC measurement in aqueous medium of the PPz-co-PGA with the hydrazide linker synthesized after Procedure 3, compared the PPz-co-PGA alone; shown with normalized intensities of the refractive index detector signal.

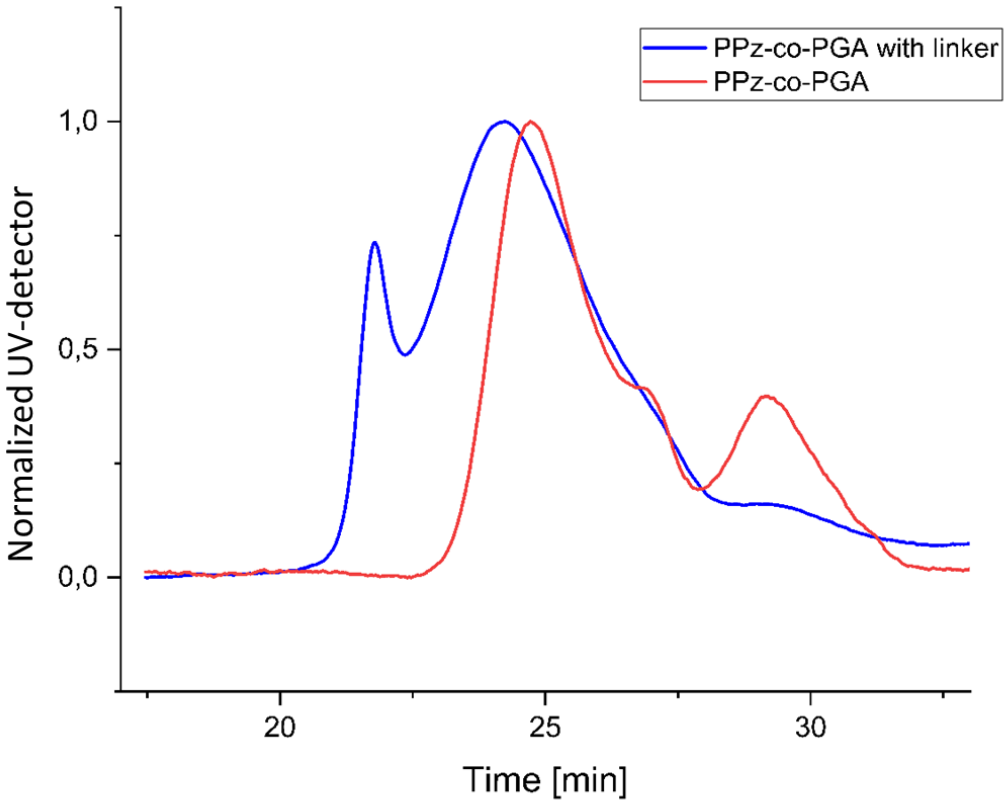

Figure 45: GPC measurement in aqueous medium of the PPz-co-PGA with the hydrazide linker synthesized after Procedure 3, compared to the PPz-co-PGA alone; shown with normalized intensities of the UV detector signal.

In summary, albeit some impurities in the ^{1}H-NMR spectra of the prepared hydrazide functionalized PPz-co-PGA bottlebrush polymers, the clear signal of the Boc-protecting group indicates a successful reaction. Additional optimization of the reaction and the purification the material are still remaining, nevertheless, a potential functionalization could be proven.

5. Conclusion and Outlook

During the course of this thesis, various biomedical co-polymers based on polyphosphazenes were prepared. First, a novel PPz-co-pHPMA copolymer was successfully synthesized *via* copper-catalysed azide-alkyne cycloaddition CuAAC. The successful synthesis was confirmed by GPC and NMR measurements. The influence of various reaction parameters on the reaction conversion was investigated, including changes in molecular weight, solvent, reducing agents, and the linker species on the PPz backbone. The optimal conditions were found to be a reaction in DMF at room temperature, using $Cu^{(II)}SO_4$ and ascorbic acid as reactants, yielding a conversion of 81%. The size of the pHPMA did not significantly affect the conversion rate. A decrease in reaction temperature, DMAc or water as solvent, CuBr as reducing agent, as well as exchanging a glycine linker to valine significantly decreased the conversion. Future work could further explore additional modifications to the reaction protocol, such as different combinations of solvents and copper species, as described in the literature [57].

In the second part, a novel PPz-co-PGA-drug conjugate was synthesized. It was demonstrated that the loading of the novel peptide therapeutic *via* peptide coupling reactions led to the formation of the desired polymer-drug conjugate. Confirmed by GPC and NMR data. Preliminary cell studies further confirmed the success of the conjugation and the suitability of the carrier for transporting the peptide therapeutic. The polymer-drug conjugate exhibited cell cytotoxicity, indicating successful loading and release of the peptide therapeutic. However, peptide solubility complicated the procedure and purification. These challenges might be overcome by further optimizing the reaction conditions, such as specific buffer solutions as solvents, as peptide folding was suspected to hinder the conjugation reaction.

Finally, a novel PPz-co-PGA equipped with a linker bearing a hydrazide functionality could be synthesized *via* peptide coupling reactions. Although some impurities remained in the product, complicating the accurate assignment of the ^1H NMR spectra, the overall spectrum could be attributed to the correct structure. Additionally, GPC data indicated an increase in molecular weight, accompanied by an unexpected increase in dispersity. In the next step, the new PPz-co-PGA with the hydrazide linker would need to be deprotected, further characterized, and used for a coupling reaction to provide a proof-of-concept of the targeted simplified conjugation chemistry.

7. Abbreviations

Boc…*tert*-butyloxycarbonyl protection group

Boc_2O…di-*tert*-butyldicarbonate

Cbz…benzyloxycarbonyl (Z) protection group

$CDCl_3$… deuterated chloroform

$CHCl_3$… chloroform

CuAAc… copper catalysed azide-alkyne cycloaddition

CuBr… copper$^{(I)}$bromide

Cy5… cyanine 5 NHS ester

dH_2O… distilled water

DMAc… dimethylacetamide

DMAP… 4-dimethylaminopyridine

DMF… dimethylformamide

DMSO… dimethylsulfoxide

DMSO-d6… deuterated DMSO

EDC.HCl… 1-ethyl-3-(3-dimethylaminopropyl)carbodiimide.hydrogen chloride

GPC_{aqu}… gel permeation chromatography, with aqueous solvent

GPC_{max}… gel permeation chromatography, with DMF as solvent

kDa… kilo Dalton

Millipore water… ultrapure water, trademark of the company 'Merck' for

MilliQ… ultrapure water, trademark of the company 'Merck' for

MeOD… deuterated methanol

MeOH…methanol

MES… 2-(*N*-morpholino)ethanesulfonic acid, buffer

M_w… weight averaged molecular weight [$g.mol^{-1}$]

MWCO… molecular weight cut off

NCA…5-benzyl-L-glutamate-*N*-carboxyanhydride / (4S)-2-,5-Dioxo-4-oxazolidinepropanoic acid phenylmethyl ester

NEt_3…triethylamine

NHS…*N*-hydroxysuccinimide

PBS…phosphate buffered saline

pHPMA…poly-*N*-(2-hydroxypropyl)methacrylamide

PPz…polyphosphazene

rpm…rounds per minute

TBTA… tris[(1-benzyl-1H-1,2,3-triazol-4-yl)methyl]amin

LIST OF FIGURES

References

[1] Thakor, P., Bhavana, V., Sharma, R., Srivastava, S., Singh, S.B., and Mehra, N.K., *Drug discovery today*, Vol. 25, 1718–1726, 2020.

[2] Junyaprasert, V.B., and Thummarati, P., *Pharmaceutics*, Vol. 15, 2023.

[3] Ratanji, K.D., Derrick, J.P., Dearman, R.J., and Kimber, I., *Journal of immunotoxicology*, Vol. 11, 99–109, 2014.

[4] Oh, J.K., *Molecular pharmaceutics*, Vol. 14, 2459, 2017.

[5] Javia, A., Vanza, J., Bardoliwala, D., Ghosh, S., Misra, L.A., Patel, M., and Thakkar, H., *International journal of pharmaceutics*, Vol. 623, 121863, 2022.

[6] Ekladious, I., Colson, Y.L., and Grinstaff, M.W., *Nature reviews. Drug discovery*, Vol. 18, 273–294, 2019.

[7] Duncan, R., and Spreafico, F., *Clinical pharmacokinetics*, Vol. 27, 290–306, 1994.

[8] Kopecek, J., and Kopecková, P., *Advanced drug delivery reviews*, Vol. 62, 122–149, 2010.

[9] Andrianov, A.K., and Allcock, H.R., eds., *Polyphosphazenes in Biomedicine, Engineering, and Pioneering Synthesis,* American Chemical Society, Washington, DC, 2018.

[10] Scales, C.W., Vasilieva, Y.A., Convertine, A.J., Lowe, A.B., and McCormick, C.L., *Biomacromolecules*, Vol. 6, 1846–1850, 2005.

[11] Zhang, Y., Song, W., Lu, Y., Xu, Y., Wang, C., Yu, D.-G., and Kim, I., *Biomolecules*, Vol. 12, 2022.

[12] Teasdale, I., and Brüggemann, O., *Polymers*, Vol. 5, 161–187, 2013.

[13] Jain, A.K., and Thareja, S., *Artificial cells, nanomedicine, and biotechnology*, Vol. 47, 524–539, 2019.

[14] Zhao, Z., Xu, Z., Chen, J., Zhong, M., Wang, J., and Chew, J.W., *Journal of Energy Storage*, Vol. 85, 111049, 2024.

[15] Rothemund, S., and Teasdale, I., *Chemical Society reviews*, Vol. 45, 5200–5215, 2016.

[16] Allcock, H.R., and Chen, C., *The Journal of organic chemistry*, Vol. 85, 14286–14297, 2020.

[17] Potin, P., and Jaeger, R. de, *European Polymer Journal*, Vol. 27, 341–348, 1991.

[18] Allcock, H.R., and Kugel, R.L., *J. Am. Chem. Soc.*, Vol. 87, 4216–4217, 1965.

[19] Ullah, R.S., Wang, L., Yu, H., Abbasi, N.M., Akram, M., -ul-Abdin, Z., Saleem, M., Haroon, M., and Khan, R.U., *RSC Adv.*, Vol. 7, 23363–23391, 2017.

[20] Honeyman, C.H., Manners, I., Morrissey, C.T., and Allcock, H.R., *J. Am. Chem. Soc.*, Vol. 117, 7035–7036, 1995.

[21] Ilayaperumal, P., Chelladurai, P., Vairan, K., Anilkumar, P., and Balagurusamy, B., *Macro Materials & Eng*, Vol. 308, 2023.

[22] Allcock, H.R., and Morozowich, N.L., *Polym. Chem.*, Vol. 3, 578–590, 2012.

[23] Strasser, P., and Teasdale, I., *Molecules (Basel, Switzerland)*, Vol. 25, 2020.

[24] Allcock, H.R., Pucher, S.R., and Scopelianos, A.G., *Biomaterials*, Vol. 15, 563–569, 1994.

[25] Li, Z., Tang, M., Liang, S., Zhang, M., Biesold, G.M., He, Y., Hao, S.-M., Choi, W., Liu, Y., Peng, J., and Lin, Z., *Progress in Polymer Science*, Vol. 116, 101387, 2021.

[26] Ogueri, K.S., Ogueri, K.S., Allcock, H.R., and Laurencin, C.T., *Journal of vacuum science and technology. B, Nanotechnology & microelectronics : materials, processing, measurement, & phenomena : JVST B*, Vol. 38, 30801, 2020.

[27] SHARMA, A., and PANDE, P.P., *JPM*, Vol. 36, 175–194, 2019.

[28] Weikel, A.L., Cho, S.Y., Morozowich, N.L., Nair, L.S., Laurencin, C.T., and Allcock, H.R., *Polym. Chem.*, Vol. 1, 1459, 2010.

[29] Allcock, H.R., Synthesis, Structures, and Emerging Uses for Poly(organophosphazenes), American Chemical Society, Vol. 1298, 3–26, 2018.

[30] Allcock, H.R., *Dalton transactions (Cambridge, England : 2003)*, Vol. 45, 1856–1862, 2016.

[31] Foster, J.C., Varlas, S., Couturaud, B., Coe, Z., and O'Reilly, R.K., *J. Am. Chem. Soc.*, Vol. 141, 2742–2753, 2019.

[32] Ajvazi, E., Bauer, F., Strasser, P., Brüggemann, O., Preuer, R., Kracalik, M., Hild, S., Abbasi, M., Graz, I., and Teasdale, I., *ACS polymers Au*, Vol. 4, 56–65, 2024.

[33] Verduzco, R., Li, X., Pesek, S.L., and Stein, G.E., *Chemical Society reviews*, Vol. 44, 2405–2420, 2015.

[34] Ruiz-Rodado, V., Lita, A., and Larion, M., *Nature methods*, Vol. 19, 1048–1063, 2022.

[35] Teasdale, I., Wilfert, S., Nischang, I., and Brüggemann, O., *Polym. Chem.*, Vol. 2, 828–834, 2011.

[36] Chytil, P., Etrych, T., Konák, C., Sírová, M., Mrkvan, T., Říhová, B., and Ulbrich, K., *Journal of controlled release : official journal of the Controlled Release Society*, Vol. 115, 26–36, 2006.

[37] Pan, X., Zhang, F., Choi, B., Luo, Y., Guo, X., Feng, A., and Thang, S.H., *European Polymer Journal*, Vol. 115, 166–172, 2019.

[38] Francini, N., Purdie, L., Alexander, C., Mantovani, G., and Spain, S.G., *Macromolecules*, Vol. 48, 2857–2863, 2015.

[39] Šubr, V., Kostka, L., Strohalm, J., Etrych, T., and Ulbrich, K., *Macromolecules*, Vol. 46, 2100–2108, 2013.

[40] Sincari, V., Petrova, S.L., Konefał, R., Hruby, M., and Jäger, E., *Reactive and Functional Polymers*, Vol. 162, 104875, 2021.

[41] Yang, J., and Kopeček, J., *Current opinion in colloid & interface science*, Vol. 31, 30–42, 2017.

[42] Chytil, P., Kostka, L., and Etrych, T., *Journal of personalized medicine*, Vol. 11, 2021.

[43] Kissel, M., Peschke, P., Subr, V., Ulbrich, K., Strunz, A.M., Kühnlein, R., Debus, J., and Friedrich, E., *European journal of nuclear medicine and molecular imaging*, Vol. 29, 1055–1062, 2002.

[44] Bobde, Y., Biswas, S., and Ghosh, B., *European Polymer Journal*, Vol. 139, 110018, 2020.

[45] Li, Q., Yang, S., Zhu, L., Kang, H., Qu, X., Liu, R., and Huang, Y., *Polym. Chem.*, Vol. 6, 2869–2878, 2015.

[46] Rani, S., and Gupta, U., *Drug discovery today*, Vol. 25, 997–1012, 2020.

[47] Duro-Castano, A., England, R.M., Razola, D., Romero, E., Oteo-Vives, M., Morcillo, M.A., and Vicent, M.J., *Molecular pharmaceutics*, Vol. 12, 3639–3649, 2015.

[48] Park, S.-B., Sung, M.-H., Uyama, H., and Han, D.K., *Progress in Polymer Science*, Vol. 113, 101341, 2021.

[49] Chen, W.-H., Chen, Q.-W., Chen, Q., Cui, C., Duan, S., Kang, Y., Liu, Y., Liu, Y., Muhammad, W., Shao, S., Tang, C., Wang, J., Wang, L., Xiong, M.-H., Yin, L., Zhang, K., Zhang, Z., Zhen, X., Feng, J., Gao, C., Gu, Z., He, C., Ji, J., Jiang, X., Liu, W., Liu, Z., Peng, H., Shen, Y., Shi, L., Sun, X., Wang, H., Wang, J., Xiao, H., Xu, F.-J., Zhong, Z., Zhang, X.-Z., and Chen, X., *Science China. Chemistry*, Vol. 65, 1010–1075, 2022.

[50] Zhang, K., Song, L., Wang, J., Yan, S., Li, G., Cui, L., and Yin, J., *Acta biomaterialia*, Vol. 51, 246–257, 2017.

[51] Stevanović, M., Bračko, I., Milenković, M., Filipović, N., Nunić, J., Filipič, M., and Uskoković, D.P., *Acta biomaterialia*, Vol. 10, 151–162, 2014.

[52] Liu, Q., Chen, S., Chen, J., and Du, J., *Macromolecules*, Vol. 48, 739–749, 2015.

[53] Strasser, P., Montsch, B., Weiss, S., Sami, H., Kugler, C., Hager, S., Schueffl, H., Mader, R., Brüggemann, O., Kowol, C.R., Ogris, M., Heffeter, P., and Teasdale, I., *Small (Weinheim an der Bergstrasse, Germany)*, Vol. 19, e2300767, 2023.

[54] Baumgartner, R., Kuai, D., and Cheng, J., *Biomaterials science*, Vol. 5, 1836–1844, 2017.

[55] Hein, J.E., and Fokin, V.V., *Chemical Society reviews*, Vol. 39, 1302–1315, 2010.

[56] Pineda-Castañeda, H.M., Rivera-Monroy, Z.J., and Maldonado, M., *ACS omega*, Vol. 8, 3650–3666, 2023.

[57] Liang, L., and Astruc, D., *Coordination Chemistry Reviews*, Vol. 255, 2933–2945, 2011.

[58] Héron, J., and Balcells, D., *ACS Catal.*, Vol. 12, 4744–4753, 2022.

[59] Madhu, C., NageswaraRao, P., Narendra, N., and Sureshbabu, V.V., *Int J Pept Res Ther*, Vol. 20, 353–363, 2014.

[60] Rothemund, S., Aigner, T.B., Iturmendi, A., Rigau, M., Husár, B., Hildner, F., Oberbauer, E., Prambauer, M., Olawale, G., Forstner, R., Liska, R., Schröder, K.R., Brüggemann, O., and Teasdale, I., *Macromolecular bioscience*, Vol. 15, 351–363, 2015.

[61] Henke, H., Wilfert, S., Iturmendi, A., Brüggemann, O., and Teasdale, I., *Journal of polymer science. Part A, Polymer chemistry*, Vol. 51, 4467–4473, 2013.

[62] Hackl, C.M., Schoenhacker-Alte, B., Klose, M.H.M., Henke, H., Legina, M.S., Jakupec, M.A., Berger, W., Keppler, B.K., Brüggemann, O., Teasdale, I., Heffeter, P., and Kandioller, W., *Dalton transactions (Cambridge, England : 2003)*, Vol. 46, 12114–12124, 2017.

[63] Rostovtsev, V.V., Green, L.G., Fokin, V.V., and Sharpless, K.B., *Angew. Chem. Int. Ed.*, Vol. 41, 2596–2599, 2002.

[64] Androvič, L., Woldřichová, L., Jozefjaková, K., Pechar, M., Lynn, G.M., Kaňková, D., Malinová, L., and Laga, R., *Macromolecules*, Vol. 54, 3139–3157, 2021.

[65] Chan, T.R., Hilgraf, R., Sharpless, K.B., and Fokin, V.V., *Organic letters*, Vol. 6, 2853–2855, 2004.

[66] Jakubek, P., Suliborska, K., Kuczyńska, M., Asaduzzaman, M., Parchem, K., Koss-Mikołajczyk, I., Kusznierewicz, B., Chrzanowski, W., Namieśnik, J., and Bartoszek, A., *Free radical biology & medicine*, Vol. 209, 239–251, 2023.

[67] Tang, H., Guo, H., Yang, F., and Zhu, S., *Liquid Crystals*, Vol. 44, 1566–1574, 2017.

[68] Wilfert, S., Iturmendi, A., Schoefberger, W., Kryeziu, K., Heffeter, P., Berger, W., Brüggemann, O., and Teasdale, I., *Journal of polymer science. Part A, Polymer chemistry*, Vol. 52, 287–294, 2014.

[69] Chary, A., Groff, K., Stucki, A.O., Contal, S., Stoffels, C., Cambier, S., Sharma, M., Gutleb, A.C., and Clippinger, A.J., *Toxicology in vitro : an international journal published in association with BIBRA*, Vol. 83, 105423, 2022.

[70] Cooper, J.R., Abdullatif, M.B., Burnett, E.C., Kempsell, K.E., Conforti, F., Tolley, H., Collins, J.E., and Davies, D.E., *PloS one*, Vol. 11, e0164438, 2016.

[71] Hauptmann, S., and Wilde, H., *Chem. Ber.*, Vol. 101, 1349–1353, 1968.

[72] Sonawane, S.J., Kalhapure, R.S., and Govender, T., *European journal of pharmaceutical sciences : official journal of the European Federation for Pharmaceutical Sciences*, Vol. 99, 45–65, 2017.

[73] Etrych, T., Subr, V., Laga, R., Říhová, B., and Ulbrich, K., *European journal of pharmaceutical sciences : official journal of the European Federation for Pharmaceutical Sciences*, Vol. 58, 1–12, 2014.

[74] Lu, D., Wen, X., Liang, J., Gu, Z., Zhang, X., and Fan, Y., *Journal of biomedical materials research. Part B, Applied biomaterials*, Vol. 89, 177–183, 2009.

APPENDIX

Ad linkers:

Propargylglycine amide linker:

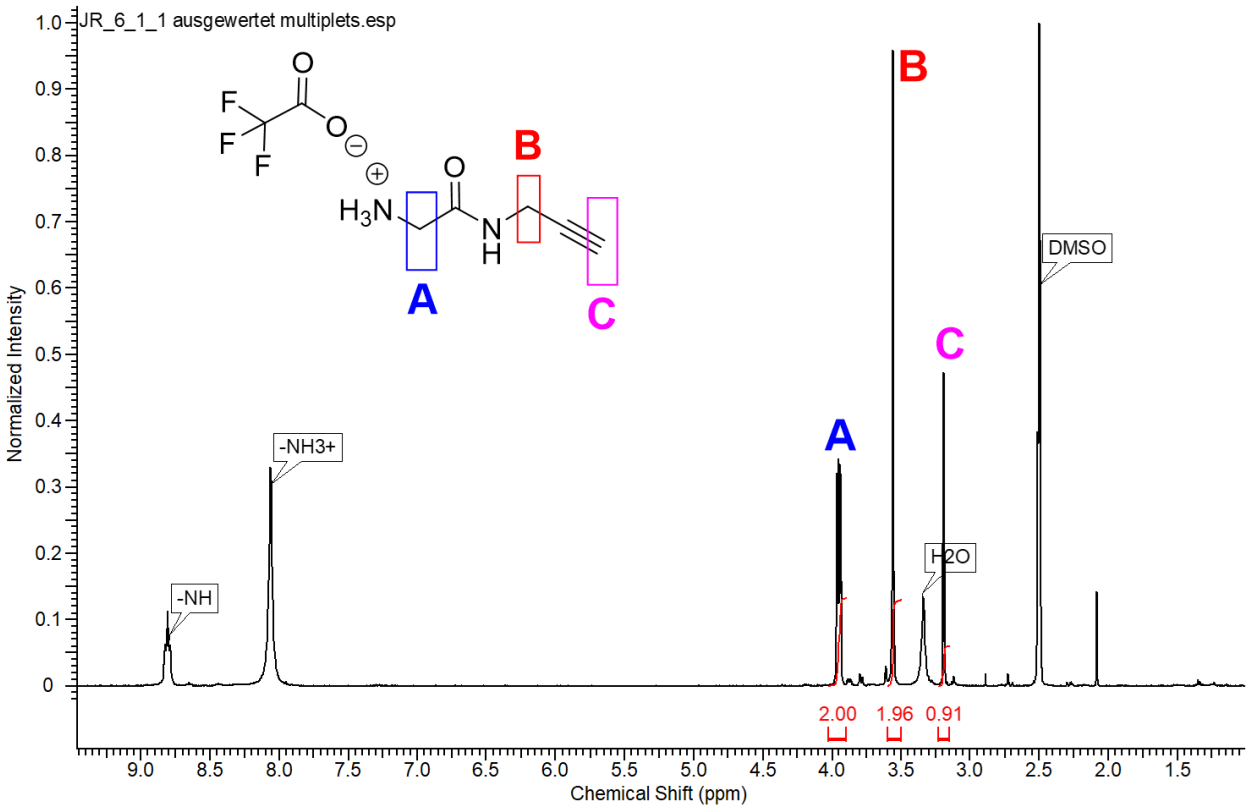

Figure 46: [1]H NMR spectrum in DMSO-d6 of propargylglycine amide linker, deprotected with TFA.

[1]H, 300 MHz, DMSO-d6: δ=3.95 (dd, J=5.5 Hz; 2.5, 2H), 3.56 (s, 2H), 3.19 (t, J=2.5 Hz, 1H) ppm.

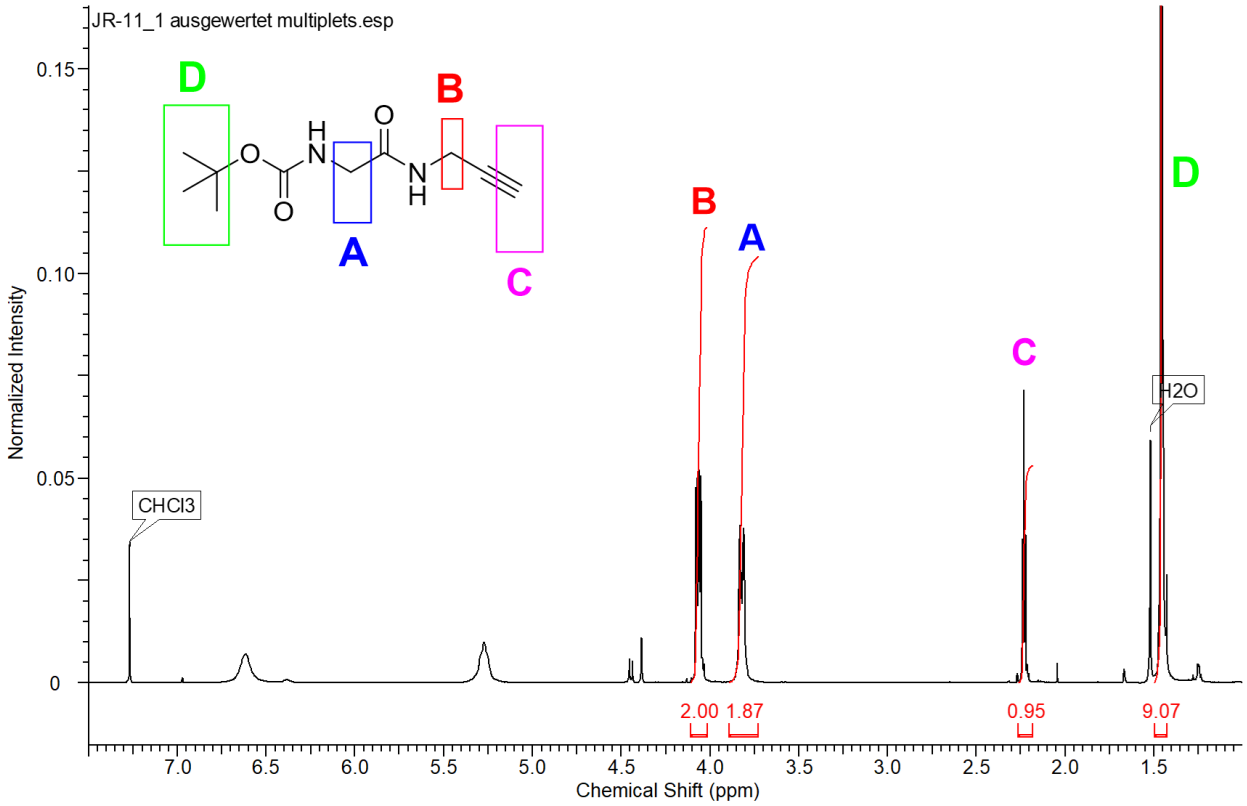

Figure 47: ^{1}H NMR spectrum in $CDCl_3$ of Boc-propargylglycine amide linker.

^{1}H, 300 MHz, $CDCl_3$: δ= 4.07 (dd, J=5.4 Hz, 2.6 Hz, 2H), 2.23 (t, J=2.6 Hz; 1H), 1.44 (s, 9H) ppm.

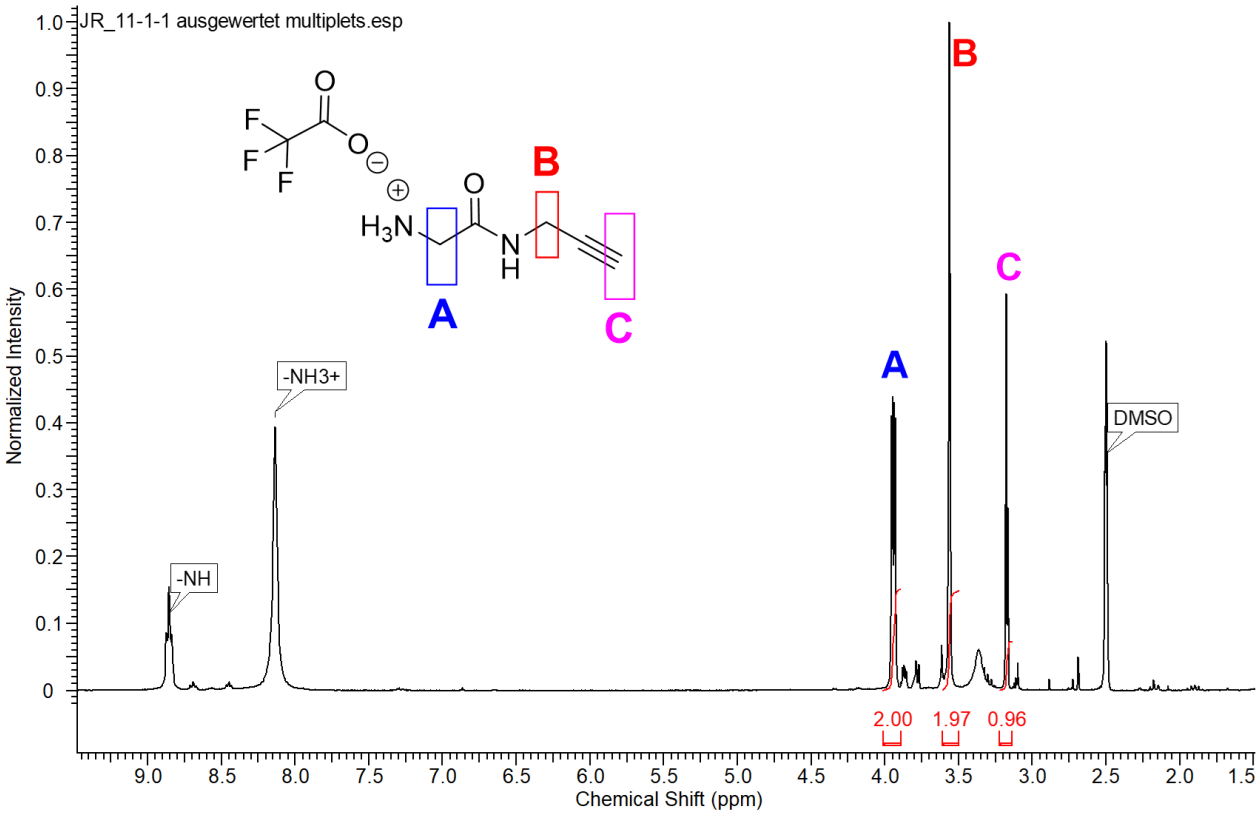

Figure 48: ^{1}H NMR spectrum in DMSO-d6 of the propargylglycine amide linker, deprotected with TFA.

^{1}H, 300 MHz, DMSO-d6: δ= 3.94 (dd, J=5.4 Hz, 2.6 Hz, 2H), 3.56 (s, 2H), 3.17 (t, J=2.6 Hz; 1H) ppm.

Propargylglycine ester linker:

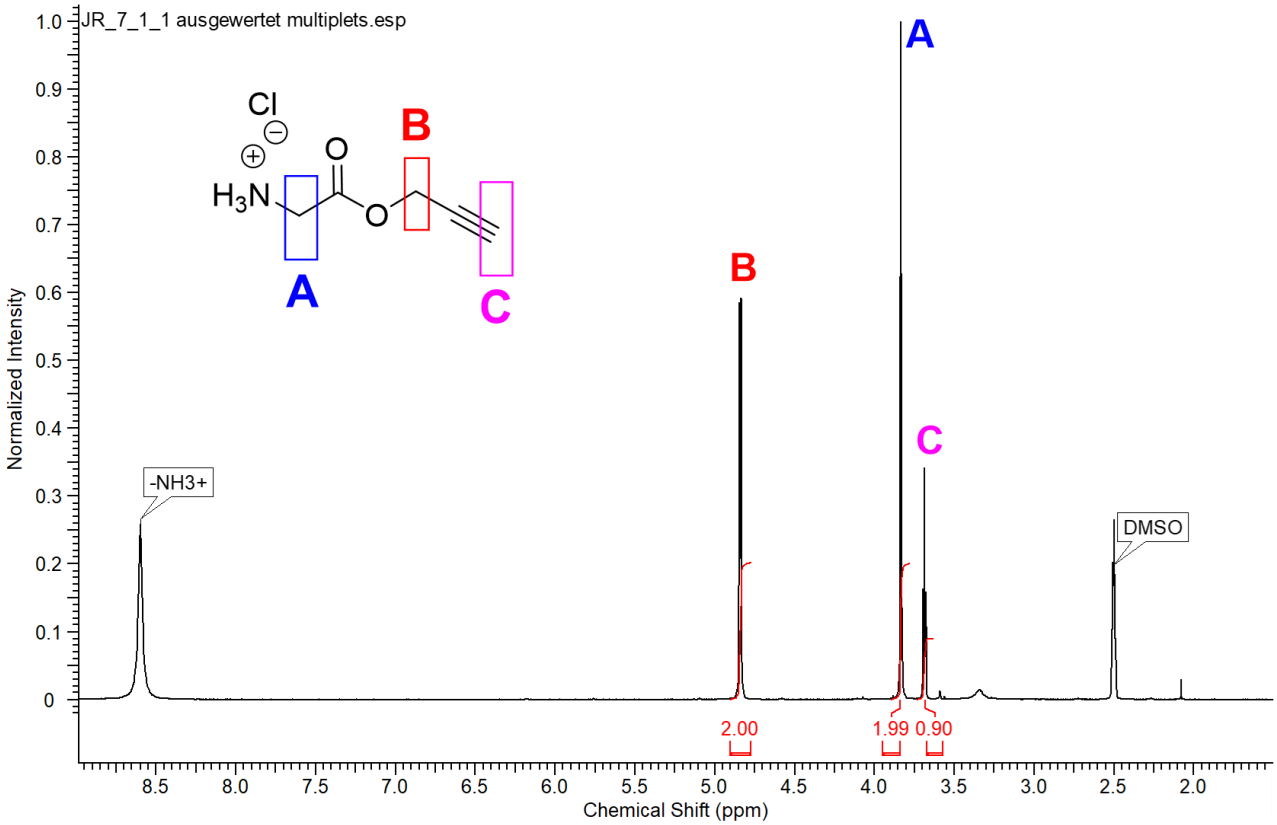

Figure 49: ^{1}H NMR spectrum in DMSO-d6 of propargylglycine ester linker, deprotected with HCl / Dioxane.

^{1}H, 300 MHz, DMSO-d6: δ= 4.84 (d, J=2.5 Hz, 2H), 3.83 (s, 2H), 3.69 (t, J=2.5 Hz; 1H) ppm.

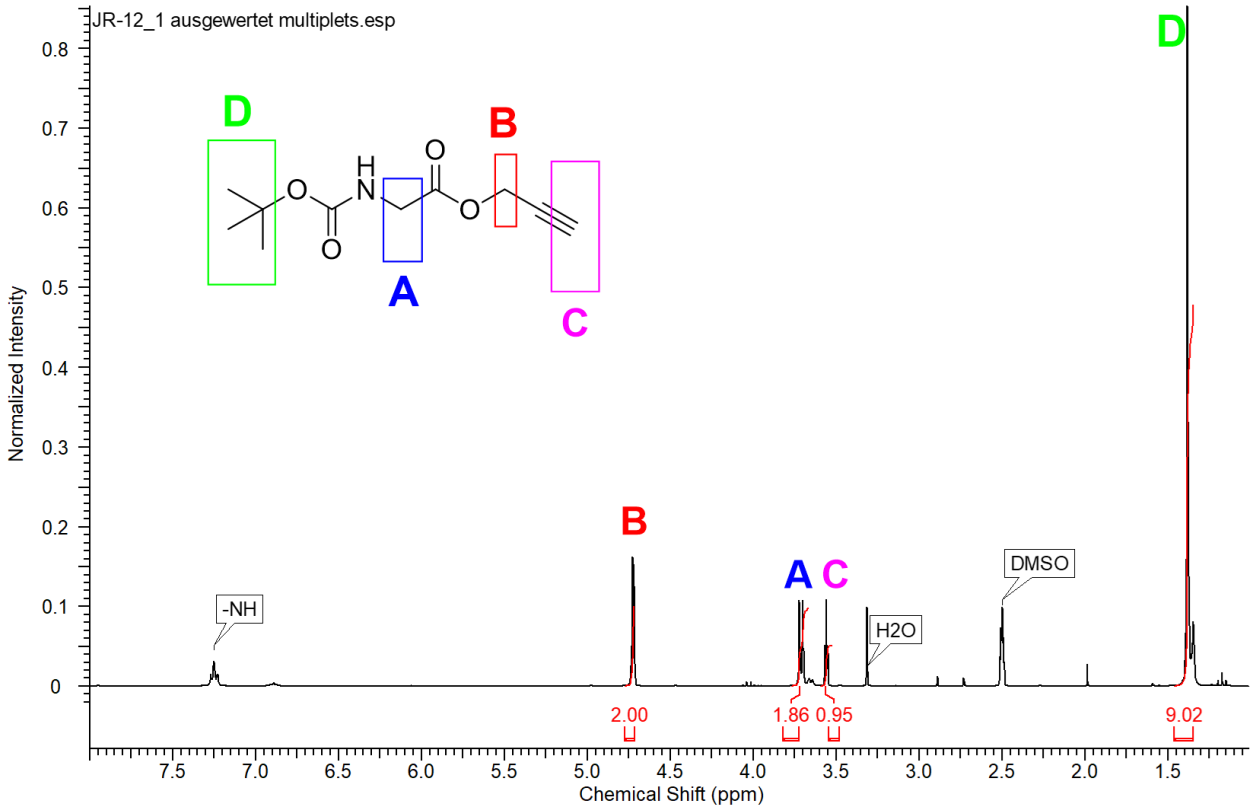

Figure 50: ^{1}H NMR spectrum in DMSO-d6 of the Boc-protected propargylglycine ester linker.

^{1}H, 300 MHz, DMSO-d6: δ= 4.72 (d, J=2.4 Hz; 2H), 3.71 (d, J=6.1 Hz, 2H), 3.56 (t, J=2.4 Hz; 1H), 1.38 (s, 9H) ppm.

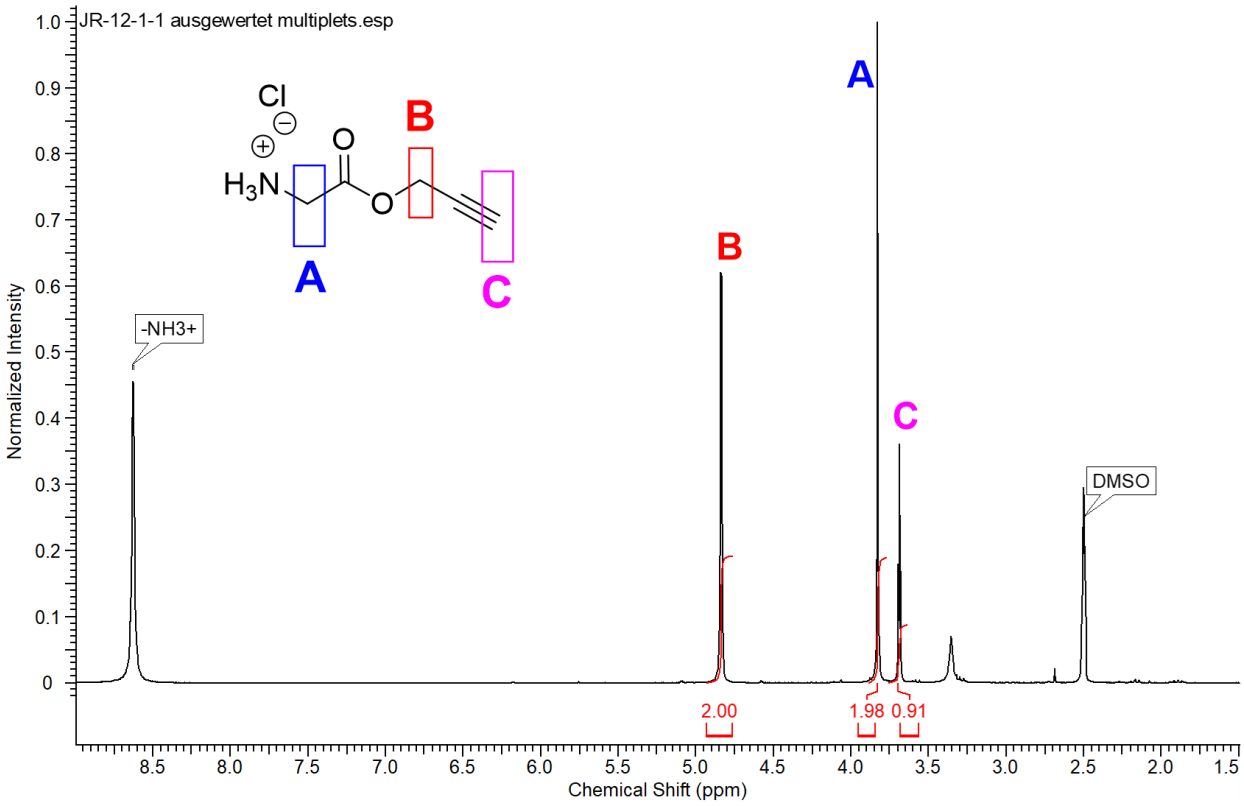

Figure 51: ^{1}H NMR spectrum in DMSO-d6 of propargylglycine ester linker, deprotected with HCl / Dioxane.

^{1}H, 300 MHz, DMSO-d6: δ= 4.84 (d, J=2.4 Hz; 2H), 3.83 (s, 2H), 3.69 (t, J=2.4 Hz; 1H) ppm.

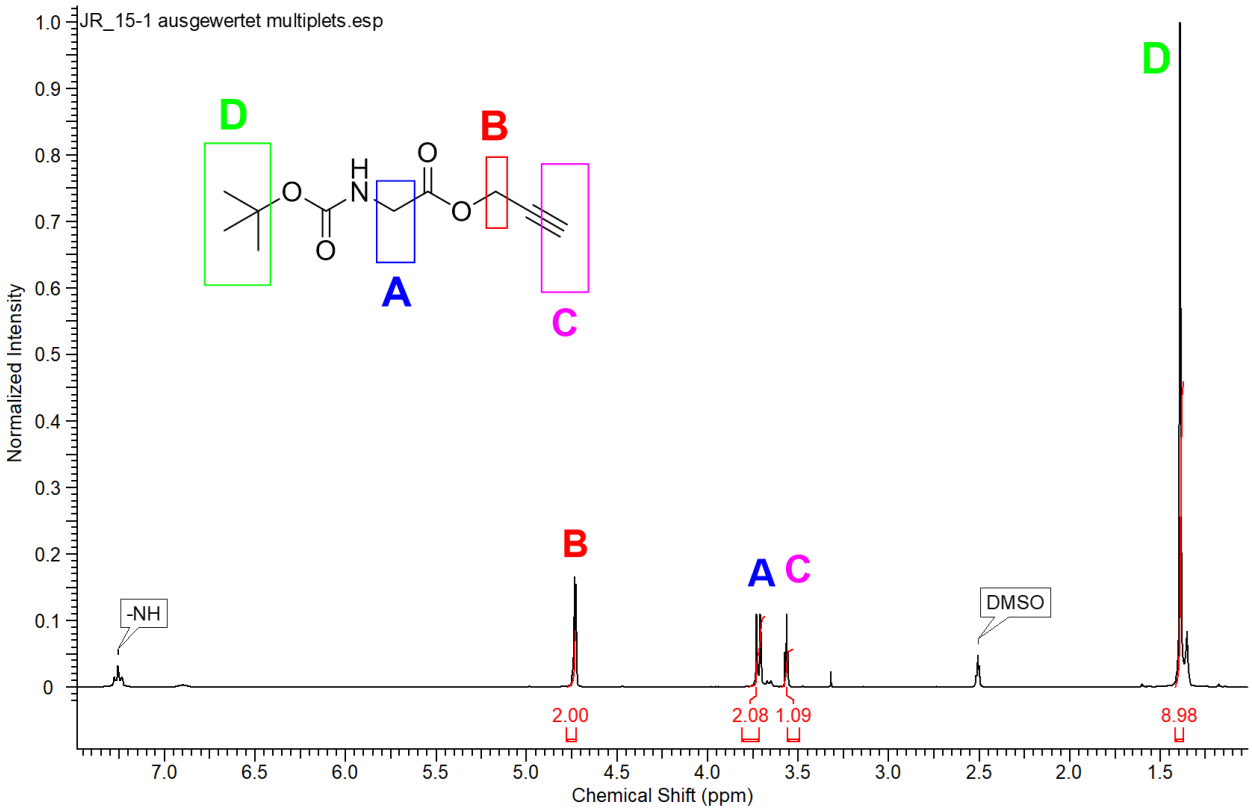

Figure 52: ^{1}H NMR in DMSO-d6 of propargylglycine ester linker, -Boc protected.

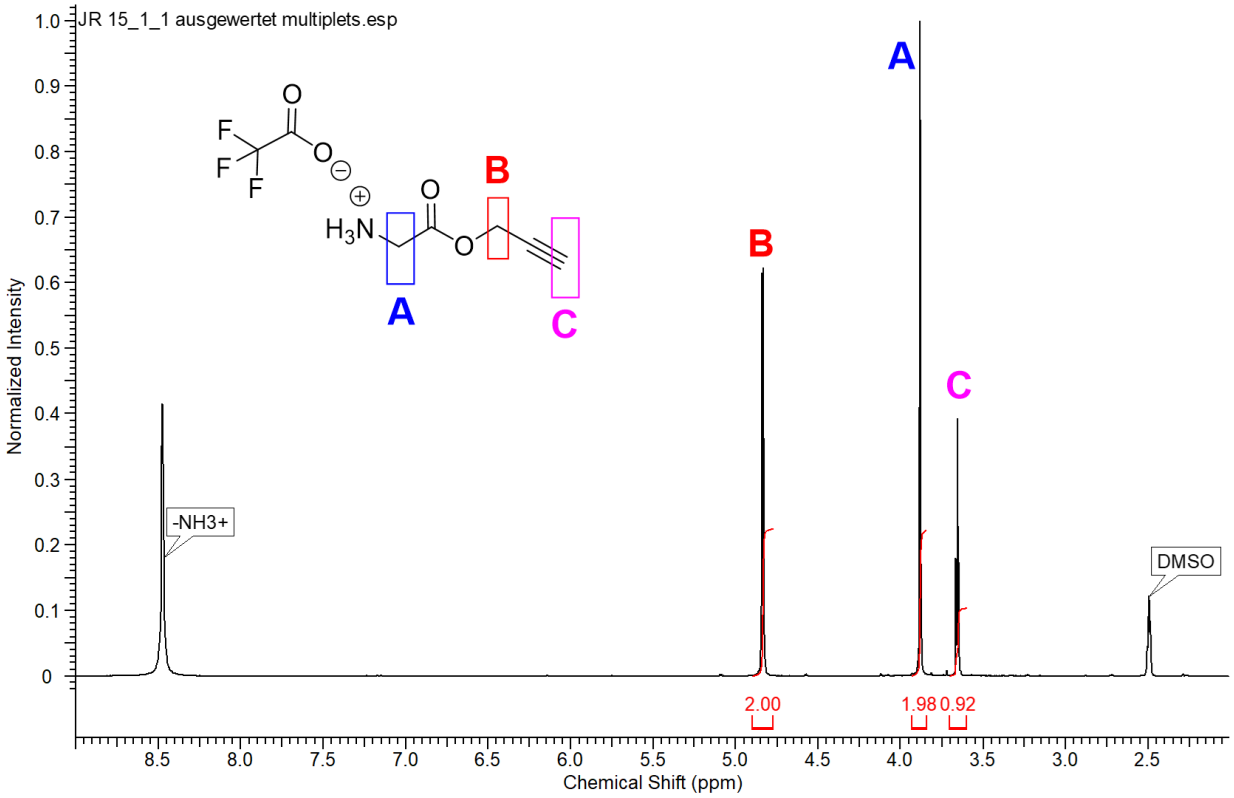

Figure 53: ^{1}H NMR spectrum in DMSO-d6 of propargylglycine ester linker, deprotected with TFA.

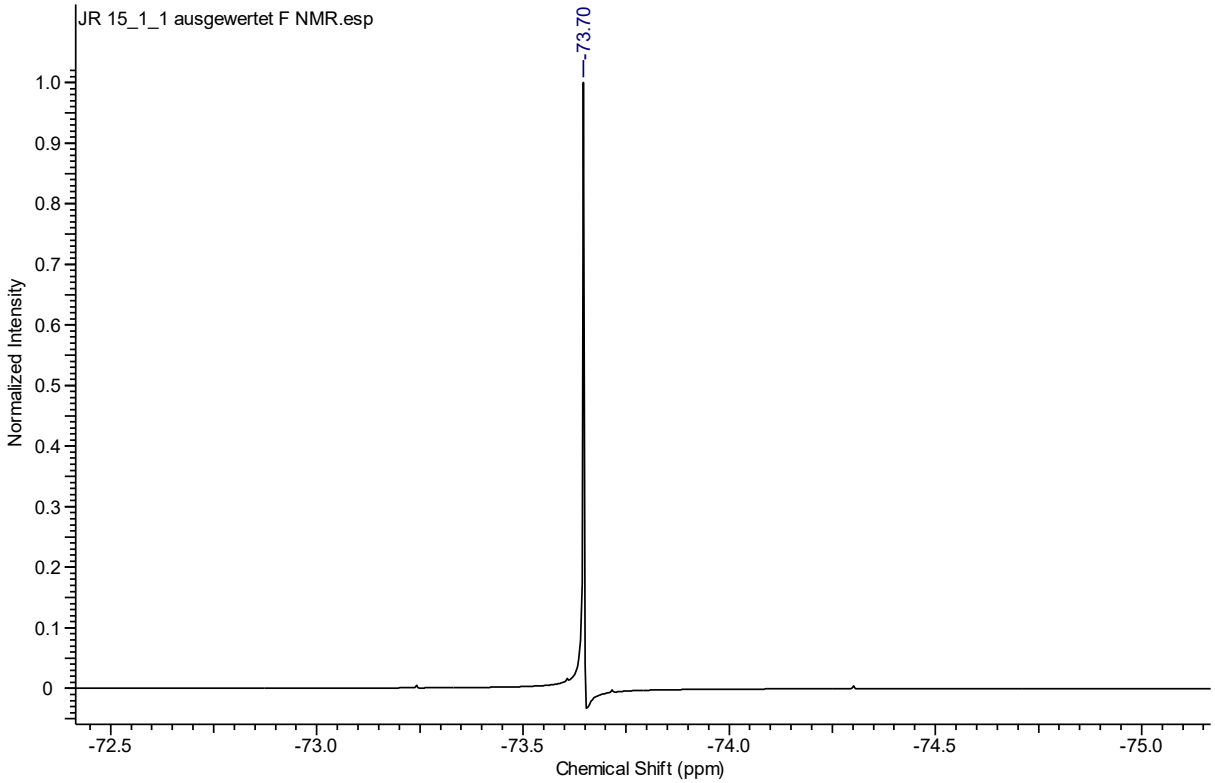

Figure 54: ^{19}F NMR spectrum in DMSO-d6 of propargylglycine ester linker, deprotected with TFA.

^{1}H, 300 MHz, DMSO-d6: δ= 4.73 (d, J=2.5; 2H), 3.72 (d, J=6.1; 2H), 3.56 (t, J=2.5 x2; 1H), 1.39 (s, 9H) ppm.

^{1}H, 300 MHz, DMSO-d6: δ= 8.47 (s, 3H -NH_3), 4.84 (d, J=2.4; 2H), 3.88 (s, 2H), 3.66 (t, J= 2.4 x2; 1H) ppm.
^{19}F, 300 MHz, DMSO-d6: δ= -73.70 ppm.

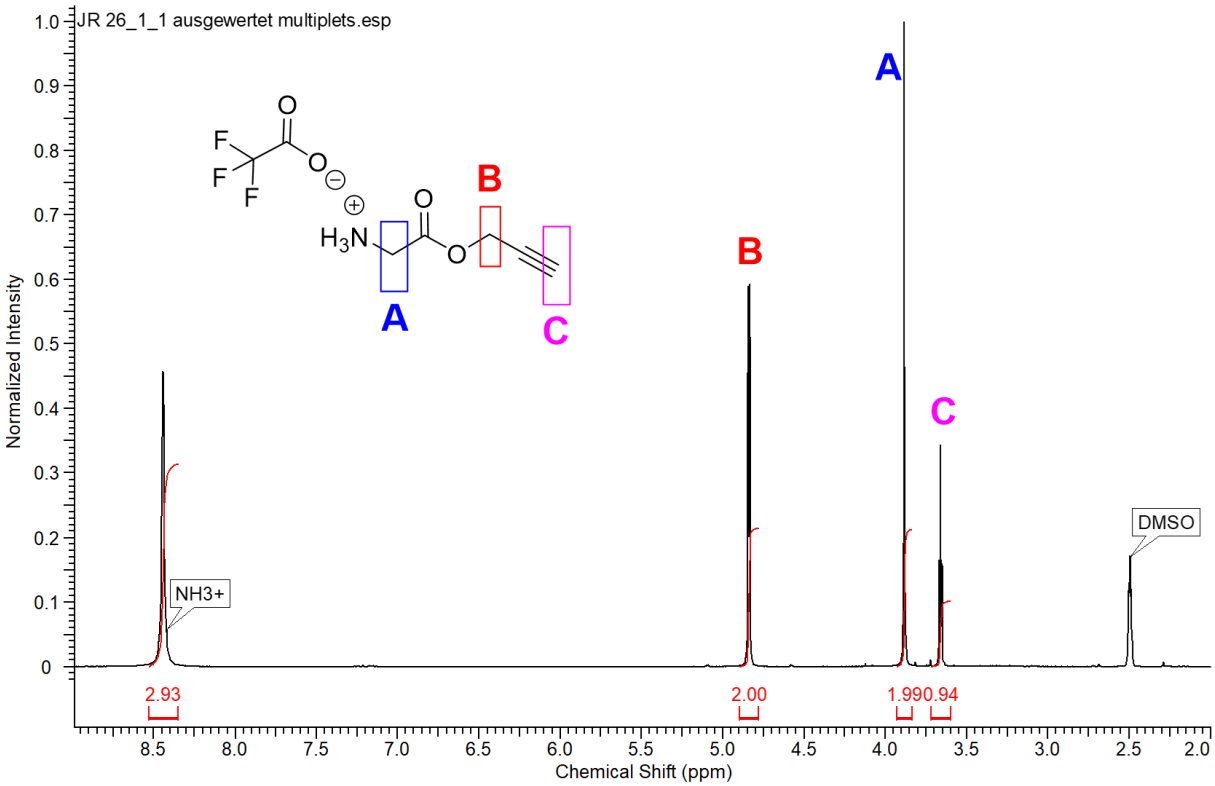

Figure 55: ^{1}H NMR in DMSO-d6 of propargylglycine ester linker, deprotected with TFA.

^{1}H, 300 MHz, DMSO-d6: δ= 8.44 (s, 3H, -NH_3), 4.84 (d, J=2.5 Hz; 2H), 3.88 (s, 2H), 3.66 (t, J=2.5 Hz; 1H) ppm.

[t]Butyl(2-(2-(2-aminoethoxy)ethoxy)ethyl)carbamate linker:

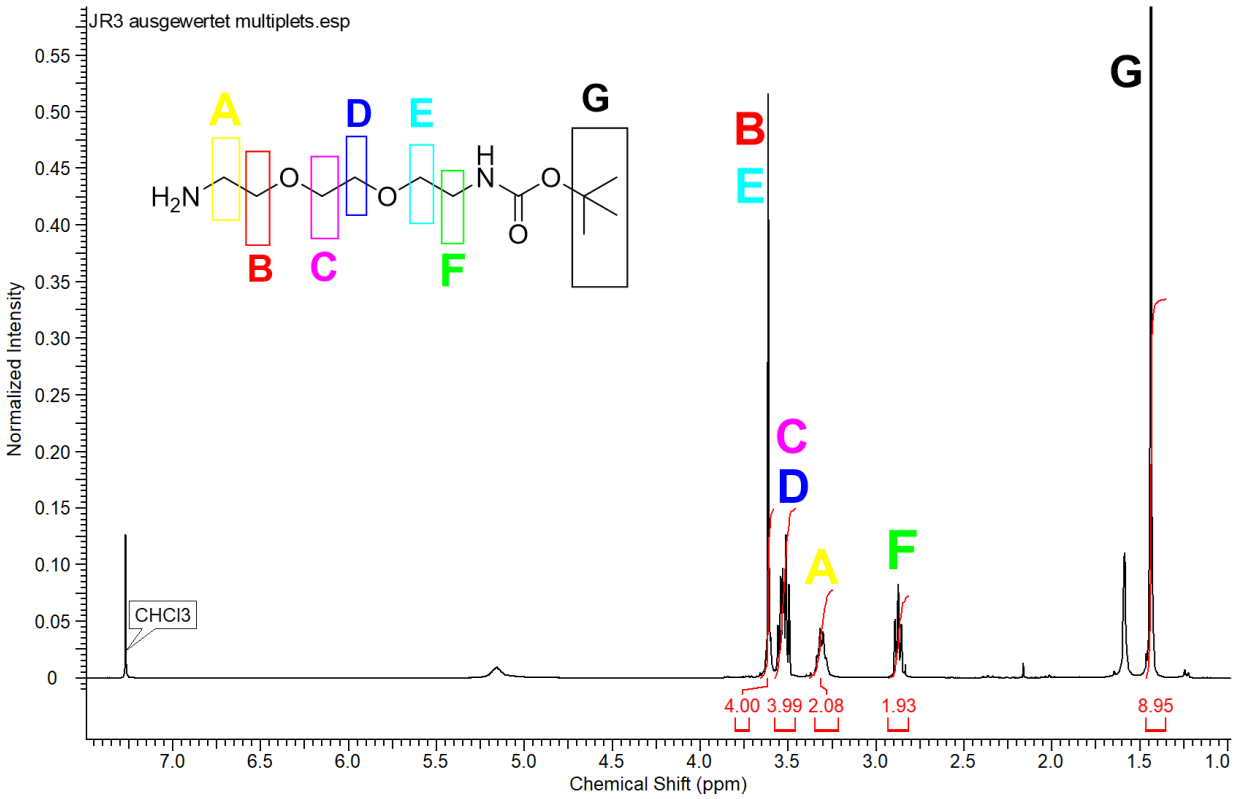

Figure 56. [1]H NMR spectrum in $CDCl_3$ of tbutyl(2-(2-(2-aminoethoxy)ethoxy)ethyl)carbamate linker.

[1]H, 300 MHz, $CDCl_3$: δ= 3.61 (m, 4H), 3.53 (m, 4H), 3.32 (m, 2H), 2.87 (t, J=5.2 Hz; 2H), 1.45 (s, 9H) ppm.

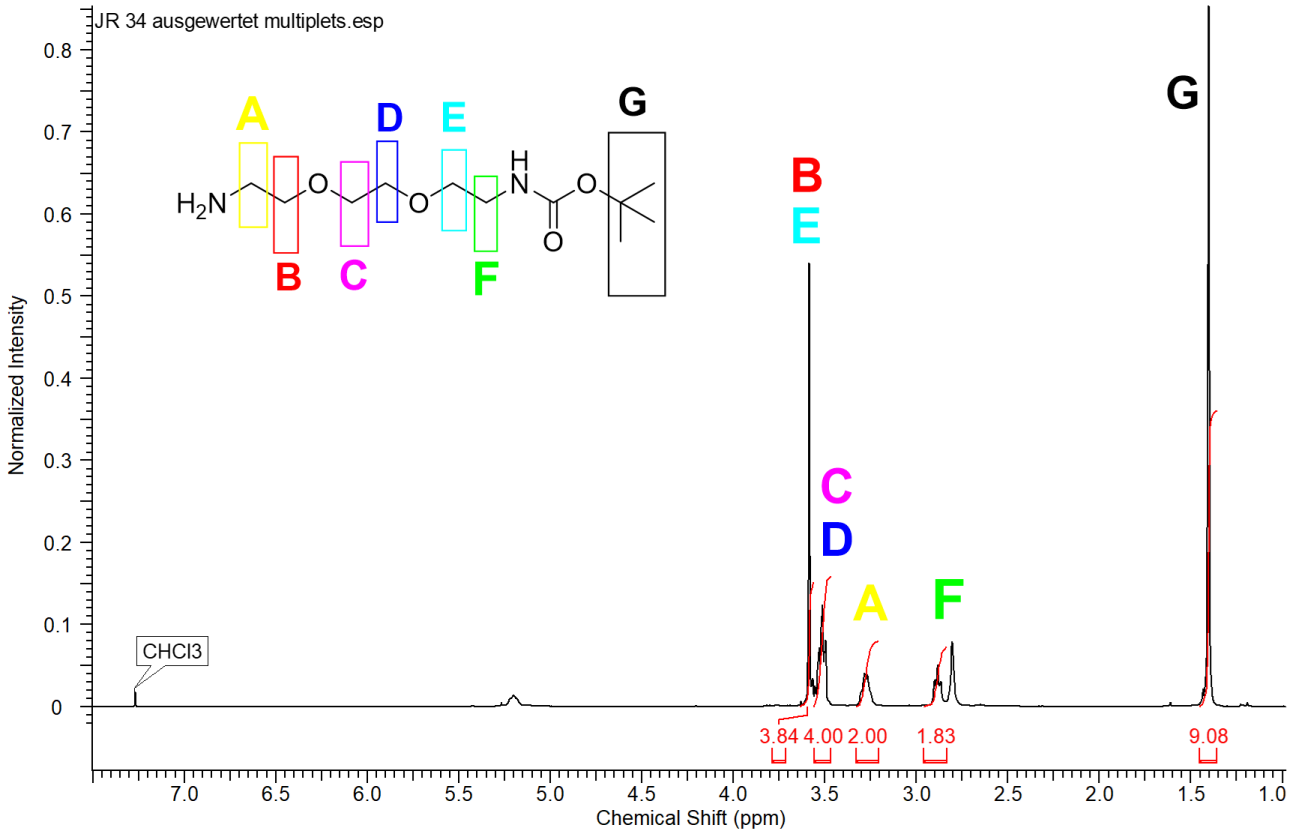

Figure 57: ^{1}H NMR in $CDCl_3$ of tbutyl(2-(2-(2-aminoethoxy)ethoxy)ethyl)carbamate linker.

^{1}H, 300 MHz, $CDCl_3$: δ= 3.59 (m, 4H), 3.51 (m, 4H), 3.28 (d, J=4.8 Hz; 2H), 2.88 (t, J= 5.0 Hz; 2H), 1.40 (s, 9H) ppm.

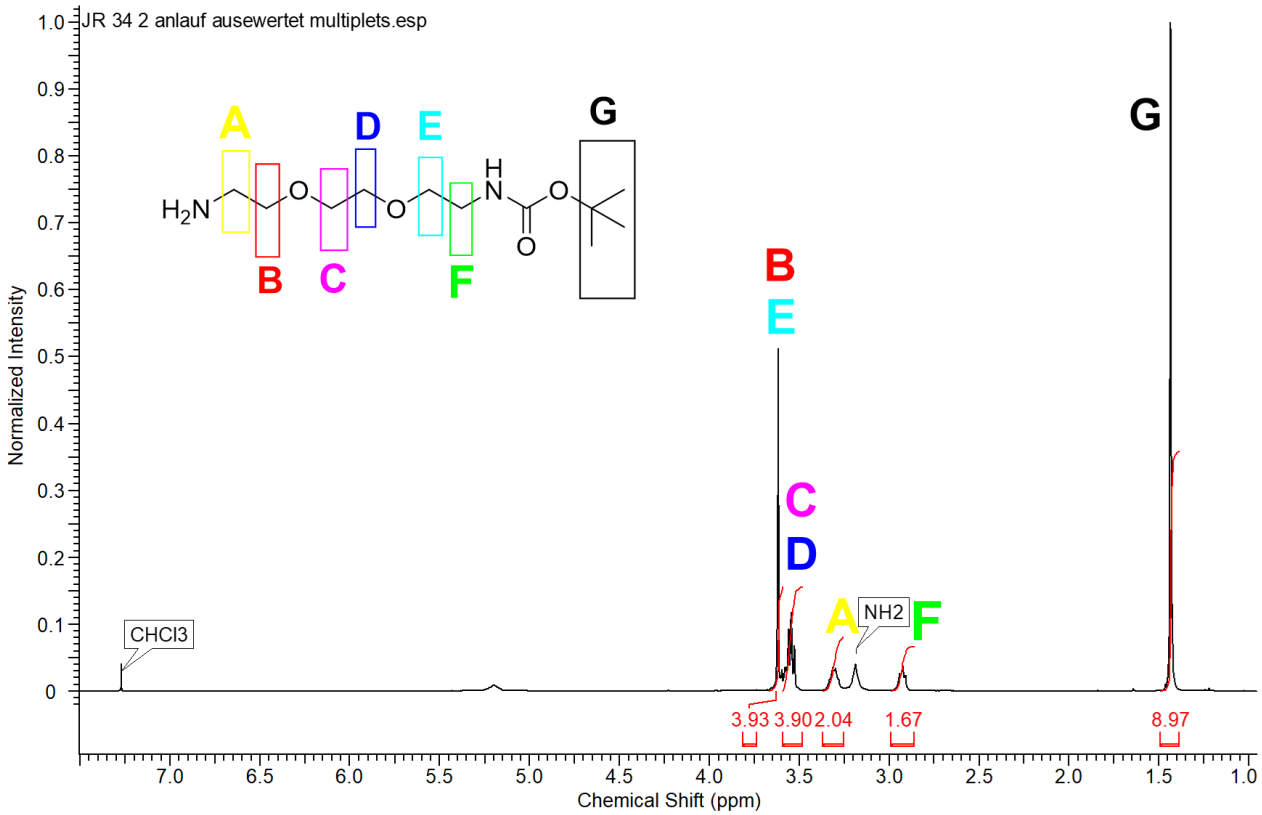

Figure 58: ^{1}H NMR in $CDCl_3$ of tbutyl(2-(2-(2-aminoethoxy)ethoxy)ethyl)carbamate linker.

^{1}H, 300 MHz, $CDCl_3$: δ= 3.62 (m, 4H), 3.55 (q, J=5.3 Hz; 4H), 3.31 (d, J=4.9 Hz; 2H), 2.93 (t, J=4.9 Hz; 2H), 1.43 (s, 9H) ppm.

Hydrazide Linker:

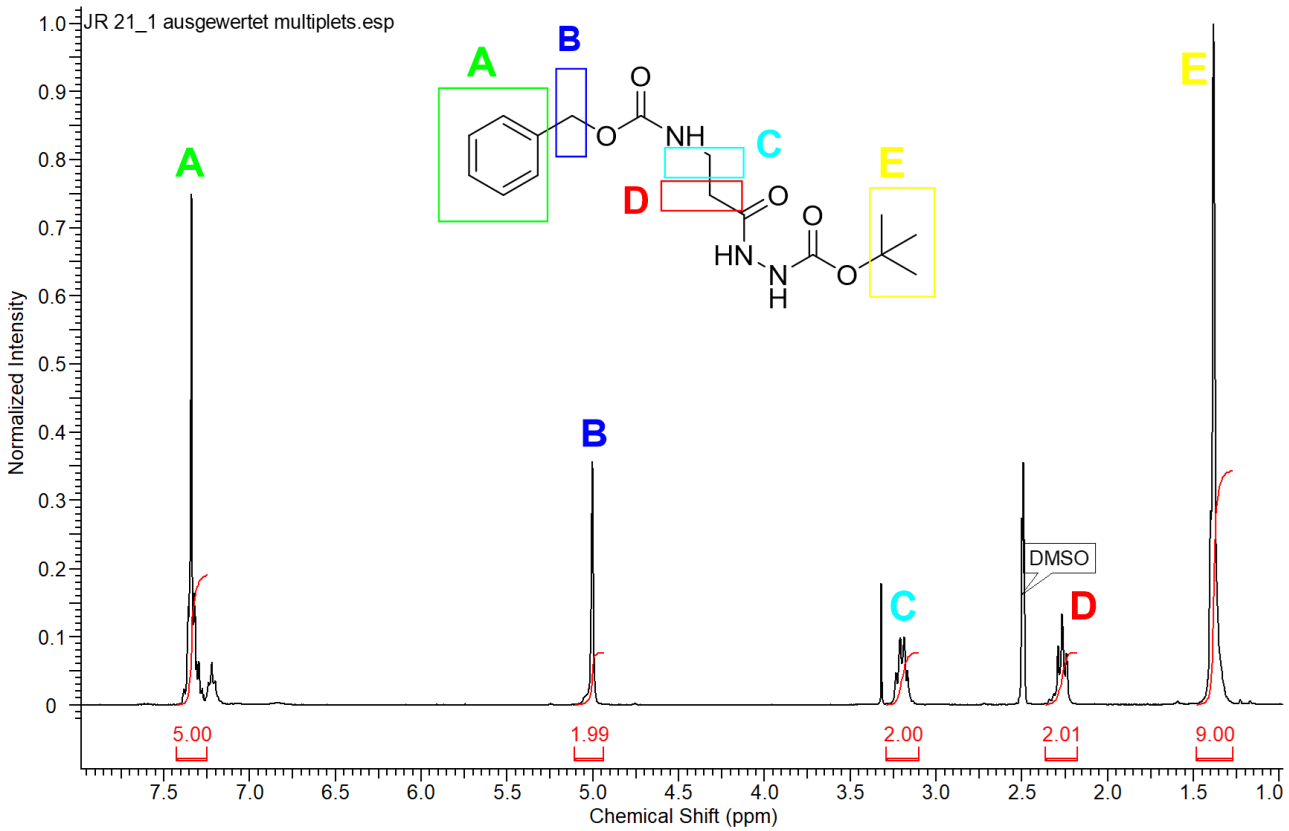

Figure 59: ^{1}H NMR spectrum in DMSO-d6 of Z- β-alanyl-Boc-hydrazide linker.

^{1}H, 300 MHz, DMSO-d6: δ= 7.33 (m, 5H), 5.00 (s, 2H), 3.20 (q, J=6.8 Hz; 2H), 2.27 (t, J=7.4 Hz; 2H), 1.38 (s, 9H) ppm

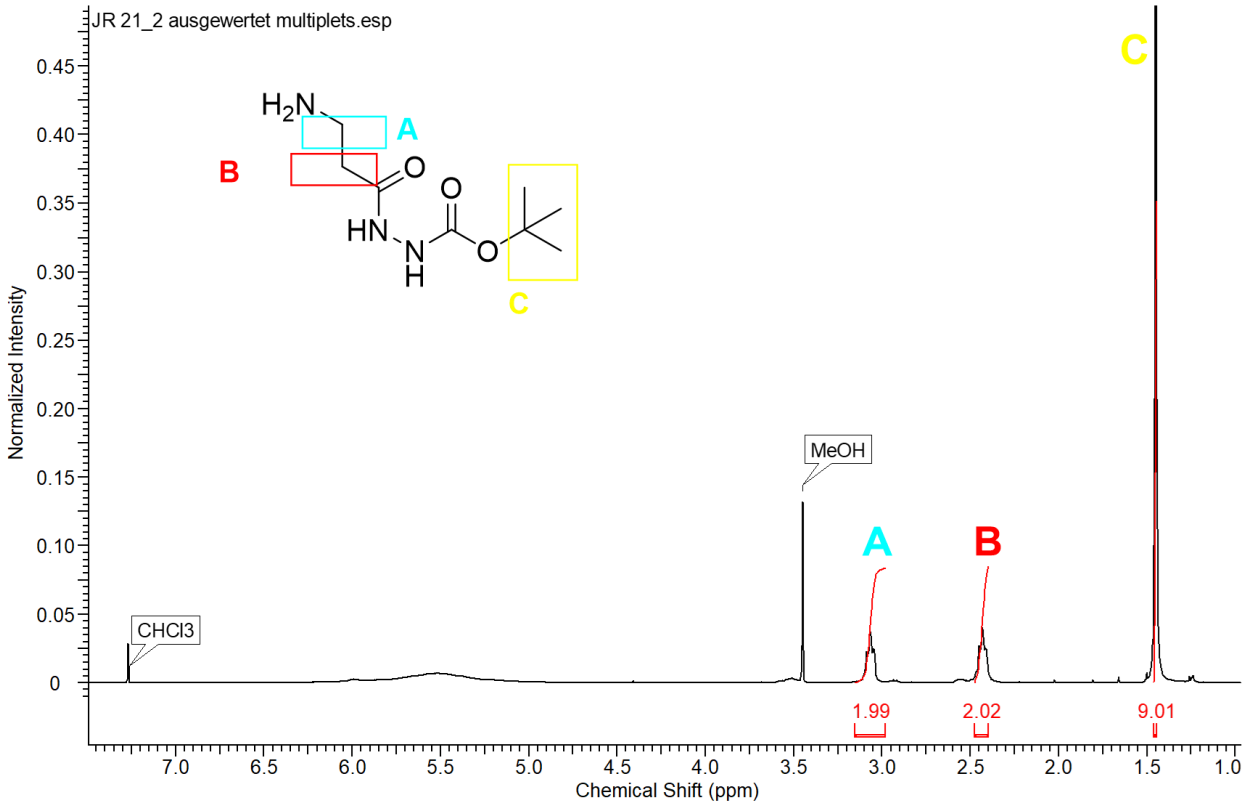

Figure 60: ^{1}H NMR spectrum in $CDCl_3$ of β-alanyl-Boc-hydrazide linker.

^{1}H, 300 MHz, $CDCl_3$: δ= 3.07 (t, J= 5.7 Hz; 2H), 2.43 (t, J=5.7 Hz; 2H), 1.45 (s, 9H) ppm.

***Ad* Macromolecular substitution:**

PPz with Propargylglycine amide linker:

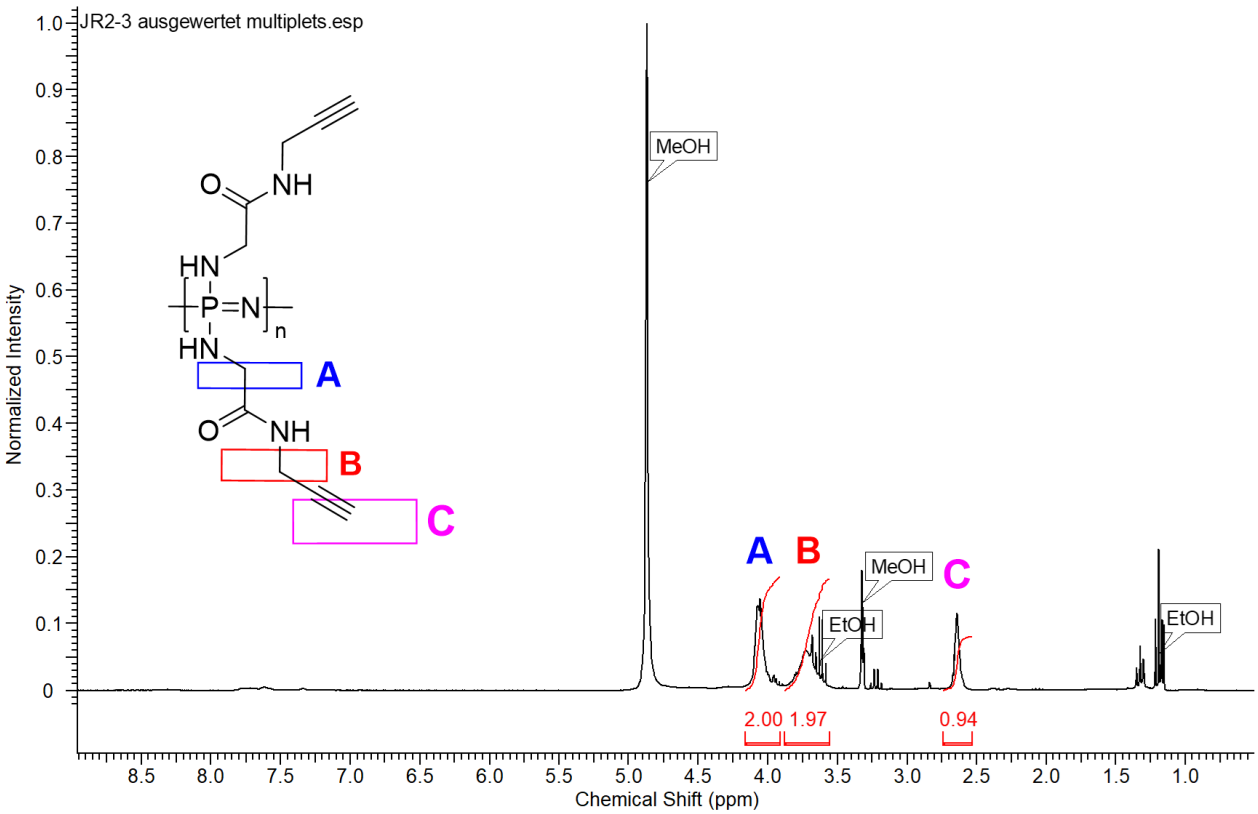

Figure 61: ^{1}H NMR spectrum in MeOD of PPz macrosubstituted with the propargylglycine amide linker.

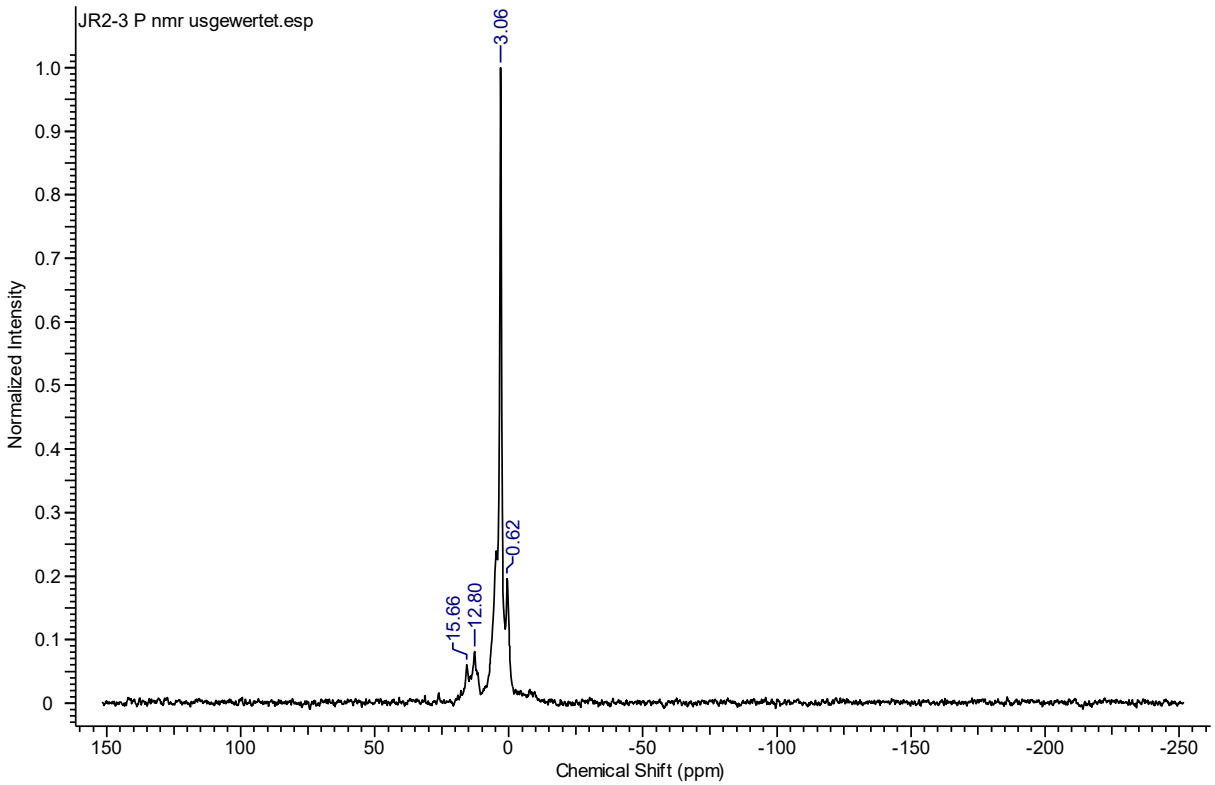

Figure 62. ^{31}P NMR spectrum in MeOD of PPz macrosubstituted with the propargylglycine amide linker.

^{1}H, 300 MHz, MeOD: δ= 4.02 (m, 2h), 3.69 (m, 2H), 2.63 (m, 1H) ppm.

^{31}P, 121.49 MHz, MeOD: δ= 3.06 ppm.

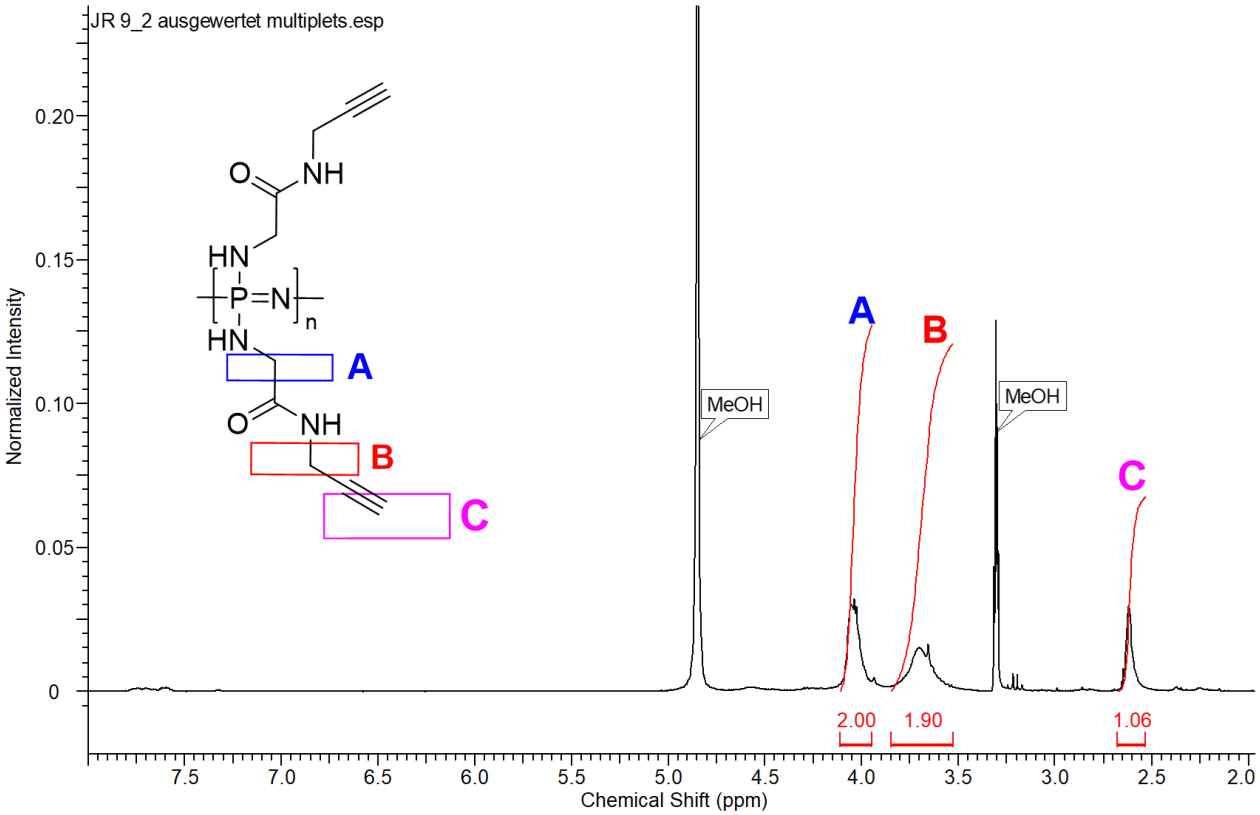

Figure 63: ^{1}H NMR in MeOD of macro substituted PPz, with propargylglycine amide linker.

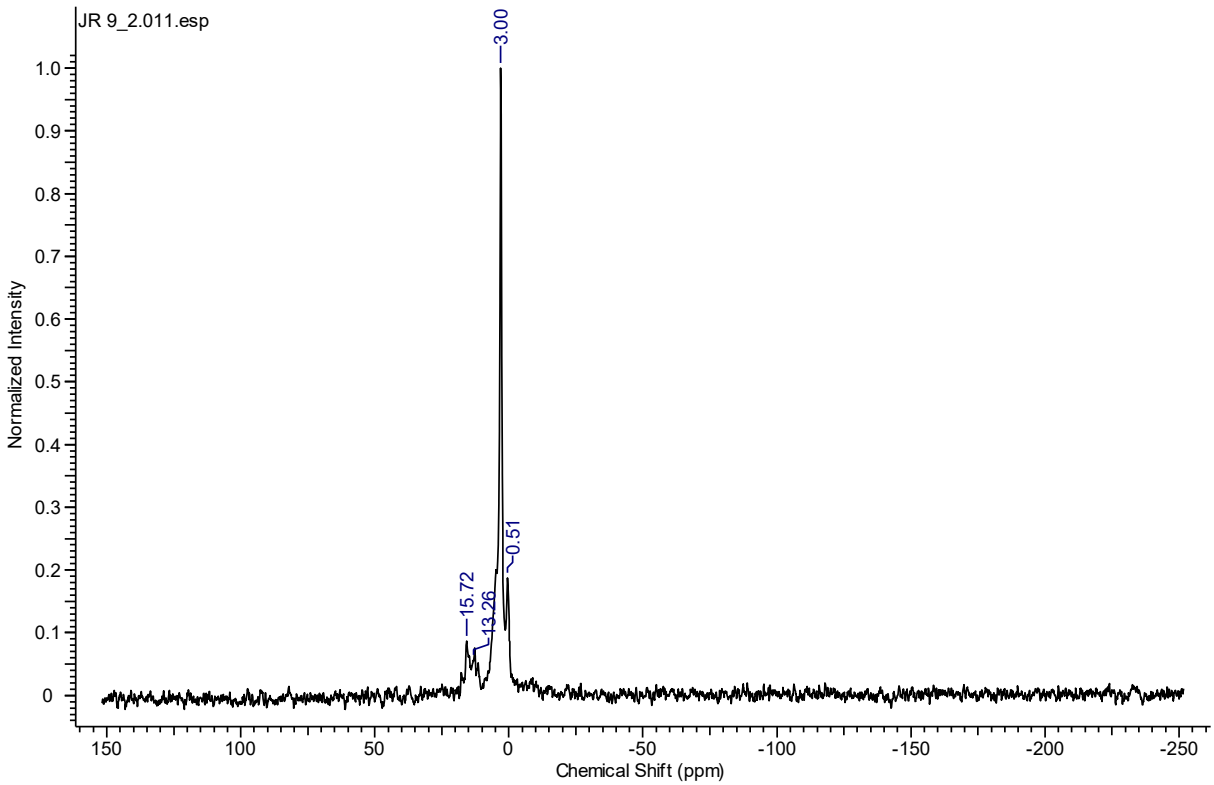

Figure 64: ^{31}P NMR in MeOD of macro substituted PPz, with propargylglycine amide linker.

^{1}H, 300 MHz, MeOD: δ= 4.06 (m, 2H), 3.69 (m, 2H), 2.64 (m, 1H) ppm.

^{31}P, 121.49 MHz, MeOD: δ= 3.00 ppm.

PPz with Propargylglycine ester linker:

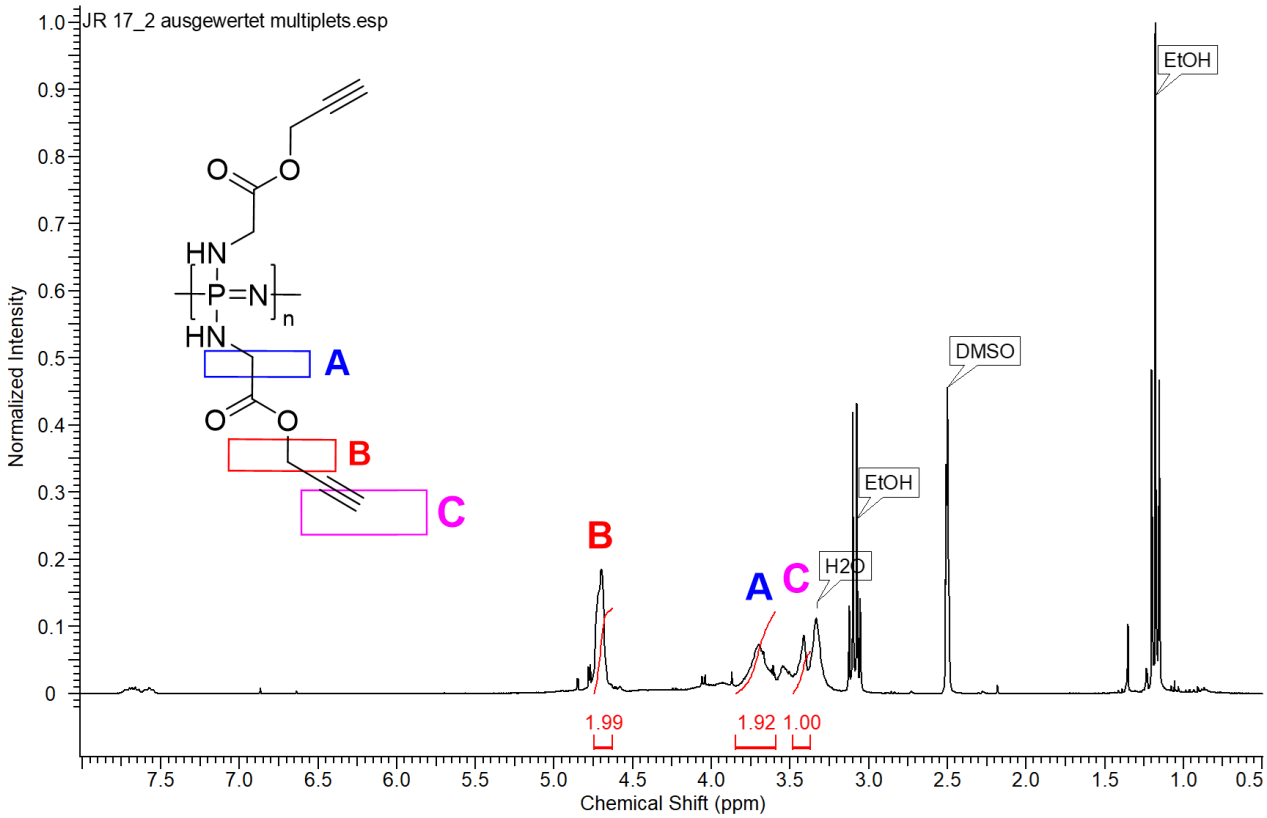

Figure 65: ^{1}H NMR spectrum in DMSO-d6 of PPz macrosubstituted with the propargylglycine ester linker.

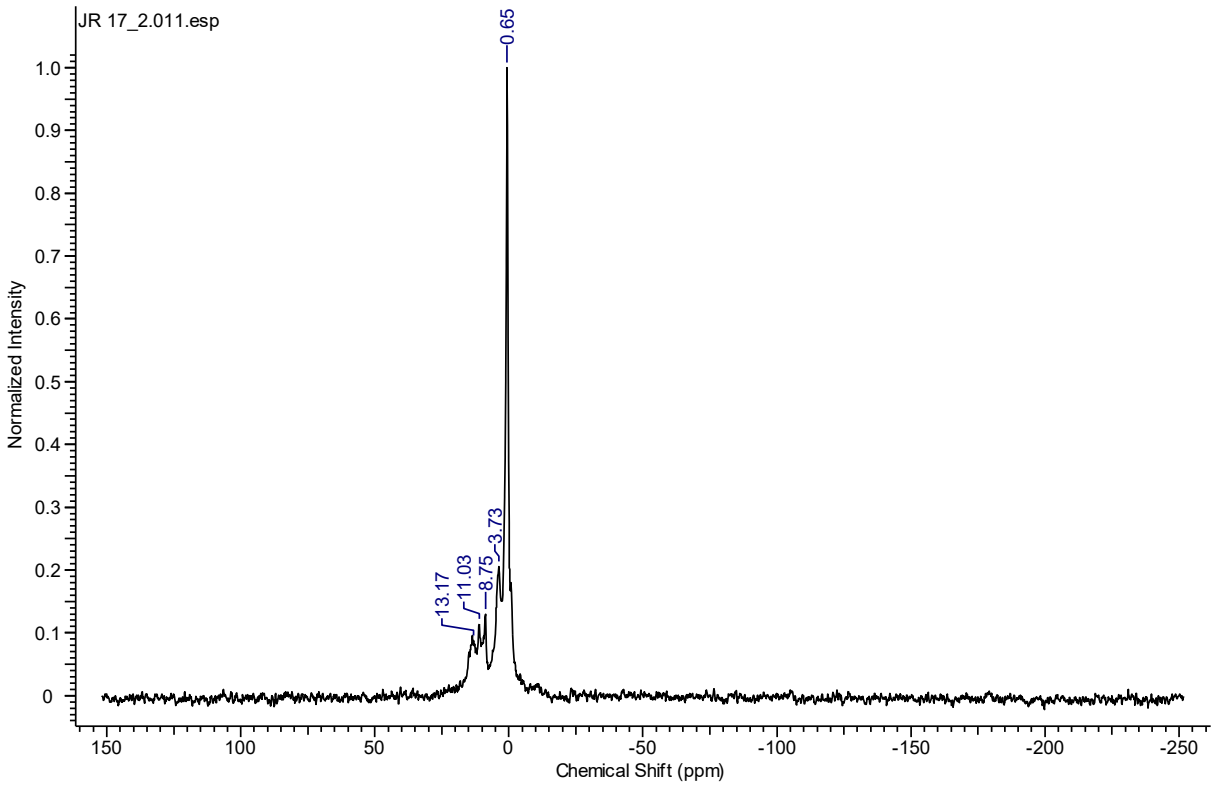

Figure 66: ^{31}P NMR spectrum in DMSO-d6 of PPz macrosubstituted with the propargylglycine ester linker.

^{1}H, 300 MHz, DMSO-d6: δ= 4.75 (m, 2H), 3.66 (m, 2H), 3.43 (m, 1H) ppm.

^{31}P, 121.49 MHz, DMSO-d6: δ= 0.65, 3.73 ppm.

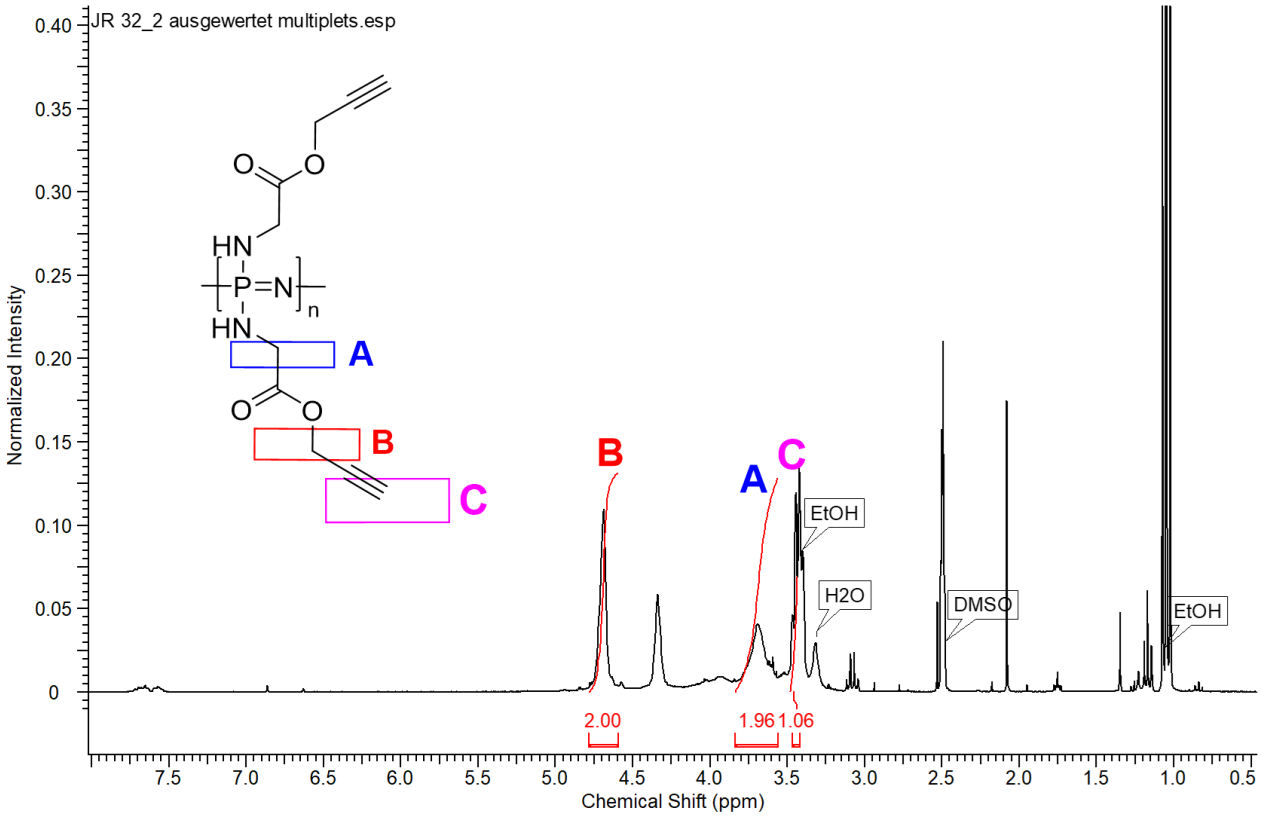

Figure 67. [1]H NMR in DMSO-d6 of macro substituted PPz, with propargylglycine ester linker.

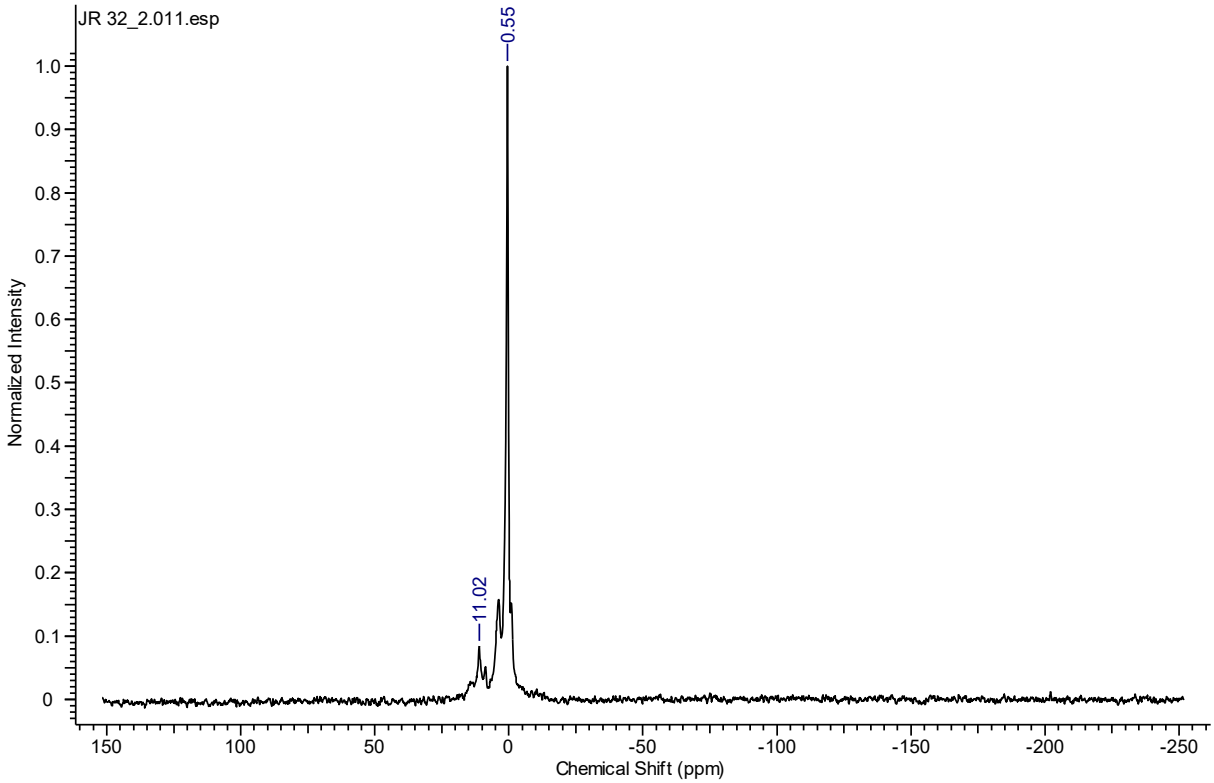

Figure 68: [31]P NMR in DMSO-d6 of macro substituted PPz, with propargylglycine ester linker).

^{1}H, 300 MHz, DMSO-d6: δ= 4.69 (m, 2H), 3.69 (m, 2H), 3.44 (m, 1H) ppm.

^{31}P, 121.49 MHz, DMSO-d6: δ= 0.55 ppm.

PPz with ^{t}butyl(2-(2-(2-aminoethoxy)ethoxy)ethyl)carbamate linker:

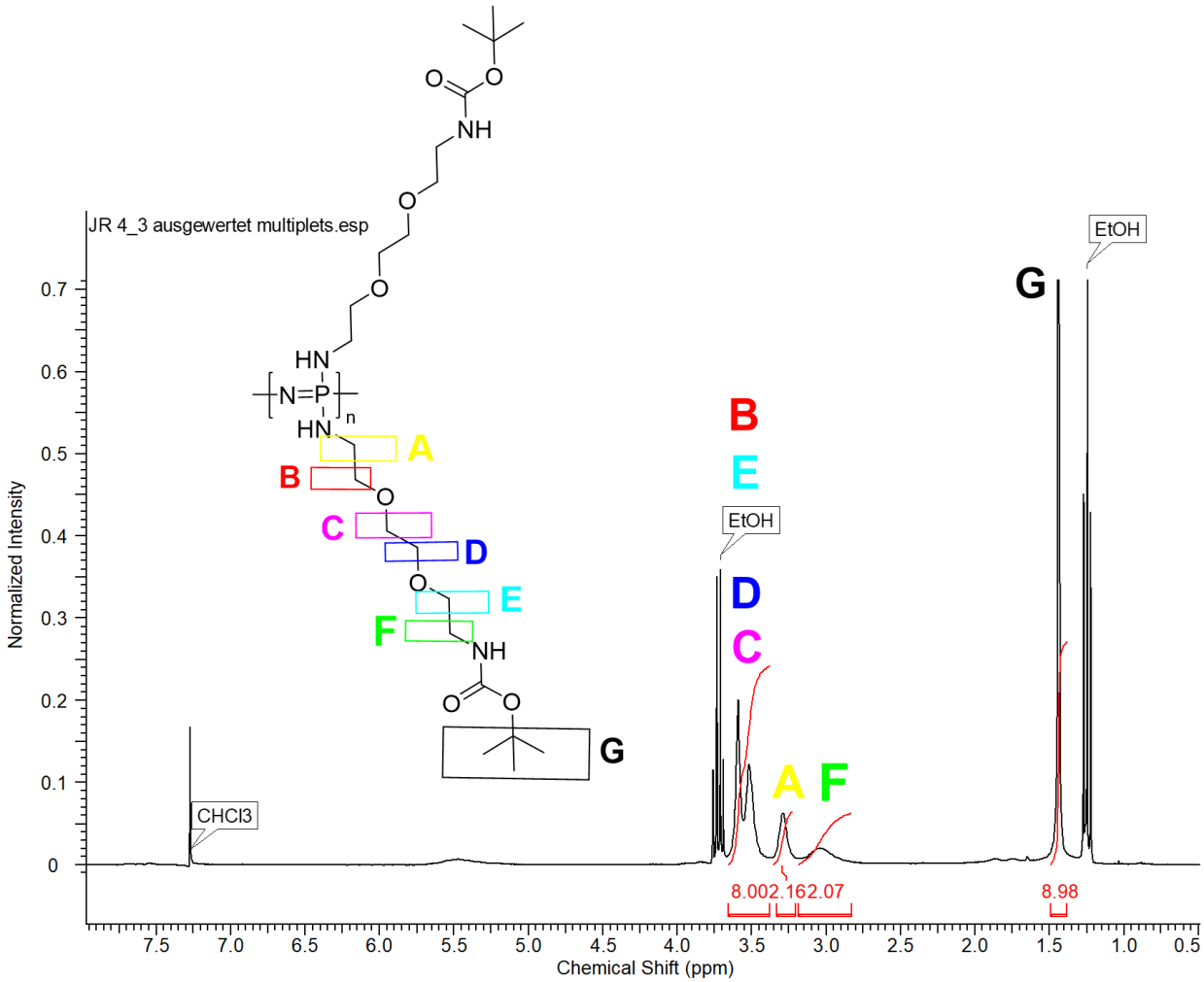

Figure 69: ^{1}H NMR spectrum in $CDCl_3$ of PPz macrosubstituted with tbutyl(2-(2-(2-aminoethoxy)ethoxy)ethyl)carbamate linker.

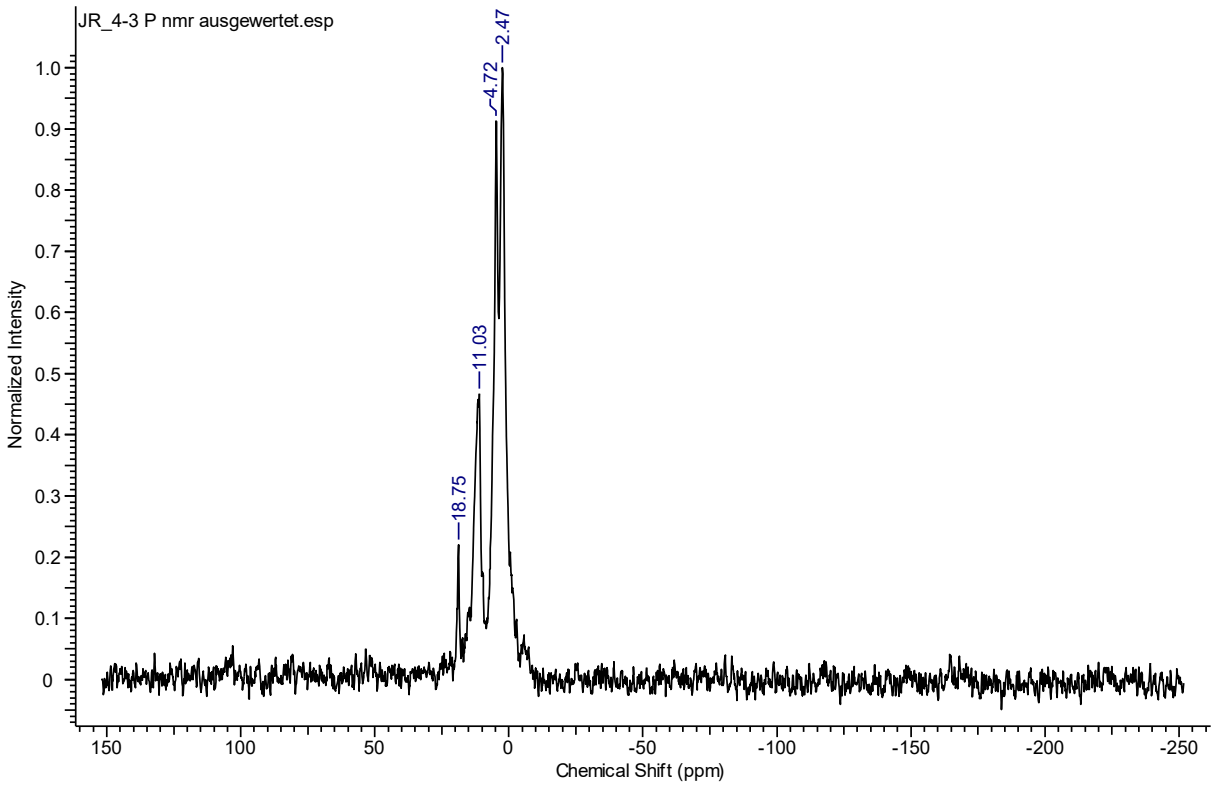

Figure 70: ^{31}P NMR spectrum in $CDCl_3$ of PPz macrosubstituted with the tbutyl(2-(2-(2-aminoethoxy)ethoxy)ethyl)carbamate linker.

^{1}H, 300 MHz, $CDCl_3$: δ= 3.59 (m, 4H), 3.52 (m, 4H), 3.29 (m, 2H), 3.04 (m, 2H), 1.44 (s, 9H) ppm.

^{31}P, 121.49 MHz, CDCl3: δ= 2.32, 4.59 ppm.

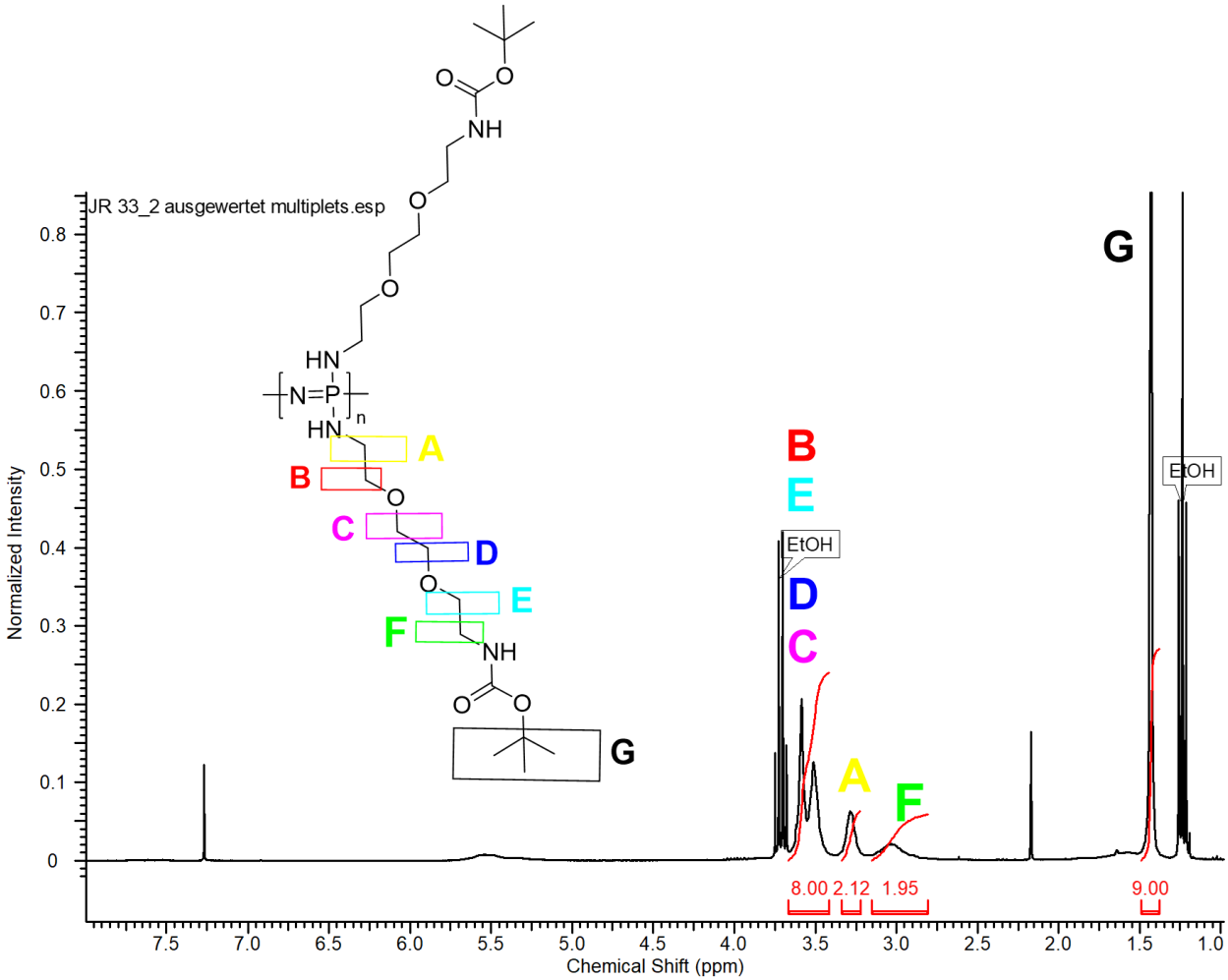

Figure 71: ^{1}H NMR in $CDCl_3$ of macro substituted PPz with tbutyl(2-(2-(2-aminoethoxy)ethoxy)ethyl)carbamate linker.

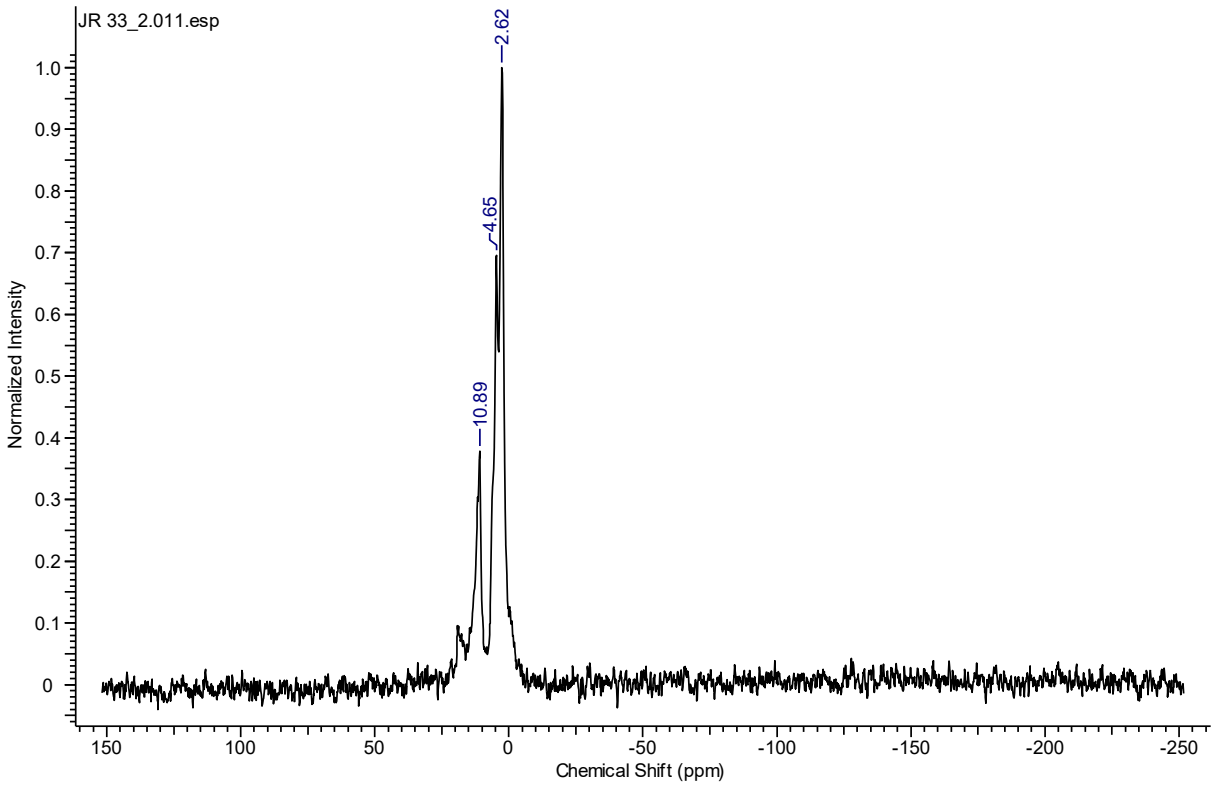

Figure 72: ^{31}P NMR in $CDCl_3$ of macro substituted PPz with tbutyl(2-(2-(2-aminoethoxy)ethoxy)ethyl)carbamate linker.

^{1}H, 300 MHz, $CDCl_3$: δ= 3.60 (m, 4H), 3.51 (m, 4H), 3.29 (m, 2H), 3.03 (m, 2H), 1.43 (s, 9H) ppm.

^{31}P, 121.49 MHz, $CDCl_3$: δ= 2.62, 4.65 ppm.

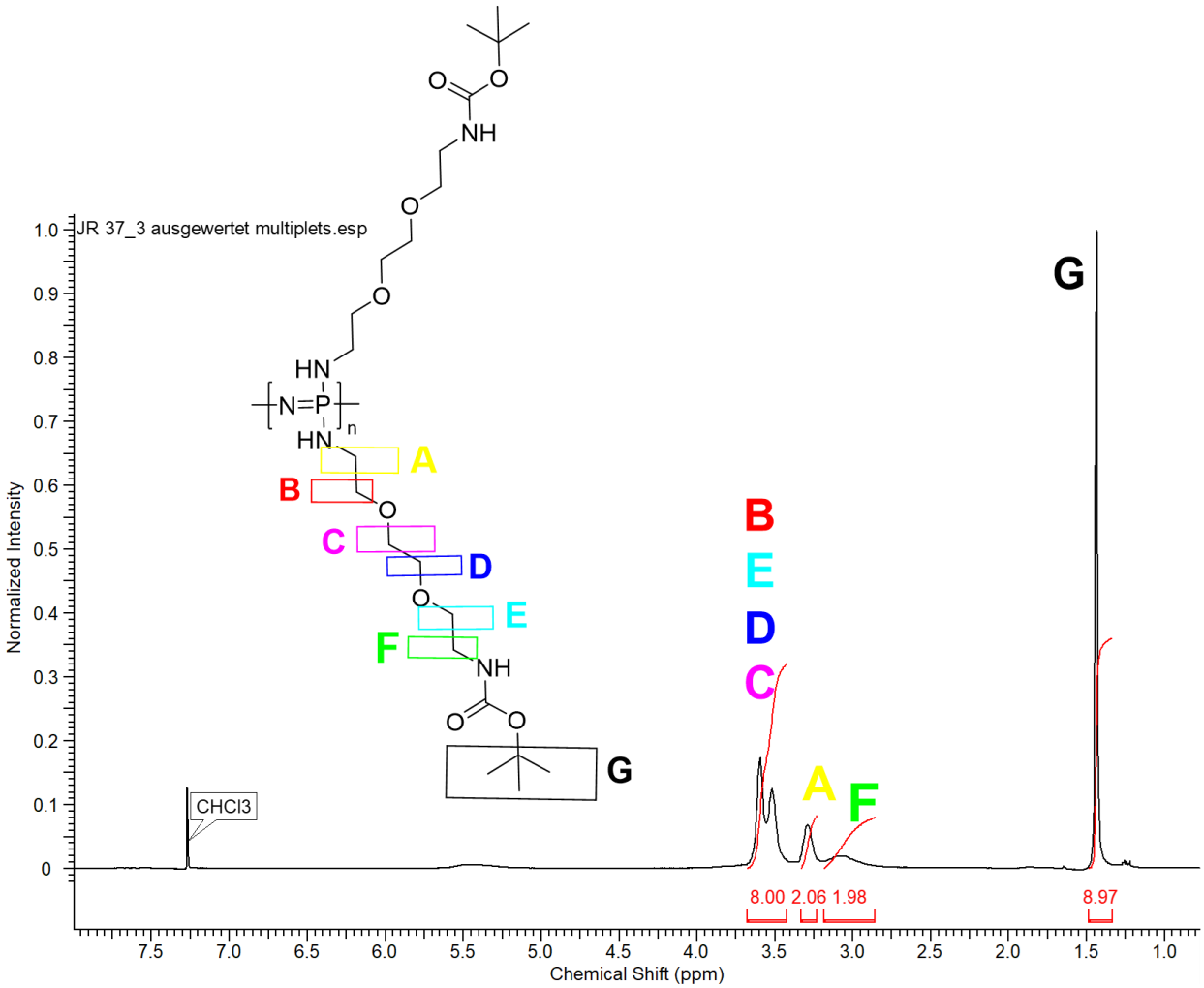

Figure 73: ^{1}H NMR in $CDCl_3$ of macro substituted PPz with tbutyl(2-(2-(2-aminoethoxy)ethoxy)ethyl)carbamate linker.

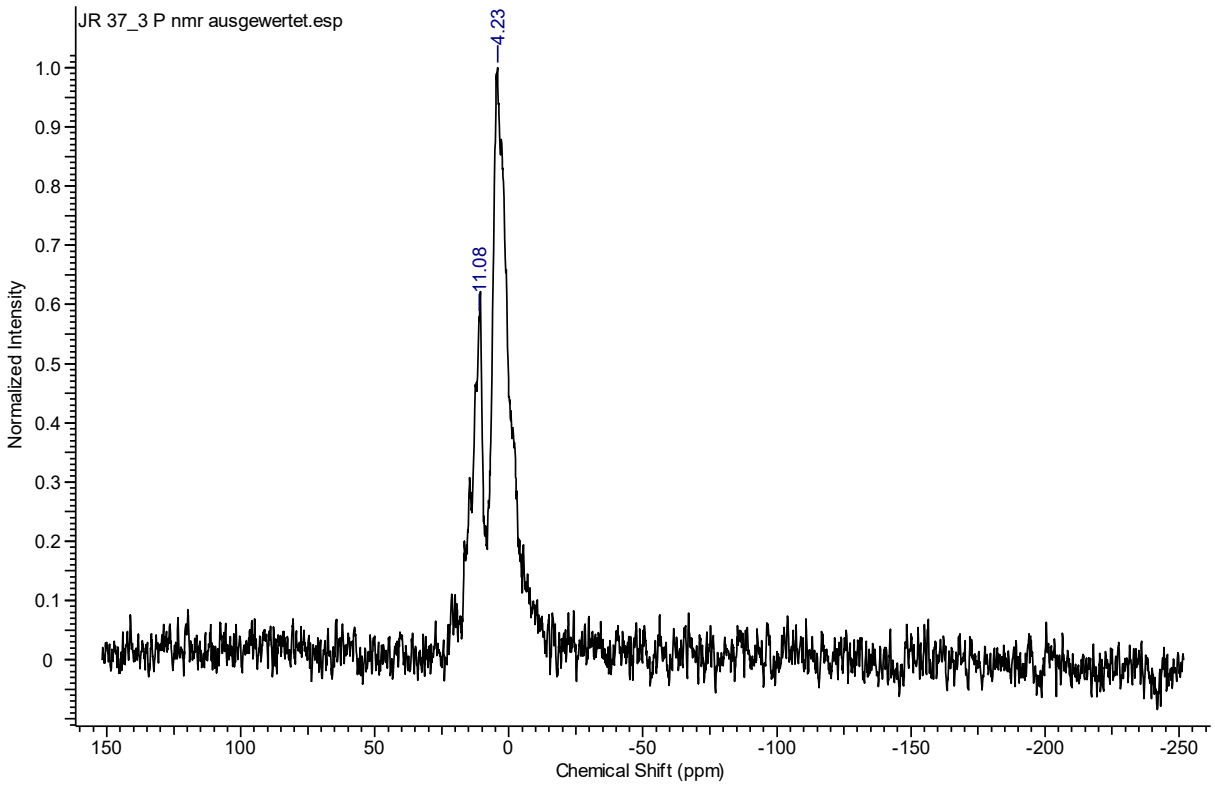

Figure 74: ^{31}P NMR in $CDCl_3$ of macro substituted PPz with tbutyl(2-(2-(2-aminoethoxy)ethoxy)ethyl)carbamate linker.

^{1}H, 300 MHz, $CDCl_3$: δ= 3.59 (m, 8H), 3.29 (m, 2H), 3.08 (m, 2H), 1.44 (s, 9H) ppm.

^{31}P, 121.49 MHz, $CDCl_3$: δ= 4.23 ppm.

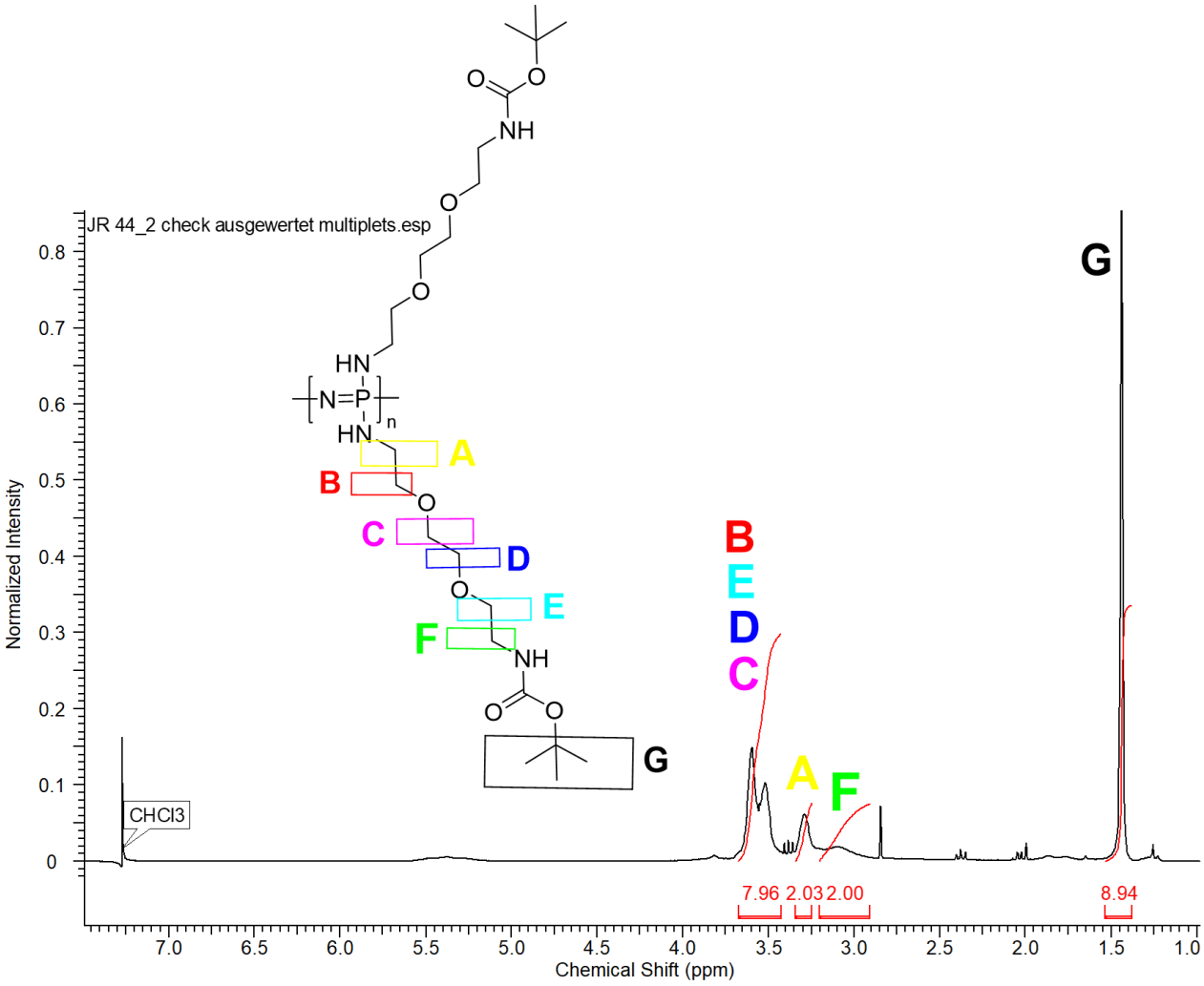

Figure 75: ^{1}H NMR in $CDCl_3$ of macro substituted PPz with tbutyl(2-(2-(2-aminoethoxy)ethoxy)ethyl)carbamate linker.

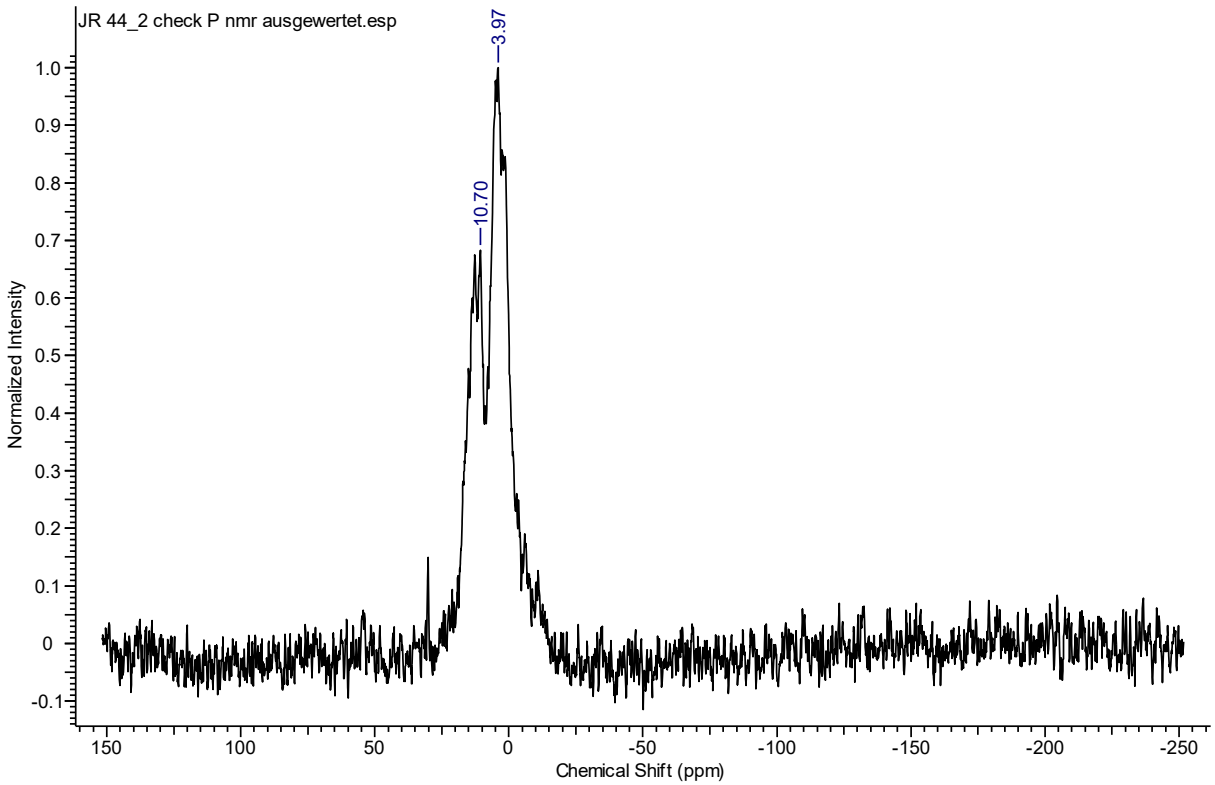

Figure 76: ^{31}P NMR in $CDCl_3$ of macro substituted PPz with tbutyl(2-(2-(2-aminoethoxy)ethoxy)ethyl)carbamate linker.

^{1}H, 300 MHz, $CDCl_3$: δ= 3.55 (m, 8H), 3.29 (m, 2H), 3.03 (m, 2H), 1.44 (s, 9H) ppm.

^{31}P, 121.49 MHz, $CDCl_3$: δ= 3.97 ppm.

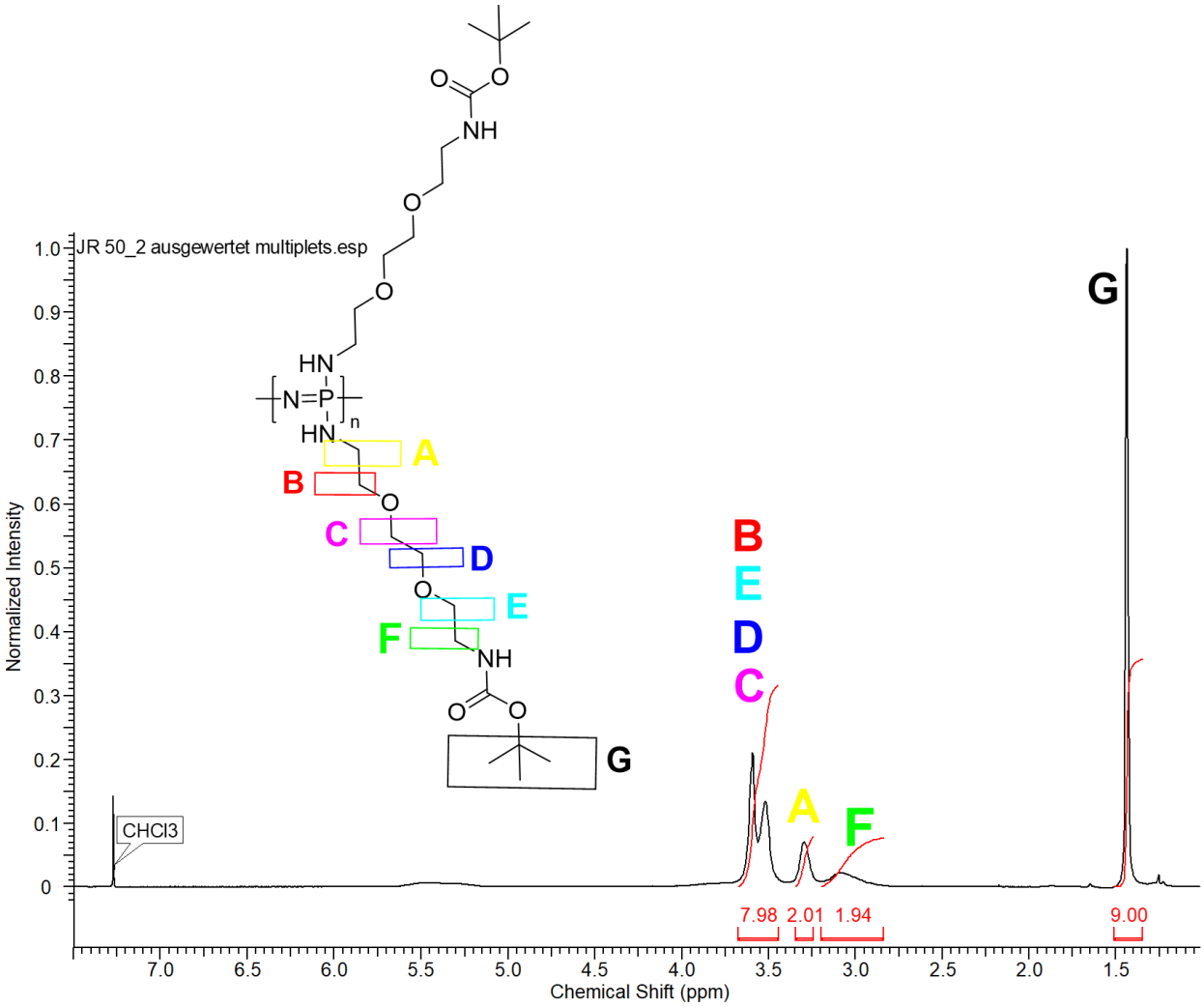

Figure 77: ^{1}H NMR in $CDCl_3$ of macro substituted PPz with tbutyl(2-(2-(2-aminoethoxy)ethoxy)ethyl)carbamate linker.

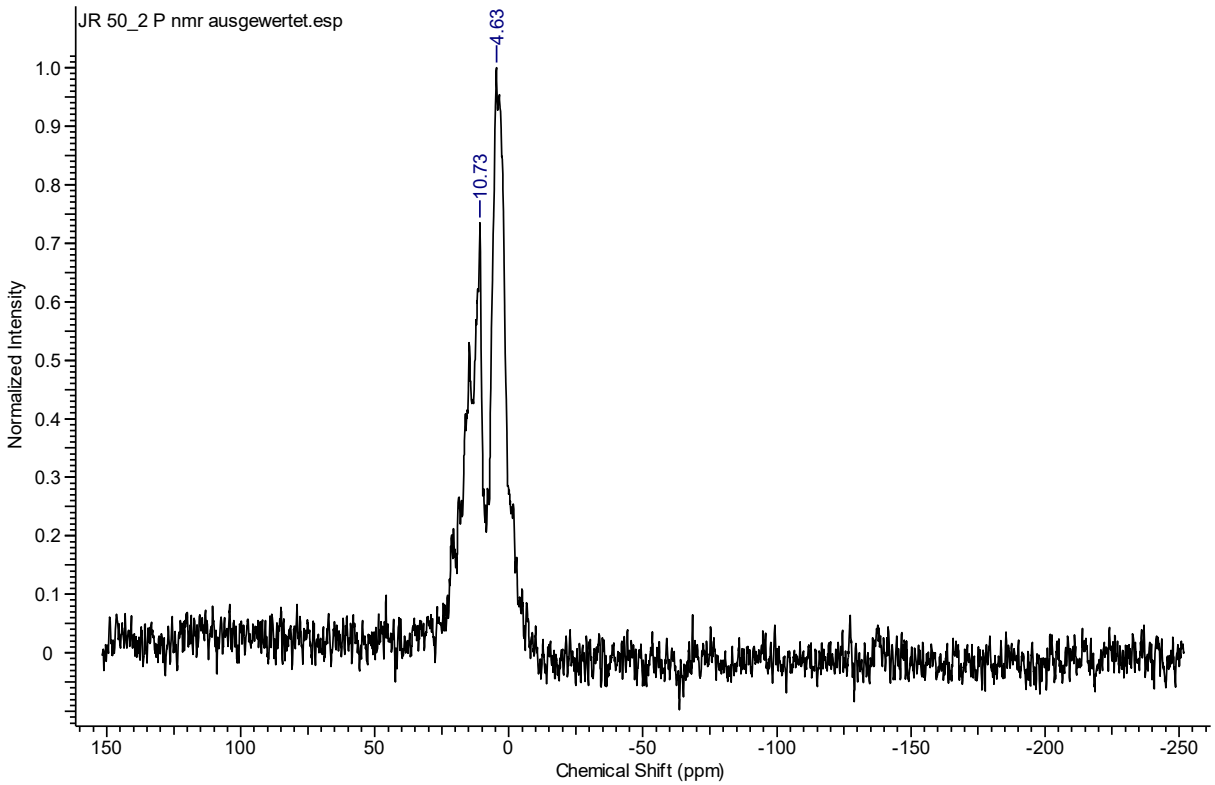

Figure 78: ^{31}P NMR in $CDCl_3$ of macro substituted PPz with tbutyl(2-(2-(2-aminoethoxy)ethoxy)ethyl)carbamate linker.

^{1}H, 300 MHz, $CDCl_3$: δ= 3.55 (m, 8H), 3.30 (m, 2H), 3.08 (m, 2H), 1.44 (s, 9H) ppm.

^{31}P, 121.49 MHz, $CDCl_3$: δ= 4.63, 10.73 ppm.

Ad PPz-co-pHPMA:

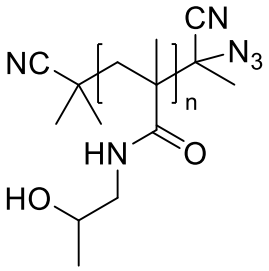

Figure 79: Structure of pHPMA ICP-IT-4.

Table 10: Characteristics of pHPMA ICP-IT-4

Sample name	**ICP-IT-4**
Description	P(HPMA)-N_3
Mw	35900 $g.mol^{-1}$
Đ	1.16

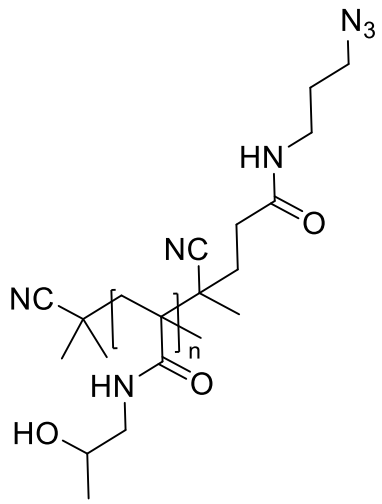

Figure 80: Structure of pHPMA ICP-IT-6.

Table 11: Characteristics of pHPMA ICP-IT-6

Sample name	**ICP-IT-6**
Description	Semitelechelic homopolymer pHPMA with terminal azide groups
Mw	8000 $g.mol^{-1}$
Đ	1.02
Functionality of azide groups	F = 0.96

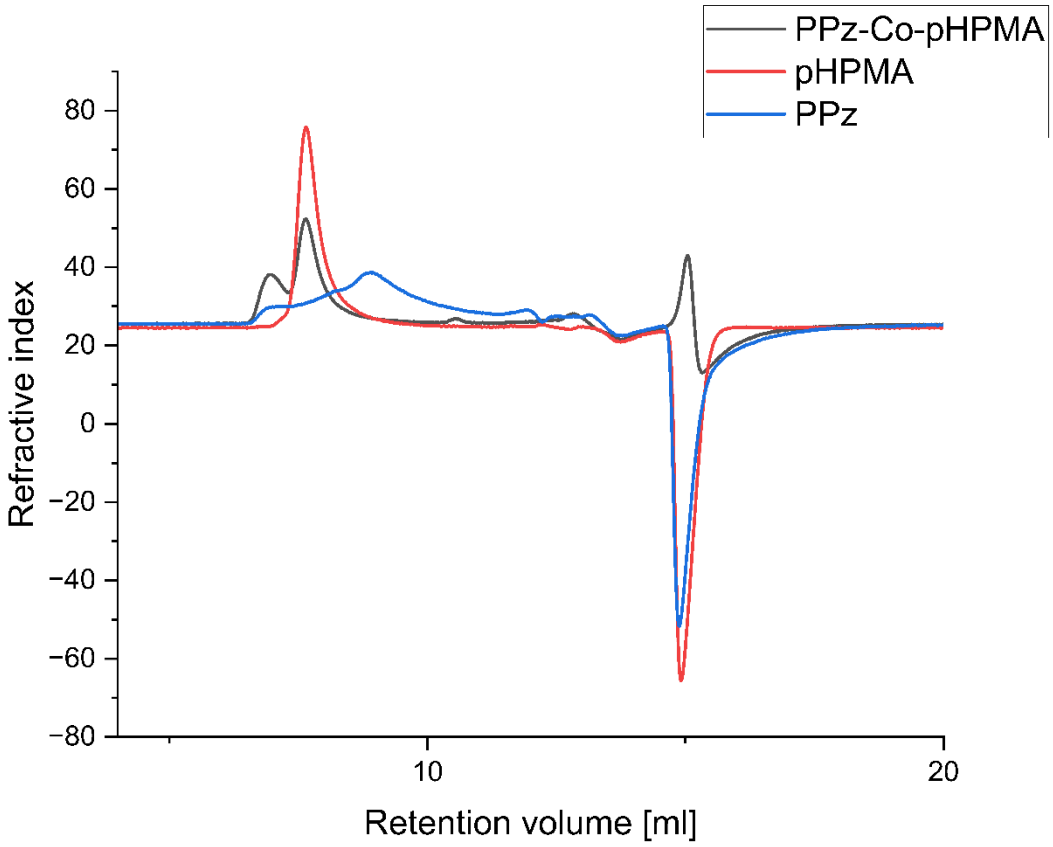

Figure 81. GPC chromatogram in DMF of PPz-Co-pHPMA, reacted in EtOH/H2O at rt for 2 days, with sodium ascorbate, $CuSO_4.5H_2O$ (Procedure 1).

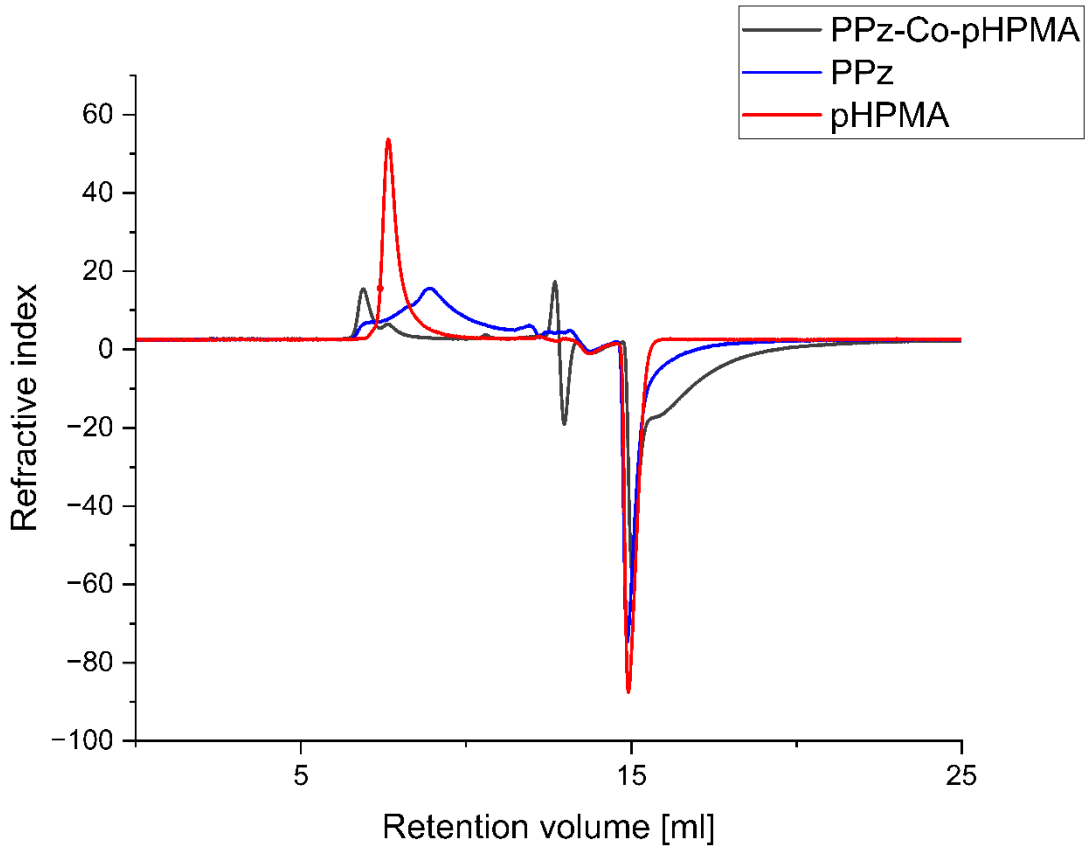

Figure 82: GPC chromatogram in DMF of PPz-Co-pHPMA, reacted in DMF at rt under argon for 2 days, with ascorbic acid, $CuSO_4.5H_2O$ (Procedure 2).

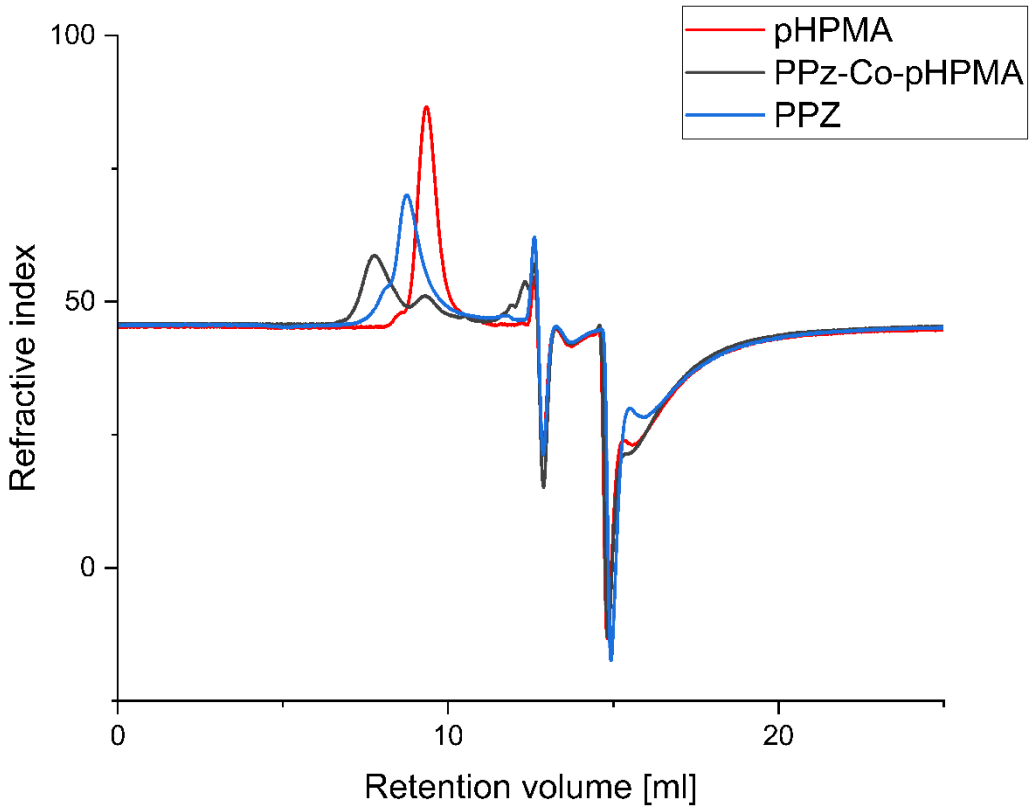

Figure 83: GPC chromatogram in DMF of PPz-co-pHPMA, reacted in DMF at rt under argon for 2 days, with ascorbic acid, $CuSO_4.5H_2O$ (Procedure 3).

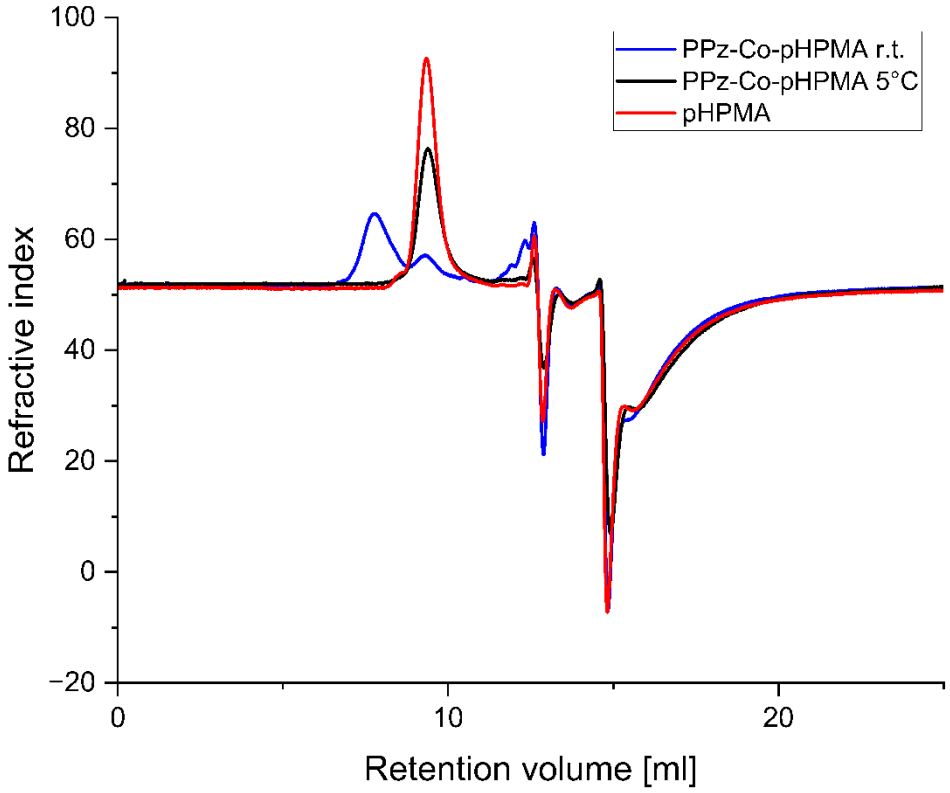

Figure 84: GPC chromatogram in DMF of PPz-Co-pHPMA, reacted in DMF, with $CuSO_4.5H_2O$ and ascorbic acid for 2 days under argon and at 5°C (Procedure 4).

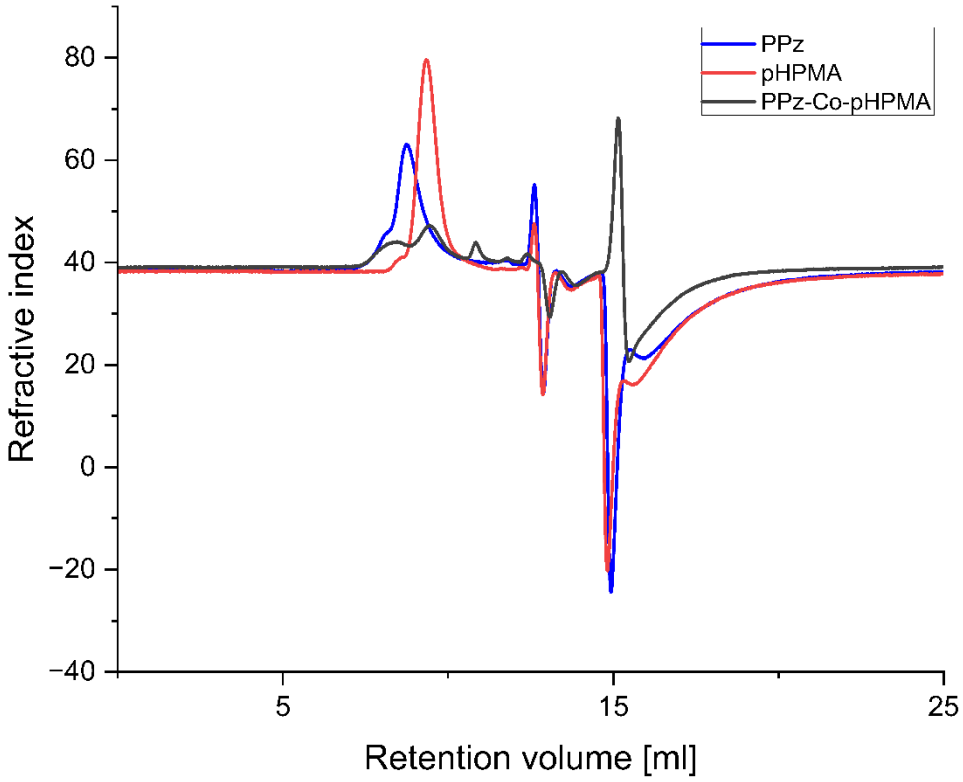

Figure 85: GPC chromatogram in DMF of PPz-Co-pHPMA, reacted in DMAc, with CuBr and TBTA, at rt under argon, for 1 day (Procedure 5).

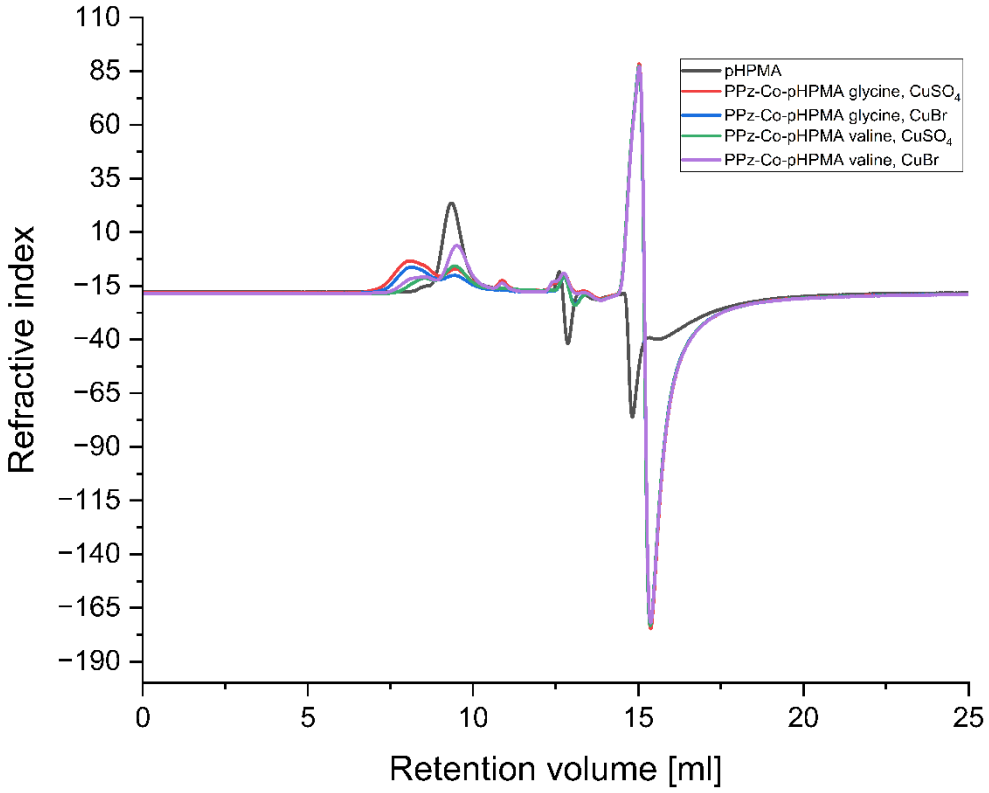

Figure 86: GPC chromatogram in DMF of PPz-Co-pHPMA, comparing different linker species (glycine versus valine) and reaction conditions (Procedure 6 and Procedure 7).

***Ad* PPz-co-PGA:**

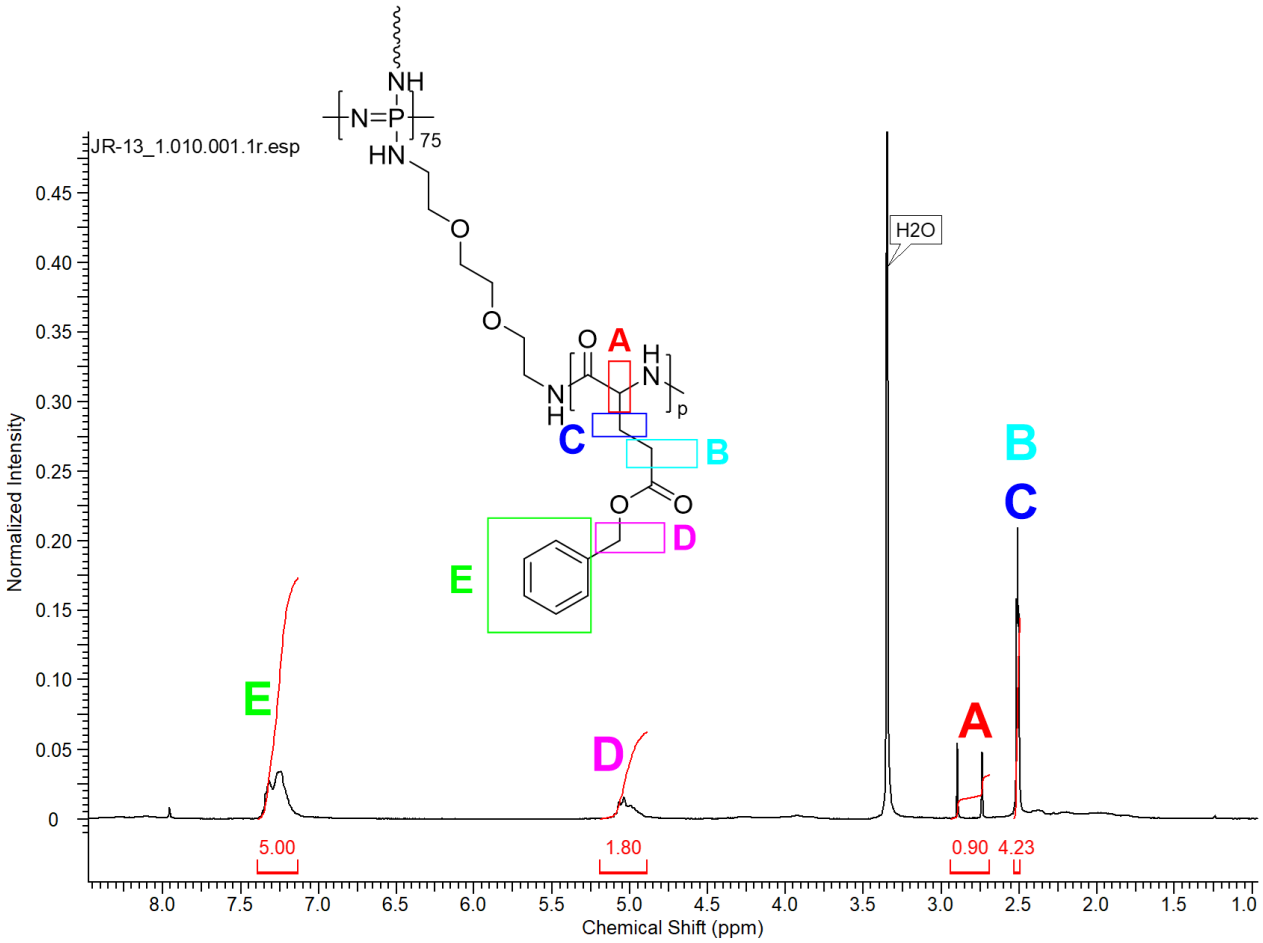

Figure 87: ^{1}H NMR spectrum in DMSO-d6 of benzyl-protected PPz-co-PGA.

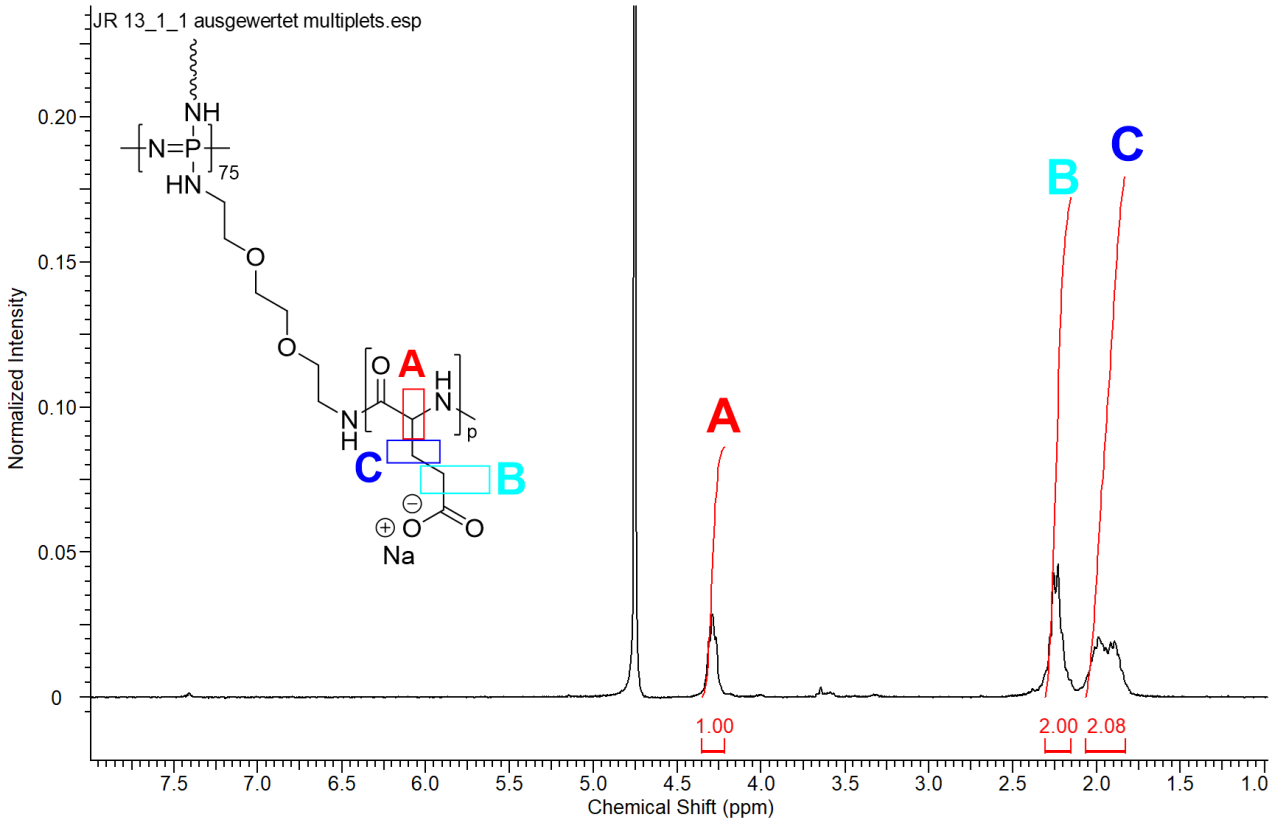

Figure 88: ^{1}H NMR spectrum in D_2O of deprotected PPz-co-PGA.

^{1}H, 300 MHz, DMSO-d6: δ=7.26 (m, 5H), 5.08 (m, 2H), 2.84 (m, 1H), 2.49 (m, 4H) ppm.

^{31}P, 121.49 MHz, DMSO-d6: δ= n.a.

^{1}H, 300 MHz, D_2O: δ= 4.29 (m, 1H), 2.23 (m, 2H), 1.99 (m, 2H) ppm.

^{31}P, 121.49 MHz, D_2O: δ= n.a.

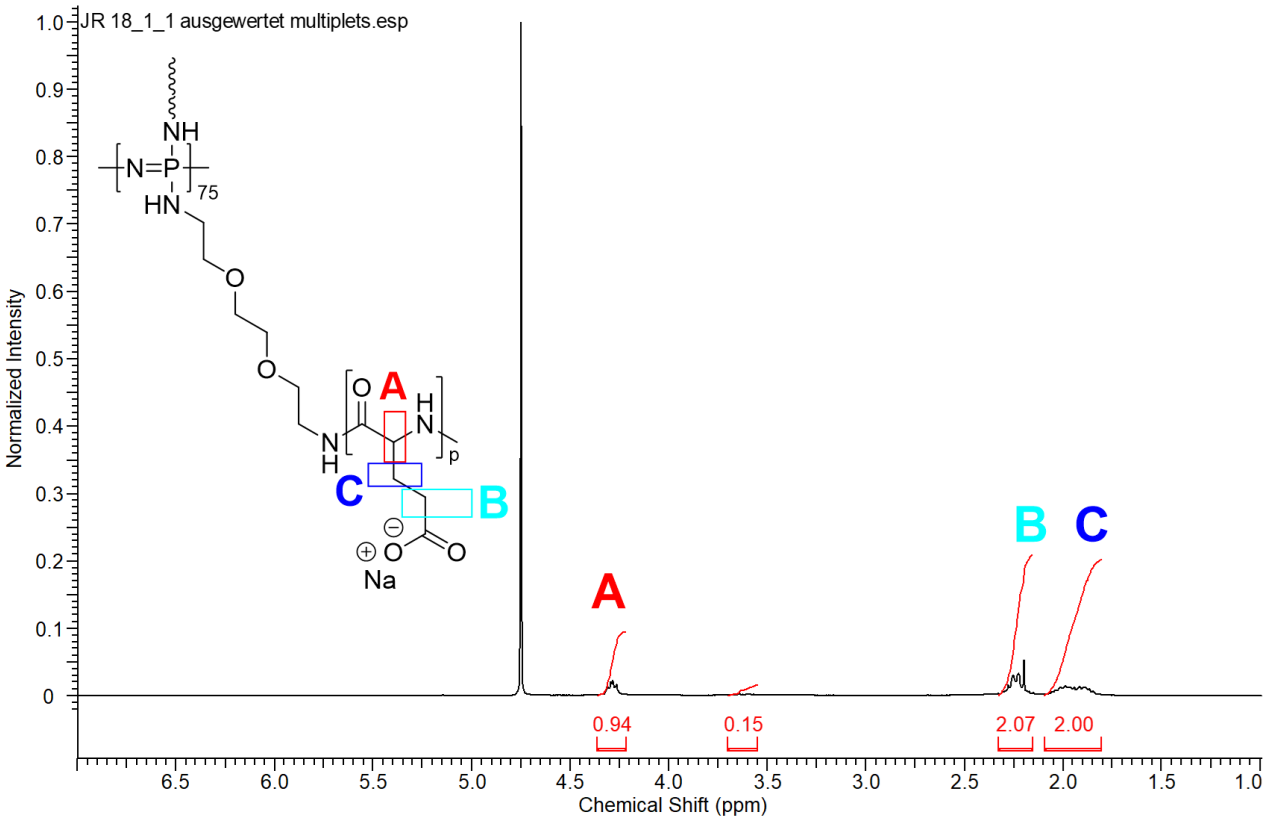

Figure 89: ^{1}H NMR in D_2O of deprotected PPz-co-PGA.

^{1}H, 300 MHz, D_2O: δ= 4.29 (m, 1H), 2.24 (m, d, J=7.4 Hz, 2H), 1.95 (m, 2H) ppm.

^{31}P, 121.49 MHz, D_2O: δ= n.a.

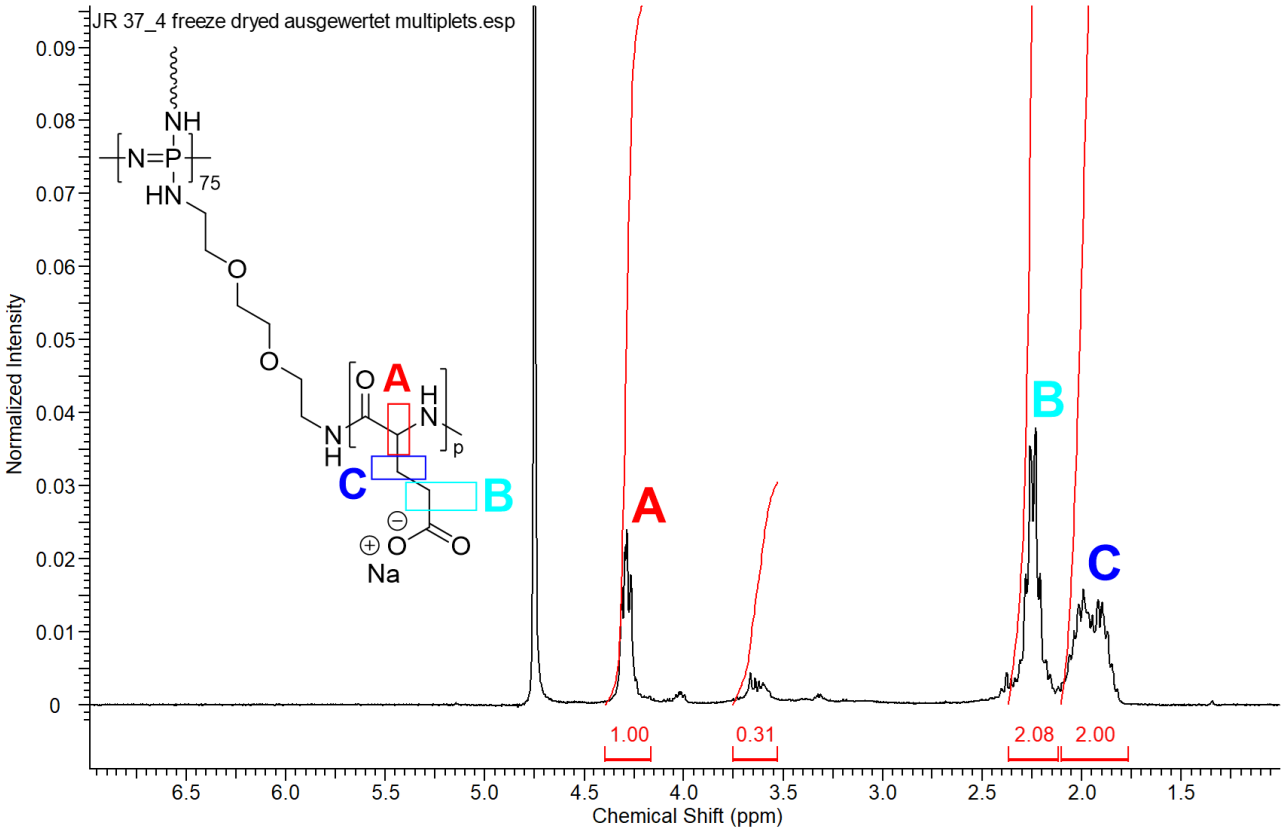

Figure 90: ^{1}H NMR in D_2O of deprotected PPz-co-PGA.

^{1}H, 300 MHz, D_2O: δ= 4.29 (d, J=2.9 Hz, 1H), 2.24 (d, J=8 Hz, 2H), 1.94 (m, 2H) ppm.

^{31}P, 121.49 MHz, D_2O: δ= n.a.

***Ad* PPz-co-PGA with peptide therapeutic:**

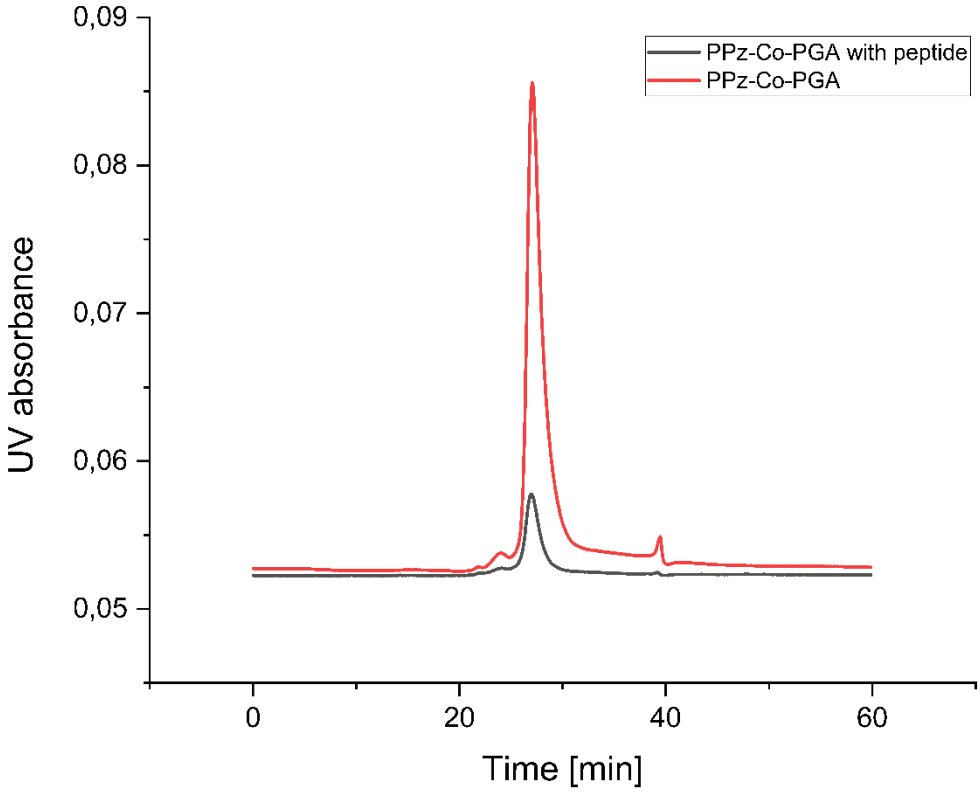

Figure 91: GPC measurement in aqueous medium of the PPz-co-PGA with peptide therapeutic, labelled with Cy5

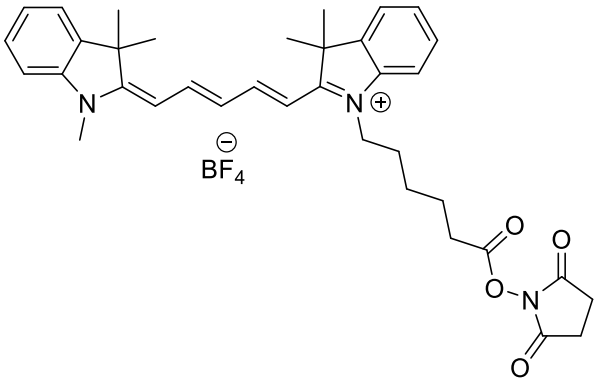

Figure 92: Chemical structure of cyanin5 NHS ester.

***Ad* PPz-co-PGA with hydrazide linker:**

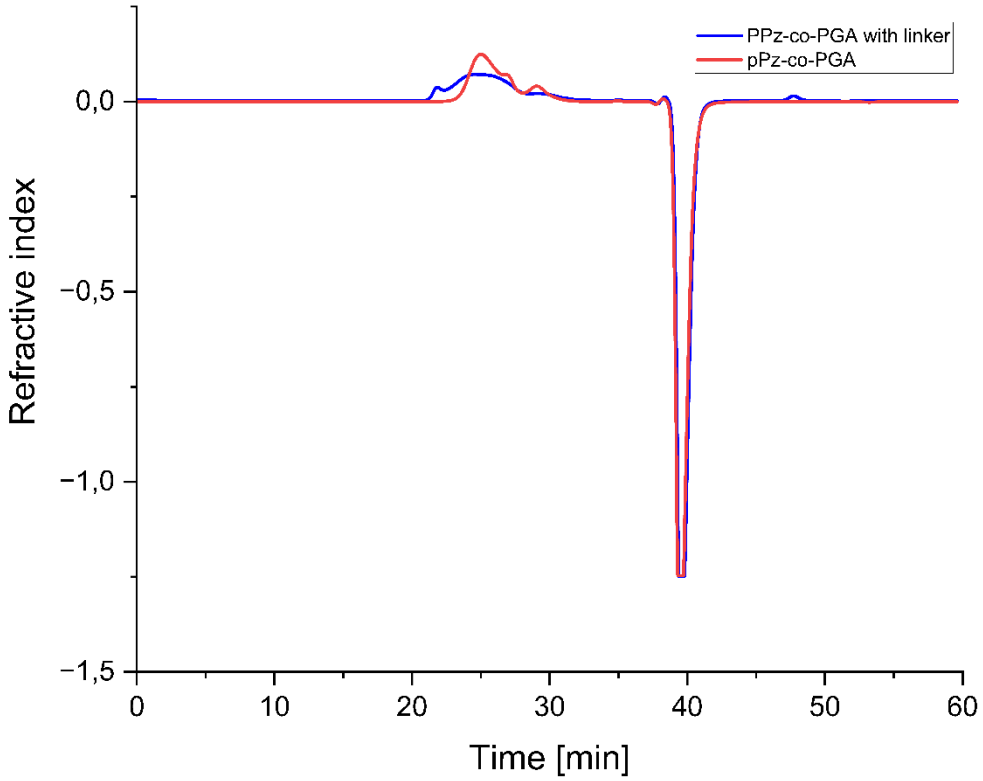

Figure 93: RI detector trace of the GPC chromatogram of the PPz-co-PGA with the hydrazide linker (Procedure 3).

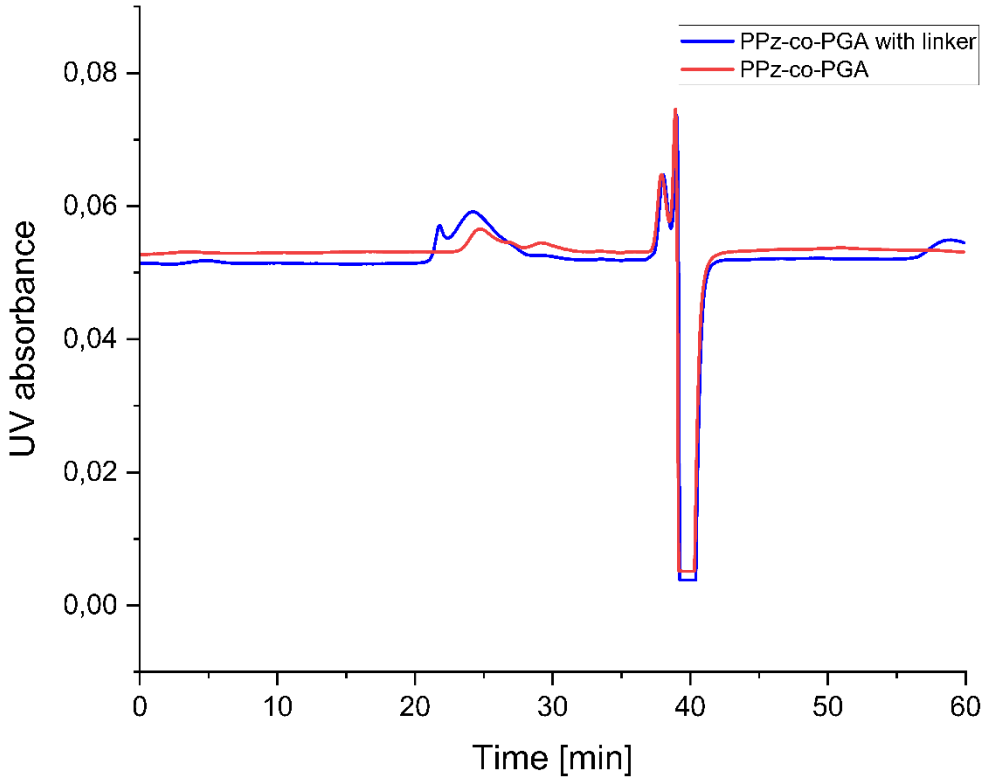

Figure 94: UV-detector trace of the GPC chromatogram of the PPz-co-PGA with the hydrazide linker (Procedure 3).